Optimal Planning and Operation of Power to Gas Energy Hubs in Transitioning Electricity Systems

by

Ushnik Mukherjee

A thesis

presented to the University of Waterloo

in fulfillment of the thesis requirement for the degree of

Doctor of Philosophy

in

Chemical Engineering

Waterloo, Ontario, Canada, 2018

Examining Committee Membership

The following served on the Examining Committee for this thesis. The decision of the Examining Committee is by majority vote.

External Examiner	Professor Rupp Carriveau Civil and Environmental Engineering, University of Windsor
Supervisor(s)	Professor Michael Fowler Chemical Engineering, University of Waterloo
Internal Member	Professor Eric Croiset Chemical Engineering, University of Waterloo
Internal-external Member	Professor Kumaraswamy Ponnambalam Systems Design Engineering, University of Waterloo
Internal Member	Professor Peter Douglas Chemical Engineering, University of Waterloo

Author's Declaration

This thesis consists of material all of which I authored or co-authored. The list of co-authors who have contributed in the publications that have come out the work presented in this thesis include Dr. Azadeh Maroufmashat, Professor. Sean Walker, Dr. Mohamed Elsholkami, Dr. Amir Hajimiragha, Ehsan Haghi, Dr. Apurva Narayan, Professor Michael Fowler, and Professor Ali Elkamel.

Dr. Mohamed Elsholkami, and Dr. Azadeh Maroufmashat have been instrumental in supporting and reviewing the optimization model logic developed for studies presented in chapters 4, 6 and 7. Professor. Sean Walker and Dr. Azdeh Maroufamashat contributed with their expertise in developing conceptual figures of the energy hub system proposed in chapters 2 and 6.

Ehsan Haghi, helped with his insights on the policy aspect of the research, especially the analysis presented in chapter 4. He (Ehsan Haghi) also helped in preparing parts of text presented in chapter 4 (section 4.3.5).

Dr. Apurva Narayan was involved in this work to direct and support the analysis presented in chapter 7. Dr. Apurva Narayan provided his background in design optimization under uncertainty and helped in understanding the stochastic nature of some of the input parameters used in chapter 7.

Professor Michael Fowler, Professor Ali Elkamel and Dr. Amir Hajimiragha have contributed by providing feedback on after reviewing the articles published from this work.

Abstract

Challenges faced by an electricity sector transitioning towards a lower carbon footprint can be seen as an opportunity for energy technologies that are able to address them. Surplus energy generation is one of the biggest issues faced by the provincial power grid of Ontario. In 2017, the IESO exported approximately 7.3 TWh of surplus electricity. This adds up to almost 5.54% of the province's annual energy demand and equivalent to meeting the electricity demand of 9.8 million homes. Power to gas energy hubs represent a novel concept that could help in effectively repurposing surplus electricity generation. This concept proposes to utilize the surplus electricity to produce hydrogen via the water electrolysis process. Hydrogen as an energy vector enables the storage and distribution of surplus electricity through an entirely different energy system (e.g. natural gas grid).

The implementation of this idea is of particular interest in the context of Ontario as this work proposes to utilize the existing natural gas distribution infrastructure to distribute the electrolytic hydrogen. Linking of the electrical distribution and natural gas distribution system will allow Ontario to form a seamless integrated energy system.

This work looks at repurposing surplus electricity via hydrogen in the natural gas and transportation sector within Ontario. More specifically, this thesis focusses on estimating the cost of reducing emissions by servicing natural gas end users with a hydrogen enriched natural gas (HENG) blend and renewable natural gas (RNG) (produced by combining electrolytic hydrogen with biogenic CO_2 from organic waste processing facilities). These costs have estimate to be \$87 and \$228 per tonne of lifecycle $CO_{2,e}$ emissions offset at the natural gas end user for using HENG and RNG, respectively. The cost of reducing emissions in the natural gas sector is then compared with what the province's electric and hydrogen vehicle incentive program offers in the transportation sector. For the 9056 (4760 battery and 4296 plug-in hybrid) electric vehicles that qualified for incentives at the end of 2016, it will cost the province of Ontario \$732 per tonne of $CO_{2,e}$ to offset emissions over an 8 year lifetime (with each vehicles mileage being 180,000 km). This comparison shows the potential incentive structures required for power to gas energy hubs, and electric vehicles, both of which represent ways to repurpose surplus electricity within the

province. Electric vehicles and power to gas both are important technologies that reduce emissions by utilizing clean low emission surplus electricity, this comparison tries to highlight how power to gas can also be a part of a holistic solution.

In addition to this, the thesis highlights the potential scale of electrolyzer systems required to absorb all of Ontario's surplus electricity and gives a brief overview of potential end uses of hydrogen in Ontario's 10 different power zones. It is seen that an electrolyzer system capacity close 3179 MW would be required to absorb all of the surplus electricity generated in 2016 (5.3 TWh) within the province. Following this, a business case analysis from a 2 MW power to gas demonstration project within the greater Toronto area has been presented. This analysis focuses on valuing: 1) The price of hydrogen as a fuel for fuel cell vehicles; 2) The incentive received by on-site electrolyzer to provide demand response ancillary service to the power grid, and 3) The $CO_{2,e}$ emission offset allowance that the power to gas requires when it offsets emissions at natural gas end users. The evaluation shows that to achieve a short payback of 8 years (desirable for the energy hub investors) hydrogen sold to the transportation sector should be valued at a price higher ($6.71 per kg) than its levelized cost of production ($3.66 per kg). The current demand response ancillary service incentive structure ($ 0.0215 per kWh) does not account for technologies such as power to gas providing demand response. Therefore for such technologies to be able to provide this service, the business cost for power to gas energy hubs to curb load while providing multiple services such as hydrogen refueling is evaluated and should be close to $0.039 per kWh. The price of carbon emission allowances in the cap and trade program (~$18 per tonne of $CO_{2,e}$) are not valued high enough and the values should increase to at least $28 per tonne of $CO_{2,e}$ emissions offset. The valuation of all these services within Ontario has been compared and seen to be well within what global trends have shown.

The last piece of analysis shown in this thesis includes assessing the impact of uncertainty in electricity price and fuel cell vehicle hydrogen demand on the sizing and operation of a power to gas energy hub. The impact of uncertainty on how the energy hub responds to deterministic data sets such as a demand response ancillary service requirement has also been evaluated. A 17 MW system has been sized with on-site tank storage capacity of 1869 kg to provide hydrogen demand for a hypothetical market penetration scenario of 1766 fuel cell vehicles within the GTA. This penetration scenario is scaled down from trends developed for the US by the Oak Ridge National

Laboratory. Positive values for the 'Expected Value of Perfect Information' ($57,211) and the 'Value of Stochastic Solution' ($104,276) highlight the value of obtaining perfect information on the uncertain parameters and the cost savings achievable when uncertainty has been accounted for.

Through the analysis presented in this thesis some of the potential barriers for the implementation of such technologies has been highlighted in chapter 8. Some of the primary challenges include the energy storage technologies being subject to market uplift charges such as global adjustment which significantly increases their cost to be competitive. If energy storage technologies are included in the electricity system operators dispatch scheduling optimization engine as dispatchable loads some of these uplift charges would reduce as a result of electricity market clearing price increasing and reaching values close to what contracted generation facilities need to be paid. Energy storage technologies have not been included in the provinces industrial conservation initiatives. There are no clear rules, regulations (including safety standards) defined by the Ontario Energy Board or in other legislations within the province. The valuation of the additional services (e.g., emission reduction, surplus baseload generation management, enabling higher penetration of renewables) has not been studied by regulators within the province. In order to drive investment in energy storage projects, the regulators of the electricity sector need to provide better access to reliable, and current data. This will help investors to understand the regions where there are potential opportunities for such projects within the province.

The four different analyses outlined above show that power to gas energy hubs can be cost competitive when compared with other technologies (such as battery and plug in hybrid electric vehicles) that repurpose surplus off-peak power or excess intermittent renewable power within a different energy sector. Power to gas energy hubs located within urban communities can provide multiple energy recovery pathways while being within agreement of current and projected market prices (H_2 enriched natural gas, H_2 as a transportation fuel, demand response ancillary service, $CO_{2,e}$ emission offset allowance). Accounting for uncertainty in parametric input data proves to be more valuable than its deterministic counterpart. Overall, this thesis tries to highlight the potential for power to gas energy hubs and what roles it could play in Ontario's long term energy future.

Acknowledgements

Pursuing my doctorate has helped me grow professionally and personally. These past five years have taught me a little bit about the world, the problems that we are facing and my desire to improve the quality of life for people and the planet.

However, for me to have this opportunity to come to Waterloo would not have been possible without Professor Sanjeev Bedi of the Mechatronics and Mechanical Engineering Department at the University of Waterloo. I will forever be grateful for his help in finding a supervisor for me. I would also like to acknowledge his family especially his wife Pauline Bedi for her generosity and for sharing her house with me when I was an exchange student here in 2012. The love, and care that I felt here with them helped me make the decision to come back to Waterloo to pursue my PhD.

The people you surround yourself with influence how you grow, and I have been fortunate enough to have had friends and family members who come from diverse backgrounds and perspectives. Engaging with people with different perspectives at times can be challenging but in the long run, it helps us reflect on and sometimes change our way of thinking.

I would like to appreciate and acknowledge my friends Manoj Mathew, Prasad Arcot, Ehsan Haghi, Abdullah Al Subaie, Azadeh Maroufmashat, Mohamed Elsholkami, Abhishek Joshi, Ankita Saikia and Sean Walker. They have been great friends! Sharing my 5 years with them have helped me learn that despite coming from different countries we all value the basic things in life: finding a sense of belonging, a genuine purpose in life, giving and receiving respect and finally, being appreciated.

My supervisor Professor Michael Fowler has been exceptional in guiding and supporting me throughout the last 5 years. I really appreciate his practicality and frankness in life. His countless fascinating stories from working for the Canadian military are a source of great inspiration and knowledge. I will always cherish my time working with him as a research assistant.

I am very thankful to have my life partner Janna Martin in Waterloo. Her patience, kindness, and objectivity are things that I am grateful for. Janna has helped me be more appreciative of the work that other faculties such as the social sciences (especially peace and conflict studies) are doing to address human rights issues. She and her family have helped me feel that I have a home in Canada.

My parents Mousumi Mukherjee, and Abhijit Mukherjee and my sister Rupsha Mukherjee have been of great emotional support for me. Maintaining family relationships over long distance is challenging but I am appreciative of their constant support and well wishes. Their insights have always been a calming influence during times of difficulty in the past five years.

In the end I would also like to thank Dr. Hira Ahuja for his generosity in making scholarships available for students like me at the University of Waterloo. His generosity helped me sustain a financially sustainable life over the past 5 years.

Table of Contents

List of Figures

List of Tables

Chapter 1: Introduction

1.1 Problem Definition

The objective of this research is to develop an operational model of an energy hub based on electrolytic hydrogen integrated into the natural gas distribution system and transportation sector. As such, the model can be used to assess the potential of using electrolytic hydrogen as an energy vector, i.e. an energy storage and transportation medium within an energy hub framework. The model will be used to optimize the size and configuration of component and operational parameters in a power to gas facility. The study will quantitatively analyze how much of low cost surplus electricity exports occurring from the province of Ontario can be curbed.

Use of electrolytic hydrogen as an energy vector can also have a significant impact in meeting the environmental emission reduction targets set by the province. Therefore it is of interest both from cost and environmental perspective to optimize the sizing and operation of electrolyzer systems that form a link between the power grid, natural gas grid, and Ontario's transportation sector.

Overall this work will aid in the development pricing structures or policy frameworks that will enable the collaboration of electrical utilities, natural gas utilities as well as hydrogen energy system technology companies to contribute to the development of an adaptable energy framework for Ontario.

Although there are few power to gas demonstration projects at various stages of development, there currently are no operational models. The facilities are not optimized for their respective markets, they do not consider environmental and economic considerations, nor do they consider the provision of a variety of services.

As such, this thesis explores the potential outlined in the above paragraph via techno-economic optimization models that account for the technological, costing and environmental aspects concerning the components of a power to gas energy hub. An environmental benefit assessment of hydrogen and renewable natural gas within the transportation and natural gas sector has also been carried out. The thesis also looks in to the influence of uncertain parametric data on the planning and operation of the power to gas energy hubs. The goal of the thesis is to address the

economic feasibility and potential policy modifications that could benefit the implementation of hydrogen as an energy vector within the province. Through the analysis presented within, this thesis develops potential incentive mechanisms in terms of $CO_{2,e}$ emission pricing, hydrogen fuel pricing for transportation application (vs. gasoline prices), and ancillary service pricing. These are the contributions of this thesis to the scientific literature and could be utilized as a guide to how energy policy decisions can be framed for novel clean energy technologies (especially one's that utilize hydrogen as an energy vector).

1.2 Motivation

The shift to cleaner renewable energy is imperative to counteract the harmful effects that the fossil fuel based energy system has had on the global climate. In Canada, the Province of Ontario has been one of the biggest promoters of renewable and low carbon energy generation. However, the path to this transition has also created issues of growing electricity prices to customers and significant amount of surplus electricity being exported at a low price to neighboring jurisdictions. Therefore, a brief overview of: 1) The formulation and changes in renewable energy policy; 2) The change in generation portfolio and 3) The gradual decrease of electricity demand within the province is necessary.

1.2.1 Renewable energy policies within Ontario

From 2004 to 2018, the province of Ontario has seen significant changes in its power sector. The year 2004 marked the laying out of Ontario's plan to phase out 4500 MW of coal fired power plant **[1]**. Although initially planned to be phased out by 2007, the transitioning to cleaner alternatives such as wind, hydroelectric, solar and bioenergy took time and in order to maintain reliability of the power system, the phase out was delayed until 2014.

In order to promote the adoption of renewable energy sources, the province in 2006 introduced its first renewable energy policy called the 'Renewable Energy Standard Offer Program, RESOP' **[1]**. The RESOP was a policy formulated to offer 20 year contracts to wind, bioenergy, solar and hydroelectric power projects with a maximum size of 10 MW. The contract proposed prices to such generation sources based on an average bid price obtained from request for proposal reports **[1]**. However, the low contract prices offered especially to solar PV projects and long approval

times of projects led to the RESOP policy experiencing significant opposition from advocates of renewable energy within the province.

A growing opposition to RESOP followed by the recession of 2008 leading to manufacturing jobs moving out of the province, the Minister of Energy in 2009 formulated a new policy called the 'Green Energy and Green Economy Act, GEGEA'. The GEGEA or the green energy act, was used as a move to reduce the provincial electricity sector's greenhouse gas footprint and create green energy jobs **[1]**. Similar to the RESOP, the GEGEA offered renewable generators such as wind and solar 20 year contracts. However, this new policy introduced new project size ranges which were less than 10 kW and more than 10 kW. Wind power projects were not limited to 10 MW in the GEGEA program **[1]**. The price paid to projects under the GEGEA program were however, far greater than what was offered by the RESOP program. The prices were determined based on the cost of producing electricity from a type of generator under the assumption that the project had internal rate of return between 10-12% **[1]**.

Table 1.1 compares the price offered in the RESOP and GEGEA programs.

Table 1.1: Incentive Structure for Renewable Generators

Types of Generators	**RESOP (2006, ¢ per kWh)**	**GEGEA (2009, ¢ per kWh)**
Wind (No Size Limitation)	11	13.5
Solar ≤ 10 kW	42	80.2
Rooftop Solar (between 10 – 250 kW)	42	71.3
Rooftop Solar (between 250 – 500 kW)	42	63.5
Rooftop Solar (>500 kW)	42	53.9
Ground Solar (between 10 kW – 10 MW)	42	44.3
Hydroelectric generator (≤50 MW)	11	12.2-13.1
Bioenergy	11	10.3-19.5

The setting of such high prices led to a large number of applicants filing for project approval in Ontario. According to Stokes, there were 50,000 applicants for projects ≤ 10 kW **[1]**.

1.2.2 The transformation of electricity generation and demand in Ontario

Following the passing of the GEGEA (2009), the province had added 3570.3 MW of wind and 370 MW of solar farms that were directly connected to the grid through transmission lines at the end of 2017 **[2]**. In the period between 2009 and 2018, the net increase in transmission connected generation capacity has been approximately 3756.3 MW **[2]**. As of March 2018, Ontario has 36,946 MW of transmission connected generation capacity. Nuclear, gas/oil fired, and hydroelectric power plants individually contribute to 35%, 28%, and 23% of the generation capacity. Wind, solar and biofuel individually contribute 12%, 1% and 1%, respectively **[3]**.

At the end of 2017, the province also had an additional 3934.7 MW (634 MW of which is under development) of contracted generation assets connected to the distribution power lines **[4]**.

Figure 1.1 shows the generation output by fuel type for 2017.

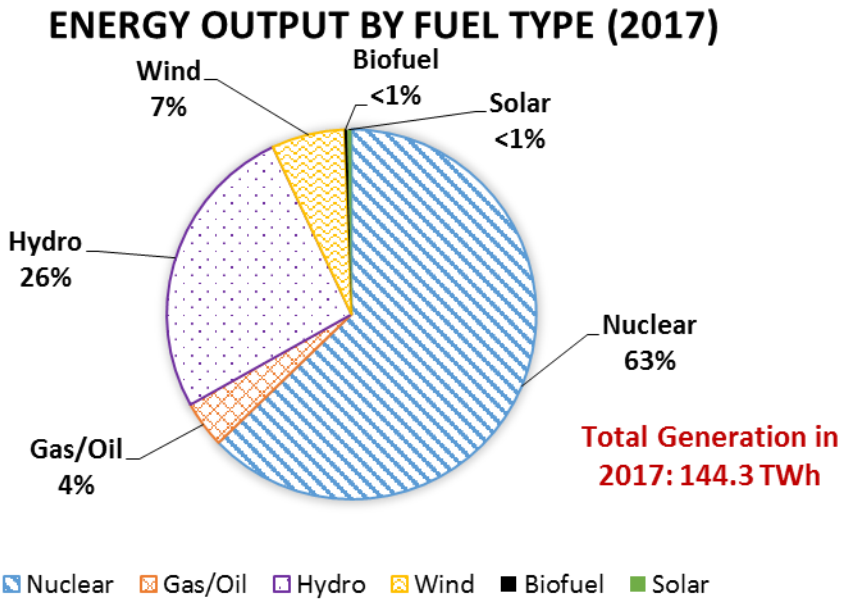

Figure 1.1: Percentage energy output by generator type in 2017 **[2]**

Based on data provided by the Independent Electricity System Operator (IESO), Ontario produced 144.3 TWh of energy in 2017. More than 60% of the electricity produced annually was supplied by the provinces nuclear power plants. They are followed by the hydroelectric power plants which have a share of 26% in the annual production. Power generated by wind farms has increased from 3% in 2012 to 7% in 2017.

However, Ontario's electricity demand has seen a net decrease of 9.75% between end of 2007 to the end of 2016 **[5]**. The 18 month outlook (IESO) released in September of 2017 highlights that the share of electricity demand met by the transmission connected grid since 2009 has remained fairly constant **[6]**. The IESO highlights three primary reasons that have helped in offsetting the energy demand met by the power grid. These include: 1) Industrial conservation initiatives; 2) Shifting of demand by employing the time of use rates for residential end users, and 3) Growing capacity of distributed connected generation units. Despite the subsequent increase in demand with the increase in population, the above three factors have offset a net increase in provincial power demand.

The on-peak and off-peak hours in Ontario during the summer season are 11 AM – 5 PM, and 7 PM – 7 AM, respectively. During the winter season, the on-peak hours are 7 AM – 11 AM and 5 PM – 7 PM. The off-peak hours during the winter season are 7 PM – 7 AM. Ontario's average hourly energy demand during on-peak hours in 2017 was 16,412 MWh. The average hourly off-peak electricity demand was 14,417 MWh **[5]**.

1.2.3 Issues within Ontario's power sector

The transition to cleaner energy technologies will come at a cost, but these costs have generally shown a trend to drop over time with innovation and further research into these technologies. Despite this fact, Stokes **[1]** raises a key point highlighting the impact that rate of adoption of new renewable energy projects have on customer electricity charges. Over time the province of Ontario has restructured its planning and incentive pricing structure. As of 2016, the highest cost bracket for rooftop solar installations (< 6 kW) is ¢31.3 per kWh. This is a significant decrease from ¢80.2 per kWh initially set by the GEGEA program **[7]**. The province in 2016 also cancelled the procurement of large renewable projects (>500 kW) **[8]**. Despite these measures, there is a case for the government to have potentially revaluated their plan at an earlier time point during this transition.

The sheer number of applicants to the GEGEA program, and the high number approved renewable energy projects has contributed to an increase in cost to rate paying customers. Stokes cites the Auditor General of Ontario while highlighting a 25% increase in electricity bills within Ontario in 2014 compared to 2009 levels **[1]**. Another factor influencing the increase in electricity bills is the $12.8 billion refurbishment of the aging Darlington nuclear power plant.

An additional issue that the province is trying to combat on top of growing electricity charges to customers is managing periods of surplus baseload generation. Surplus baseload generation occurs when the total hourly electricity produced by the wind, nuclear, and hydroelectric generators exceeds Ontario's electricity demand **[9]**.

The issue of surplus generation is created as a result of the intermittency of wind generators, and the inflexibility of nuclear generation assets to drastically maneuver their output. The degree to which wind power output can vary in a day is significant. In the morning when the load on the grid tends to be on the higher side, output from the wind farms can drop by 15% every hour with respect to its rated output **[10]**. The exact opposite of this trend is observed in the night which is the period when wind farms produce most of their power while load on the grid remains very low. Thus the wind power generated during the night only adds to the surplus baseload already being produced by nuclear and hydroelectric power plants. On a seasonal scale, winter, spring and autumn observe some of the highest wind power outputs in Ontario. Whereas, the summer season is considered to have the lowest wind power generation.

In 2017, the IESO exported approximately 7.3 TWh of surplus electricity. This adds up to almost 5.54% of the province's annual energy demand and equivalent to meeting the electricity demand of 9.8 million homes (based on 2014 data developed by Ontario energy board for average household electricity consumption within the province: 743 kWh **[11]**).

The average hourly Ontario electricity price during the hours of surplus baseload generation was ¢0.7 per kWh in 2017. However, generators in Ontario are paid a contracted price for the energy they produce. Therefore the difference in market price and the contracted price is recovered via a global adjustment fee **[12]** to Ontario electricity users. According to the auditor general, from 2006 to 2014, electricity consumers in Ontario have paid $37 billion in global adjustment. The projected cost of global adjustment payments for the period of 2015 to 2032 is $133 billion **[13]**.

An analysis of surplus baseload generation projections from the environmental commissioner of Ontario **[14]** shows that surplus generation will decrease from 6% of net demand in 2017 to 2% of net demand in 2032. The auditor general's 2015 report highlights surplus baseload generation values close to 4.1 TWh in 2032 **[13]**.

1.2.4 Measures taken to address issues within the power sector

Measures to decrease electricity cost to rate payer: In order to counter the rising electricity bills to ratepayers, the provincial government introduced the 'Ontario Clean Energy Benefit' program in 2010 to reduce the burden on electricity customers by offering a 10% reduction on their electricity bills **[1]**. This strategy has been an expensive way to counteract the rising electricity bills and according to Stokes, it has costed the provincial government $5 billion over 5 years of offering a 10% reduction to electricity bills within the province (2011-2015) **[1]**.

Surplus Baseload Generation Management: The IESO manages surplus baseload generation by: 1) maneuvering or shutting down nuclear power plants; 2) Curtailing generation from wind farms, and 3) exporting power to neighboring electricity markets at a low price.

Ideally, the repurposing of surplus electricity within the province will enable the province to benefit from this low emission energy source. The repurposing of this electricity is possible through either devices or energy technologies that store electricity or convert electricity into another energy vector for utilization in a different energy sector.

The Beck-pumping station has provided 170 MW of storage capacity for 60 years in Ontario. The pumped-storage hydroelectric generating facility located in Niagara, is able to pump water back to its upper reservoir by utilizing surplus electricity.

Through the energy storage procurement framework, the IESO has approved projects that will bring along a rated capacity of 50 MW to the power grid. At the beginning of this program in 2012 (phase 1), the IESO contracted projects with a total capacity of 6 MW to provide grid regulation service in the form of frequency regulation (balancing mismatch between supply and demand on a second to second basis), voltage control **[15]**. The technologies in focus during the first phase of procurement include batteries (4 MW by Renewable Energy Systems Canada), and flywheels (2 MW by NRStor). The phase 1 of energy storage procurement later also included contracts equivalent to 33.54 MW of capacity. The technologies in this case also included batteries,

flywheels and hydrogen energy storage in combination with a fuel cell power module, and thermal energy storage.

In phase 2 of the energy storage procurement program, the IESO contracted projects totaling 16.75 MW of capacity. Phase 2 included technologies such as solid-state and flow batteries (Total Capacity: 15 MW) and also compressed air energy storage (Total Capacity: 1.75 MW) **[16]**. Each energy storage project will be able to provide energy storage over a 4 hour period. The unit size of the battery projects do not exceed above the 2 MW nameplate capacity **[16]**. The compressed air energy storage technology (NRStor Inc.) will provide 7 MWh of energy storage capacity (1.75 MW nameplate capacity).

The province of Ontario has also prioritized the electrification of the transportation sector to utilize clean surplus electricity from the power grid in its '*Climate Change Action Plan*' **[17]**. In Ontario, the provincial government has introduced the electric vehicle incentive program (EVIP) **[18]** to incentivize the adoption of electric vehicles. Electric vehicles can be categorized under energy conversion technologies that repurpose the use of clean electricity within the transportation sector. At the end of 2016, there were 9178 registered electric vehicles on Ontario's roads [**19**].

The average value of excess electricity when there was surplus baseload generation was 1184.14 MWh in 2017 (Maximum: 3260 MWh, and Minimum: 1 MWh). The deployment of electric vehicles although important, will still require time as public acceptance over its widespread use grows. In terms of bulk energy storage battery technologies, and compressed air energy storage systems are beneficial for short term energy storage. Walker et al. present a comprehensive analysis of the duration over which different energy storage technologies can store electricity [**20**]. Technologies such as Na-S and lead acid batteries which are commercially available can have power ratings of 50 MW and can store energy for 4 – 6 hours. Other battery chemistry concepts such as Zn/Br, Zn – air , Fe/Cr, and Vanadium are still either at demonstration stages or in the research and development phase. Compressed air energy storage systems in comparison to batteries can store energy for a longer period (8 – 20 hours). However, at times this technology requires the compressed air to be cooled down for storage. Therefore when the compressed air is required to generate power, it needs heat generated from natural gas turbines to heat the air up before it is expanded to generate electricity. Although the amount of natural gas used to heat up

the air might be low, this concept still adds emissions to energy that was initially clean before being stored in the form of compressed air.

As mentioned earlier, the province already employs the use of pumped hydro storage for long term energy storage, however, building new facilities to store Ontario's surplus electricity is not a practical option considering the time taken to build them.

Among the energy storage and energy conversion technologies mentioned above, the scope of hydrogen as an energy vector has not be explored to its full potential. The 2 MW hydrogen energy storage project procured through the IESO's energy storage procurement program explores only one of its potential i.e. its ability to provide frequency regulation.

As suggested by many researchers **[21,22,23,24,25]**, hydrogen produced via the water electrolysis process from clean electricity could provide a variety of services. These services include ancillary services, energy storage, energy arbitrage, provision of industrial hydrogen, and interlinking the power grid to the transportation and natural gas sector to form an integrated energy system.

This strategy, known as power to gas for energy storage uses the produced hydrogen as an energy vector, meaning that the energy that can be both stored and transported. Despite the fact that the capital cost associated with storing and distributing hydrogen is currently high, the concept has potential within the province because of the possible use of the existing natural gas grid and underground gas storage infrastructure for storing and distributing the hydrogen gas produced. The following chapter gives a brief overview of hydrogen as an energy carrier in Canada, the scope of power to gas research in Ontario, its implementation on the global scale, and how Ontario's natural gas infrastructure can help in deploying power to gas within the province.

Chapter 2: Literature Review and Background

2.1 Literature Review: Hydrogen as a commodity in Canada

A 2006 report by Sustainable Development Technology Canada showed that Canada was the largest producer of hydrogen on a per capita basis (annual production: 3.4 Megatonnes) **[26]**. The market for hydrogen in Canada comprise of 4 categories, namely: 1) 'The captive industrial hydrogen market'; 2) 'The byproduct hydrogen market'; 3) 'The merchant hydrogen market', and 4) 'The non-conventional hydrogen system market'.

Categories 1 and 3 includes end uses such as heavy oil upgrading, refining of oil (hydro-treating), ammonia and methanol production, heat treating of metals, glass manufacturing, hydrogenation of food oils etc. These accounted for almost 84% of hydrogen end use in 2005 **[26]** with the major share going to oil refining and heavy oil upgrading (52%). The byproduct hydrogen market is the hydrogen produced in chemical industries such as the chlor-alkali-chlorate processes (15% of total market share). The last category (non-conventional market) involves the use of hydrogen for energy applications such as fuel cells, forklifts etc. (1% of market share).

2.1.1 Current hydrogen production scenario

Most of the hydrogen produced globally, comes from fossil fuel sources like natural gas, coal, or petroleum. A 2008 data of hydrogen production in Canada shows that nearly 3 mega tons of hydrogen was produced that year with 70% of it being produced using the steam methane reforming (SMR) process **[22]**.

Despite the existence of various other technologies (e.g., electrolysis, fermented hydrogen production, renewable powered water splitting etc.), SMR is still the most widely used method due to the high availability and low prices of natural gas. This also makes it the most economical way of producing hydrogen (~$1.75-1.99 per kg of H_2) **[26]**. The process involves a series of reactions between water and methane in the presence of an external heat source. According to Bartels et al. **[27]**, the fuel is initially mixed with steam and oxygen in a reformer to produce a reaction product called syn-gas which is a combination of CO, CO_2, H_2, CH_4, and water. As the reaction with the

reformer progresses, the hydrocarbon bonds present in methane break to produce hydrogen. The process uses excess amounts of water in order to avoid coking from taking place and thus increasing the hydrogen yield. After the completion of the reactions, the end product obtained is a gas mixture comprising of hydrogen and oxides of carbon. The hydrogen is separated from the mixture with the help of a pressure swing adsorption (PSA) unit.

2.1.2 Hydrogen and integrated energy systems: Canadian Outlook

As mentioned earlier at the end of section 1.2.4, the opportunity for hydrogen to be utilized as an energy vector in 'non-conventional markets' is possible in regions which have: 1) An interest in zero-emission vehicles (Fuel Cell Electric Vehicles (Transit and Personal), forklifts); 2) An established natural gas network for storing and distributing the gas, and most importantly 3) A clean power grid.

Some of the well-known projects that existed within the non-conventional market in Canada include the Whistler fuel cell electric bus trial that used 20 such buses in the 2010 Olympics in British Columbia (ending in March 2014) [**28,29**]. The hydrogen village project that operated in the greater Toronto area between April 2004 to March 2008, incorporated the use of a wind turbine (750 kW) coupled with fuel cell modules to provide services such as powering an eco-condominium, refueling for a Purolator delivery van, and provide heat and power for 12 student house units at University of Toronto's Mississauga campus [**30,31**]. However, to sustain and grow such projects, timely investment and support from government is important. The fuel cell electric bus project in Whistler, British Columbia stopped because of the inability of transit operators to maintain and procure new fleets to expand on the initial project. Another issue for its closure was the unavailability of a robust hydrogen fuel supply chain **[29]**.

The support for hydrogen as an alternative energy vector will come with the development of coordinated policy initiatives on federal and provincial levels. In the past few years, the federal government has allocated funds to projects for supporting the developing of infrastructure of alternative fuels (Pan Canadian Framework on Clean Growth and Climate Change **[32]**) in the 2016 budget outlook. Support for clean technology projects also have come through the Sustainable Development Technology Canada's (SDTC) 'SD Tech Fund' **[32]**.

Some examples of federally coordinated projects include the $1.65 million of monetary contribution to Hydrogenics and Enbridge to develop two hydrogen refueling stations in the greater Toronto area (Mississauga and Markham) in Ontario **[31]**. A total of $160 million will be available for supporting clean alternative refueling and charging infrastructure **[31]**.

Provincially supported projects in Ontario include the feasibility analysis of using hydrogen in the GO rail transit network **[28]**. Hydrogen as a fuel source in trial project for class 8 zero emission vehicles is also being explored in Ontario. The project is being coordinated between Next Hydrogen, Ballard Power Systems and FVT Research Inc. and looks at testing a heavy duty fleet powered by hydrogen to make a 380 km round trip test in Timmins, Ontario **[33]**. The government of Quebec has planned for the acquisition and testing a fleet of 50 fuel cell electric vehicles provided by Toyota in 2018 (Toyota Mirai) **[28]**. The province of British Columbia will receive $4.3 million in spending money from the federal government to support deployment of fuel cell vehicle refueling and electric charging stations. The government of British Columbia supports buyers of hydrogen powered vehicles with a rebate of $6000 on the retail price of the vehicle **[34]**. The province of Alberta initiated a $300 million project (with Air Products, in July of 2016) that produces hydrogen for use in refineries near the Strathcona county. The hydrogen will be produced via the steam methane reforming process and will be transported via a 50 km pipeline. Daily production capacity of the project will be 4.2 million m^3 **[31]**.

The IPHE summarizes that active hydrogen projects in Canada have primarily focused on the transportation sector. The country as of April, 2017 had 20 fuel cell vehicles (which were primarily refueled in privately owned refueling stations), and approximately 400 forklifts powered with hydrogen. All over Canada there were 9 hydrogen refueling stations in total with 3 of them being owned under private-public partnerships, 1 within an academic research institution and 5 deployed on a commercial scale. In terms of stationary application of hydrogen, there is currently only one project under development (5 kW – 400 kW) within Ontario with details of the project still not clear **[31]**. Projects concerning renewable energy storage project currently under development include a 5 MW power to gas project by Enbridge and Hydrogenics in Ontario. There is an existing power to gas project that produces 300 kg of hydrogen for a mine in Quebec (200 kW) **[31]**.

2.1.3 Scope of hydrogen in Ontario

Few of the major steps taken by the province's government to reduce emission include: 1) Ontario's transition to a clean electricity system (as mentioned in Chapter 1); 2) Procurement of energy storage projects; 3) Starting of the cap and trade carbon pricing program in 2017 **[35]** 4) The updating of the provincial electric vehicle incentive program to electric and hydrogen vehicle incentive program (as of March, 9 , 2018) **[36]**; 5) Investment in hydrogen refueling stations and assessing the potential use of hydrogen in transit networks, and 6) Its goal towards investing in order to increase renewable content in its natural gas pipeline **[37]** (5% renewable content by 2025, and 10% by 2030 on a national level **[38]**).

The above mentioned steps provide an opportunity to assess how power to gas energy hubs can utilize the province's energy policy decisions to 1) Act as smart loads providing ancillary services to the power grid, and 2) Produce hydrogen and renewable natural gas as a commodity for the province's transportation sector and natural gas end users (Residential and Commercial Users).

The following section (section 2.2) introduces the power to gas concept and gives a brief overview of how these hubs can interconnect with different energy networks. Section 2.2 also presents a review on the existing projects and research work that has been carried out in relation to power to gas in the scientific literature.

2.2 Background: Power to Gas Concept

Figure 2.1 below gives a general overview of the interconnections between a power to gas system and different energy sectors. The figure is broken down into 5 categories, namely: 1) Supply; 2) Conversion; 3) Transmission and Storage; 4) Distribution, and 5) Conversion at End Users.

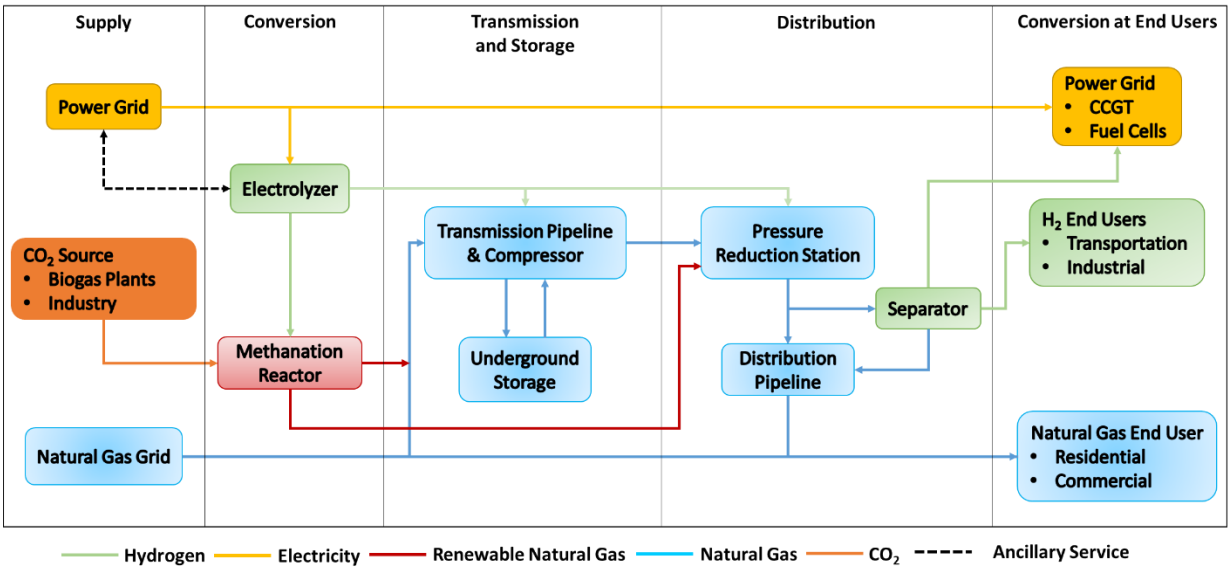

Figure 2.1: Interconnections between power to gas energy hub and other energy sectors

The first interlink is the connection between the electrolyzer and the power grid. This link will primarily occur at a substation where the electrolyzer derives energy from the grid to produce hydrogen. The hydrogen produced can then be compressed and injected within high pressure natural gas transmission pipelines to form hydrogen enriched natural gas. Renewable natural gas is another fuel that could be injected in to the transmission lines once the hydrogen produced is combined with CO_2 gas sourced either from industrial sites equipped with carbon capture and storage technology or biogas producing plants. This interlink connects the energy hubs producing hydrogen and renewable natural gas to the transmission level natural gas grid (under the transmission and storage category).

The transmission lines are primarily made out of steel (4-48 inch diameter) and operate within a pressure range of 600-1200 psig (42-84 bar) **[39]**. These pipelines can move hydrogen enriched natural gas and renewable natural gas molecules to underground storage reservoirs (depleted oil/gas fields, salt caverns or aquifers) for seasonal storage. This allows large quantities of excess electricity to be stored within the existing natural gas infrastructure. The hydrogen and renewable

natural gas can later be withdrawn from the underground storage to meet peaks in heat (residential and commercial end user via boilers and combined heat power units, see figure 2.1) and electricity demand (via combined cycle gas turbines, see figure 2.1).

The natural gas transmission pipelines can also direct hydrogen and renewable natural gas molecules to pressure reduction stations (under the *Distribution* category in figure 2.1) where the flow of gas undergoes a pressure reduction. Pressure reduction stations are also known as transmission-to-distribution transfer (or gate) stations **[39]** where the higher pressure transmission lines exchange gas with the lower pressure distribution lines.

Energy hubs producing hydrogen and renewable natural gas can also be co-located at pressure reduction stations. This way both hydrogen and renewable natural gas is injected into the distribution lines as shown in figure 2.1. This category of pipelines include distribution mains and service lines which help in distributing gas among the various conventional natural gas end users for space heating and commercial applications.

The structural material used for distribution lines include both polyethylene (PE) and steel. The mains and the service line have a diameter ranging between 0.5-8 in. and operate in a pressure range of 0.25-60 psig (1.03-5.15 bar). There also exist some distribution pipelines that may be operated at pressure levels as high as 400 psig (29 bar). Therefore gas flowing in higher pressure distribution pipelines at times will need to undergo a secondary pressure reduction cycle at a downstream location closer to the end user. Melaina et al. show that the pressure differential (29 bar to 1 bar) created at the secondary pressure reduction is suitable for pressure swing adsorption (PSA) units to separate the hydrogen mixed in natural gas **[40]**. The separated hydrogen can then be directed to end users such as hydrogen refueling stations, or industrial end users (e.g.: oil refineries, or chemical industries). Note, that this is a benefit of the power to gas concept to move large quantities of hydrogen through the natural gas system.

Therefore the energy recovery pathways of the power to gas concept highlighted in the above paragraphs include:

- Power to hydrogen: Here pure hydrogen is used at end users such as fuel cell vehicles and fuel cell power modules. Pure hydrogen can also find use in the industrial sector as a chemical compound for oil refining and heat treating of metals.

- Power to renewable natural gas and hydrogen enriched natural gas: Hydrogen produced by grid powered electrolysis can be utilized in the natural gas sector by blending it with natural gas or producing renewable natural gas (for space heating and electricity generation).
- Ancillary Service: The electrolyzer can act as a smart load to the power grid and respond to directions given by the grid operator to manage its operating level to help balance mismatches in supply and demand of electricity. Section 2.2.6 covers more details on the potential ancillary services that electrolyzers can provide.

2.2.1 Future hydrogen production methods: Electrolyzers

Electrolyzers are devices that harness the energy of the electric (DC) current supplied to them to produce hydrogen and oxygen by splitting water. Given an electricity grid which has 96% of its power coming from low emission generation sources like nuclear, wind and hydroelectric power plants in Ontario (see section 1.2.2), grid powered elecrolyzers hold an advantage over traditional SMR and coal based techniques to produce hydrogen. Therefore, they are considered to be one of the technologies that have the potential to mass produce the gas in the future.

There currently exists three types of electrolyzer technology **[22]**:

- Alkaline electrolyzers;
- Polymer Electrolyte Membrane (PEM) electrolyzers; and

The power to gas system proposes to produce electrolytic hydrogen using the polymer electrolyte membrane electrolyzers and alkaline electrolyzers due to their commercial availability in the market.

Alkaline Electrolyzers: Electrolyzers classified under this category generally consist of a cell stack consisting of numerous electrodes (cathode and anode) either connected in series (bipolar orientation) or in parallel (monopolar orientation). Every cell has a platinum cathode and a nickel or copper metal oxide anode along with an alkaline solution containing 30 wt% of either Potassium hydroxide or Sodium hydroxide used as the electrolyte.

Most of the alkaline electrolyzers generally tend to have a bipolar design (cells linked in series) as it makes them more compact when compared to the monopolar design. The compact arrangement allows the electrolyzer to have shorter current paths in the wires and the electrodes **[41]**. Thereby,

reducing the ohmic resistance offered by the electrolyte and increasing the overall efficiency of the electrolysis process.

Figure 2.2 shows a layout of a monopolar alkaline electrolyzer.

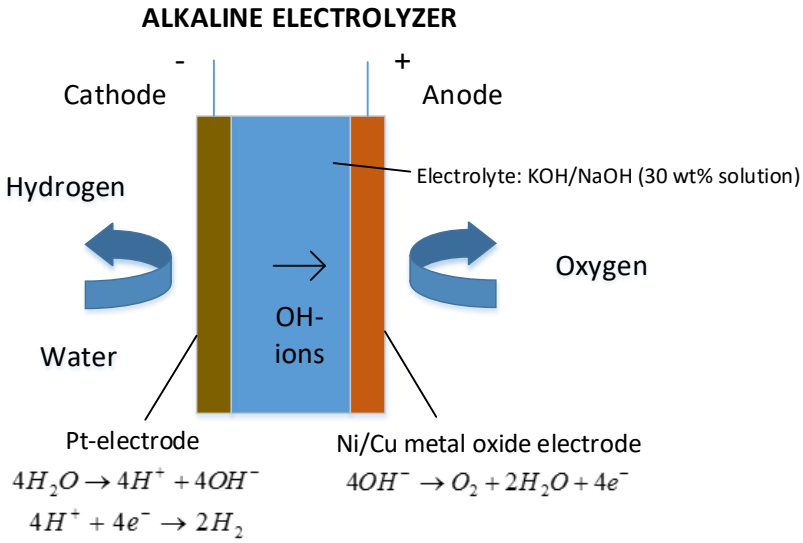

Figure 2.2: Alkaline electrolyzer cell layout

Water supplied to the electrolyzer is split into H^+ ions and OH^- ions at the cathode-electrolyte interface. The OH^- ions produced from the reaction, travels through the electrolyte towards the anode where it gets oxidized by giving off electrons and produces oxygen. The electrons produced at the anode travel to the cathode via an external circuit where they reduce H^+ ions to produce hydrogen.

Other than the components that make up the electrolyzer cell stack, there also exists auxiliary components like:

- Voltage regulator for controlling the power supply coming into the electrolyzer;
- Water supply system which includes the circulation pump, piping, and connections;
- Gas separators: The hydrogen and oxygen produced are separated from the electrolyte with the help of a microporous separator. Only Alkaline electrolyzers tend to have these because of the use of electrolyte in it; and,
- Heat exchangers (HE): HEs are used to remove any remaining moisture in hydrogen.

Polymer Electrolyte Membrane (PEM) Electrolyzers: PEM electrolyzers have electrodes made up of noble metal catalysts, typically platinum. In place of an electrolyte, the technology uses a Nafion (perfluorosulfonic acid polymer) membrane (Figure 2.3).

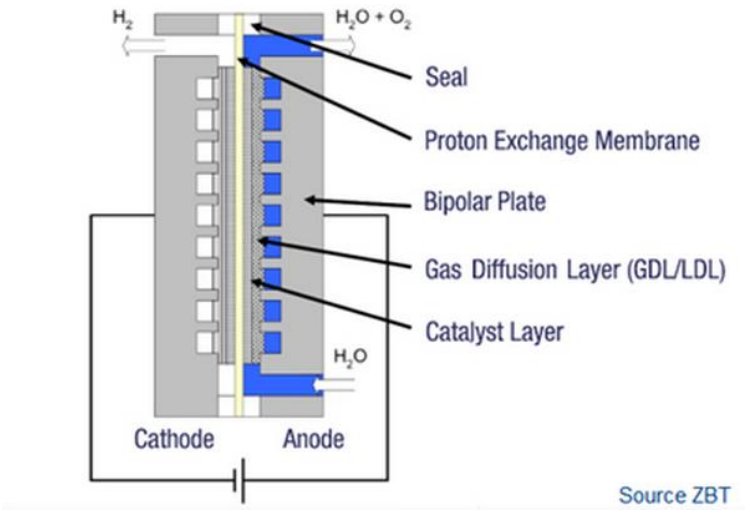

Figure 2.3: Polymer electrolyte membrane electrolyzer setup **[42]**

Water supplied to the electrolyzer is split at the anode into Oxygen, H^+ (protons) ions and electrons. While the electrons travel through the external circuit, the protons travel to the cathode through the acidic polymeric membrane. Upon reaching the cathode they combine with the electrons in a reduction reaction to form hydrogen. The electrochemical reactions that take place in the PEM electrolyzer are:

$$\text{Anode: } H_2O \rightarrow {}^1/_2\ O_2 + 2H^+ + 2e^- \tag{2.1}$$

$$\text{Cathode: } 2H^+ + 2e^- \rightarrow H_2 \tag{2.2}$$

The main purpose of the membrane is to help in separating the hydrogen from oxygen as only the protons are able to travel across it and thus rendering the use of an additional gas separation unit unnecessary. However, the hydrogen produced may have moisture content due to the transport of water across the membrane as a result of both an electro-osmotic drag and concentration gradient induced diffusion. Therefore, the use of heat exchangers to dehumidify the hydrogen gas may be necessary. PEM electrotylsis has been prototyped and is near commercialization.

Table 2.1: Comparison of electrolyzer technologies [22, 43, 44, 45]

Parameters	Alkaline Electrolyzer	PEM Electrolyzer
Operating cell pressure	<30	30-100 bar
Operating cell temperature	60-80°C	50-80°C
Lower operating limit	20-40%	5-10%

Efficiency	62-67%	67-78%
Replacement Period	~9 years	~3-7 years
Ramping Rate (% of maximum load per second)	~10-90% per second	~10-100% per second

Table 2.1 above gives a comparison of the operating characteristics of alkaline and PEM electrolyzers that are currently commercially available in the market. From the table it can be clearly seen that PEM electrolyzers have more rigorous operating conditions and can operate at load lower loads. When compared to the commercially available alkaline electrolyzers, PEM electrolyzers have the following advantages **[46]** over alkaline technology:

- More durability;
- More flexible in design and modularity;
- More flexibility and more rapid response;
- A higher efficiency;
- Compact mass-volume characteristic;

Some of the disadvantages of the technology is the high cost of the polymer membrane, the porous electrodes (Pt, Ir, Ru) and the current collectors **[50]**. Despite this disadvantage, the operational characteristic benefit justifies their use within the power to gas concept.

2.2.2 Utilizing Ontario's natural gas grid and underground storage (UGS) infrastructure for hydrogen storage and distribution

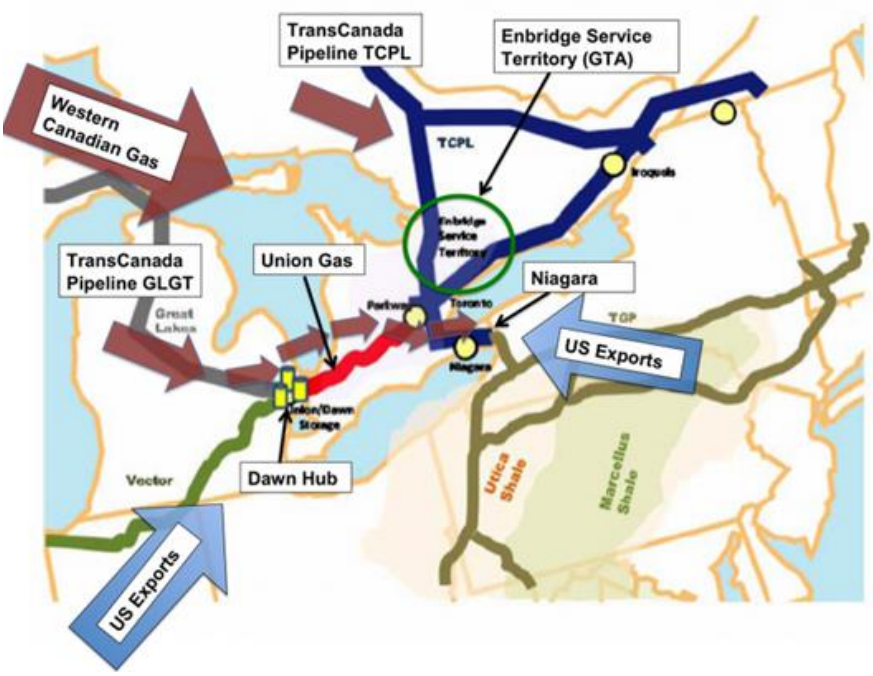

Figure 2.4: Overview of natural gas system in Ontario

Ontario's natural gas market is one of the largest in Canada, accounting for almost 40% of country's total natural gas consumption **[47]**.The daily natural gas demand of Ontario is estimated to be near 2.8 billion cubic feet (bcf) with 57% of it being consumed for residential and commercial use, 26% by the industrial sector and 17% for electricity generation **[48]**. Although Ontario has a large natural gas market, more than 95% of the supply comes from western Canada **[49]**. The major pipelines that bring natural gas into Ontario are the TransCanada pipeline (TCPL) **[50]**, which transports 4.1 bcf per day if not more **[22,47]**. The Dawn hub brings gas from the US into Ontario. The hub consists of pipelines owned by Enbridge and Union Gas (owned by Enbridge). The biggest pipeline coming into the hub is the Vector Pipeline with a rated capacity of 1.3 bcf per day (figure 2.4) **[51]**. Other pipelines coming into Dawn hub include the Great Lakes Gas Transmission (GLGT) owned by TCPL Co. **[52]**. Ontario has 35 natural gas storage facilities with a capacity of 258 bcf. Most of these facilities are depleted reservoirs located in Lambton County, Sarnia, Ontario. Underground storage reservoirs play a key role in the natural gas and energy sectors in Ontario as almost 58 % of the natural gas consumed during the winter comes from reservoirs **[53]**. The yearly consumption scale in Ontario shows that almost 25% of the gas consumed annually is

also supplied by the reservoirs, which have a capacity to store up to 80 TWH or 55% of Ontario's electrical energy demand **[51, 54]**.

From a suppliers point of view, the storage size and transportation mode of hydrogen they choose depends on the size of the market they are competing in, the distance of the end-user from the production point, and finally the method used to produce hydrogen itself **[55]**. Some of the most common methods of hydrogen transport on a global scale include railroad, tanker ship, and tube trailers. The use of pipeline systems on the other hand has not been that prominent. The first hydrogen transmission pipeline which was made in the Rhein-Ruhr area of Germany, dates back to 1938. Since then approximately 1600 km of hydrogen pipelines have been built in Europe **[39].** The US has approximately 2560 km of steel based hydrogen pipelines **[56]**.

Based on the work done by Parker **[57]**, the cost associated with laying down pipelines for commodities like natural gas, oil, and other petroleum products is influenced by the following factors:

- *Geographical location*: Building a pipeline along a topography which is not easily alterable or accessible can increase construction costs by almost 5 times in comparison to laying down a pipeline of similar length in a densely populated area.
- *Cost associated with material of construction*: On an average, this factor accounts to up to 26% of the total costs.
- *Labor and right of way*: The portion contributed by labor costs for constructing the pipelines is close to 45%. The right of way accounts for almost 22% of the total costs and primarily includes the legal bindings and contractual agreements associated with getting permissions to construct pipelines on either private or government owned lands or properties.
- *Miscellaneous costs*: According to Parker **[57],** the miscellaneous category includes the costs associated with "surveying, engineering, supervision, contingencies, allowances, overhead, and filing fees.

The contribution of the above factors except labor costs can be subject to variations based on the diameter of the pipeline being installed **[57]**. Due to the lack of any existing set industrial standards for installing hydrogen pipelines, the cost associated with their construction can be even higher. As mentioned above that the different factors contributing to the total construction cost of pipelines are primarily dependent on their diameter, the cost of a hydrogen pipeline can be 50-80% higher

than natural gas pipelines **[55,57]**. Therefore, Tabkhi et al. **[55]** mentions that when the hydrogen has a big market, the utilization of the existing pipeline network proves to be an economically feasible option to move electrolytic hydrogen through the long transmission pipelines.

2.2.3 Safeguards associated with using natural gas pipeline infrastructure

Several researchers have tried to assess the conditions under which hydrogen can be injected within the natural gas grid **[40,58,59,60,61]** with tolerable repercussions on safety, material lifetime, and durability of the existing components in the natural gas network including the end user appliances of natural gas.

The operating conditions of a natural gas grid might have to be altered when hydrogen is added to it due to safety reasons related to the differences in the chemical and physical properties between the two gases. When compared to hydrogen, methane (or natural gas) is ~8 times heavier and has higher viscosity, density, energy content per unit volume and is more soluble in water. Hydrogen on the other hand is known to have a higher heat capacity, energy content per unit mass, diffusibility, maximum flame temperature, auto-ignition temperature and also wider explosive and firing ranges **[61]**.

According to Haeseldocx **[60]**, under normal conditions the higher heating values of hydrogen and natural gas are 13 MJ Nm^{-3} and 40 MJ Nm^{-3}, respectively. Therefore it can be clearly seen that to satisfy the same amount of energy demand, almost three times the volume of hydrogen needs to be transported through the pipeline. Thus the amount of gas that the compressor needs to compress increases, which indirectly increases its operating power consumption.

Despite the fact that the electrolyzers that are commercially available in the market nowadays produce hydrogen at high pressures ranging from 16-30 bars, the gas needs to be compressed before being injected into the pipeline because big transmission pipelines are known to have higher operating pressures that can range from 41-83 bars. Therefore, hydrogen is normally compressed to a pressure slightly higher than the pipeline pressure just as a safeguard to avoid backflow of the gas from the injection point. Once the hydrogen enters the system, its pressure drops to the line pressure which in turn increases its volume and temperature. In general when a gas expands, its

temperature drops but for the case of hydrogen the exact opposite is seen. This phenomena is primarily attributable to the Joule-Thomson effect and the low inversion temperature of hydrogen (202 K). The term inversion temperature ($T_{inversion}$) is defined as the critical temperature below which a real gas that is expanding at constant enthalpy experiences a drop in its temperature and above which it experiences an increase in temperature. As most of the pipelines systems operate well above 202 K, the temperature of hydrogen is seen to increase with the drop in its pressure. Work done by Von der Grün et al. **[61]** shows that at a maximum hydrogen concentration level of 5 vol.% within the pipeline system will not create a temperature rise of greater than 5 K. Haeseldockx **[60]** mentions that upon throttling from 80 bar to 15 bar its temperature only increases by just 2°C.

Another important parameter that needs to be discussed is the admissible levels of hydrogen within the natural gas pipeline. Lines that are exposed to flows with high hydrogen concentration are prone to a phenomena termed as hydrogen embrittlement, where hydrogen breaks into H atoms and diffuses into the small voids existing within the steel pipelines where they again form molecular hydrogen gas. As time goes by, the pressure builds up within these voids creating fractures that affect the ductility and reduce the strength of the pipeline material. Hydrogen attack **[39]** is another phenomena observed in HENG transportation when the gas temperature and pressure exceeds 200°C and 100 bars, causing H atoms to react with the carbon present in steel and thereby eroding it.

The cracks caused due to hydrogen embrittlement can lead to gas leaks, and since hydrogen has a higher leakage rate with respect to natural gas **[55]**, the flow losses across the pipelines needs to be kept under constant check. The leakage rates are also influenced by the pipeline material. According to Haeseldockx **[60]**, fibrous cement and cast iron pipelines are more prone to leaks in comparison to steel and polyethylene pipelines. Despite the higher leak rates for hydrogen, they also highlight the fact that the percentage of gas lost via leaks only amount to 0.0005-0.001% of the total volume transported over the course of a year **[22,60]**. “Cathodic charging” is one of the most common methods adopted to test the strength degradation of steel when subject to a hydrogen rich environment **[61]**. Strength tests (NaturalHy project) have shown that pipelines can carry 50% hydrogen in them without having significant reduction in material strength **[60]**. Various other studies say that only 17% hydrogen can be accommodated within the pipelines. There are

significant risks of leakage while using cast iron and cement pipelines, and therefore the use of polyethylene (PE) pipelines have been popular among distributors. PE pipelines also observe leakages but the amount of leakage is negligible when compared to the amount of hydrogen passed through them on a yearly basis **[60]**. Pipelines subjected to frequent fluctuations or pressure swings may be more prone to hydrogen embrittlement and therefore need to be tested properly before being used in order to avoid disasters. Melaina et al. **[40]** define a scale between 0 to 50 for categorizing the risk of a particular blend to catch fire in the pipeline. A value less than or equal to 10 means that the risk is minor, 30 means it is moderate and 50 means severe. So pipeline systems having hydrogen volumetric concentrations below 20% are categorized under the minor risk situation. The Power to Gas project proposes to produce a blend with less than or equal to 5 vol.% of hydrogen concentration within the pipeline which is well within the limits of safe injection.

2.2.4 Hydrogen storage systems

Hydrogen has conventionally been stored in both gaseous and liquid form. A lot depends on the end use application for the type of storage. Some of the different storage technologies that are currently being used for hydrogen storage are **[21]**:

- *Compressed storage in tanks*: This method is favored by most of the fuel cell vehicle (FCV) manufacturers because of a more reasonable storage cost when compared to liquefaction. Commercially available high pressure storage tanks under this category include tanks capable of storing 89 kg of hydrogen at 172 bar **[62]**. Higher pressure storage vessels include 420 bar and 875 bar vessels that store 21.7 kg of hydrogen **[62]**. These storage tanks are primarily used in fuel cell vehicle refueling stations. The cost of compressing hydrogen and high storage tank material cost (e.g.: carbon fiber) are currently factors that requires further reduction in price.
- *Liquefied Hydrogen*: One of the advantages of storing hydrogen in liquid form is that it has a higher energy content and density even at lower pressures. This allows storage units to be lighter and more compact. Its only drawback is that the liquefying process increases the power demand by 30 % **[21]**. Therefore liquid hydrogen costs 4-5 times more than compressed hydrogen gas. This kind of technology is more suitable for delivery over long distances if pipeline transport of hydrogen is not an option **[56]**.

- *Solid Hydride*: Hydrogen can also be stored in the form of metal hydrides by combining it with Magnesium based alloys, Carbon based compounds, and Boron compounds. Here hydrogen can be bonded to the metal compound at normal temperature and pressure, and when the demand arises it can be released from the hydride by either heating or increasing the pressure. Large scale deployment of such storage approach has not been seen yet.

The costs of these technologies (especially gaseous and liquid storage) are still high and will remain high unless market demand for the use of hydrogen in the transportation sector goes up. Economies of scale, reduction in material cost, development of recognized standards for tank sizes will enable hydrogen storage costs to lower in the future **[56]**.

A techno-economic review on the different hydrogen storage methods carried out by Taylor et al. **[63]** shows that large scale underground storage of hydrogen proves to be much more cost competitive when compared to liquid hydrogen and high pressure tube storage even after a significant amount of capital is invested in developing a cavern and installing the required auxiliary equipment for the functioning of the underground storage system. An economic assessment of cavern and depleted gas/oil field hydrogen storage shows that, cavern storage is more cost effective due to the high throughput of the storage unit. However, it should be noted that since the system is catered to store natural gas, further research on how storage of hydrogen enriched natural gas affects the capacity and the dynamics of the system needs to be carried out. The research in to this warranted as Ontario holds a vast underground capacity of depleted oil/gas field, enabling it to store 80 TWh of energy (see section 2.2.1). This storage capacity translates to approximately 55% of Ontario's annual electricity demand in 2017. Depleted oil and gas fields are naturally occurring formations below the surface of the Earth that previously contained either oil, or gas or both and served as a source of these fossil fuels. Gas in these storage utilities is cached in the storage volume existing within the fissures and porous rock formations located in the core of the reservoir. Other than the permeable rocks, these reservoirs have a cap rock at the top and a strata of impervious rocks on the sides that help in containing the accumulated gas within the boundaries of the reservoir. However, for the scope of this research the focus will remain primarily on gaseous hydrogen tank storage.

2.2.5 Demonstration projects and analytical research supporting power to gas

A review by Gahleitner **[64]** shows that there are a few Power to gas pilot plants located in Germany, most of which involve producing hydrogen electrolytically and storing the H_2 in hydrogen tanks; few of the plants also make use of natural gas pipelines and underground gas storage reservoirs to distribute and store the gas for longer periods of time. One such example, is the power to gas plant in Falkenhagen, Germany which began operation in 2013 **[65]**. The plant, developed by E-ON with technology partner Hydrogenics, is a 2 MW energy storage plant that uses surplus energy from renewable sources to produce hydrogen and injects it into a natural gas (NG) pipeline network. Under full operation the facility feeds approximately 360 Nm^3 per hour of hydrogen into the NG pipeline system.

The Audi e-gas project (6 MW nameplate capacity) is another such project that combines hydrogen produced via renewable energy with CO_2 procured from biogas plants to produce methane. This methane is then upgraded to a fuel standards appropriate for its use in Audi's compressed natural gas vehicles **[66]**. The application of power to gas in context of Germany is effective and is helping in the transition towards Germany's goal of meeting 50% of the energy demand by 2030 via renewable energy generation by linking its power system with the natural gas and transportation sector. This demonstrates the potential that power to gas energy systems hold particularly in the context of Ontario.

The unique advantage of Ontario for having natural gas pipeline infrastructure will also allow for easier development of power to gas systems in the province compared to other regions which don't have that infrastructure. As power to gas acts as an intermediate energy conversion technology that links the existing power and natural gas grids, its sizing is flexible. In other words, the size of a power to gas system can change/increase with the change in penetration of renewable generation sources over the years. While natural gas is considered as a transition fuel toward 100% renewable energy systems, hydrogen can aid in the reduction of emissions associated with natural gas combustion. The following concurrent research work have looked at the potential of power to gas energy hubs to address similar issues in the European context.

de Boer et al. **[67]** carry out a comparative analysis of the benefits of the integration of large scale energy storage systems like pumped hydro storage, compressed air energy system and power to gas energy hubs in an electricity grid with growing penetration of wind farms. In their rigorous analysis it is seen that the power to gas energy hub concept can be effective energy storage systems in countries which have existing natural gas systems that can act as a sink to store large amounts of surplus electricity. Walker et al. benchmark power to gas with respect to other existing energy storage technologies (in the context of Ontario) and highlight that the concept has a potential storage capacity that is orders of magnitude greater than competing technologies **[20]**. They also highlight the power to gas's ability to provide energy storage over a longer time period (weeks or seasonally). The hydrogen injected in to the natural gas grid can also find direct end use at natural gas end users.

Nastasi et al. **[68]** analyze the benefits of linking the power and natural gas grids by suggesting an effective way of utilizing intermittent power generated by renewable energy storage systems. In their work Nastasi et al. look at the 'greening' of the natural gas grid by injecting renewable hydrogen produced via electrolyzers into the natural gas distribution network. The hydrogen enriched natural gas blend produced, helps in offsetting CO_2 emissions at the natural gas end user and is seen as a more efficient way of using hydrogen in comparison to its storage and re-use at a later time point to produce electricity. The linking of the heating and the electricity network is a potential solution for easing the transition to a renewable energy economy and forming a seamlessly interlinked energy network or a 'smarter energy network'.

Collet et al. **[69]** carry out an environmental and techno-economic analysis on yet another potential energy recovery pathway of the power to gas energy hub concept where, hydrogen produced from both renewable and non-renewable energy sources is combined with CO_2 from biogas to produce bio-CH_4. The bio-CH_4 can then be injected in to the natural gas distribution network once it meets the specific standards set by natural gas utilities for it to be used by the end user. Maroufmashat et al. look at the feasibility of incorporating a Power to gas energy hub in an urban community and their analysis shows how different energy vectors including hydrogen can be exchanged between hubs, thus forming smart urban energy systems **[70]**.

Götz et al. and Rönsch et al. [**71**,**72**] show the potential of combining the hydrogen with carbon dioxide to produce renewable natural gas. Otto et al.'s **[73]** work also focusses on utilizing the

energy recovery pathways that produce hydrogen and methane and put them to use in the steel industry. The case study is based on the German steel industry and highlights the versatility and CO_2 emission reduction potential of using the power to gas concept to couple the industry with renewable energy generators. Garcia et al. **[74]** highlight the various energy recovery pathways of the power to gas concept. Jempa et al. **[75]** explore the potential of 'green gases' such as hydrogen and renewable natural gas produced via methanation in Europe. They address some of the policy challenges that these concepts might face in their implementation across Europe. Their work highlights the initial implementation will be slow and by 2030, green gases produced via the power to gas concept will represent a few percent of the EU wide gas volume in use.

2.2.6 Power to Gas system in ancillary services market

The ancillary service market can provide additional revenues for power to gas facilities with modern polymer electrolyte membrane (PEM) electrolyzers which can alter their load and output quickly in order to provide this service. To determine the appropriateness of electrolyzers for offering regulation and load following services, Eichman et al. **[76]** carried out ramping tests. The tests were carried out on a 40-kW alkaline and a 40-kW PEM electrolyzer. The results show that a polymer electrolyte membrane (PEM) electrolyzer takes less than ½ a second to complete almost all of a 25% ramp down from its maximum operating level to a lower operating level. Eichman et al's work also shows that it takes ½ a second for the PEM electrolyzer to complete a 75% ramp up from when the electrolyzer was turned off, and restarted again within a quick succession. The alkaline electrolyzer lagged the PEM electrolyzer significantly in the study and is thus less suitable for providing demand response services. The provision of high value ancillary services help to make the installation and operation of electrolysis technology more economical.

There are a number of disturbances that can lead to a disjoint between energy supply and demand **[77]**. To accommodate the disturbances and manage the grid, the Independent Electricity Systems Operator (IESO) purchases ancillary services from generators and consumers **[78,79,80,81,82]**. Ancillary services can be divided into operating reserves (OR) and demand response (DR), as shown in Table 2.2.

Table 2.2 Ancillary Services provided for IESO [81]

Type	Service	Procured from	Service Time
1. Operating Reserves	Supplementary energy for unforeseen circumstances	Dispatchable loads and generators	2 hours **[81]**
2. Demand Response			
a. Regulation **[82]**	Manipulation of consumption profile	End-users	Second-to-second
b. Load following **[77]**, **[83]**	Match fluctuations in demand and supply	Generators and loads can participate directly or as aggregated load **[84]**	5-minute to 1-hour

As can be seen from Table 2.2, the goal of the demand response program is to procure loads which react to signals to modify their energy use. One way to encourage a modification of energy use is to provide a price-based program **[83,84]**. This system mimics the nature of the Time of Use energy pricing for residential consumers in Ontario, and of the wholesale Hourly Ontario Energy Price (HOEP) for industrial and commercial consumers **[77,85]**. The eventual goal in Ontario is to have various demand response contractors bid through an auction to provide demand response services, as laid out by IESO's pre-auction report **[86,87]**.

Although there are costs from offering demand response services, such as lost business and inconvenience, end users offering the service may have reduced total electrical costs from the use of low cost off-peak power **[83,88,89]**. When a high amount of energy demand is shifted to off-peak periods, it becomes easier to utilize renewable energy and manage the province's baseload nuclear power and makes more efficient use of all generation assets. The benefits are not only limited to the customers, but also extends to the operator of the program. If the IESO purchases demand response services from multiple loads, it will reduce electricity prices and its own capital and operations costs **[90]**. The IESO hopes to reach a demand response capacity of 80 MW through a number of contracts for loads up to 35 MW **[82]**. Chapter 6 presents a study where a power to gas energy hub acts as a responsive load to provide demand response in the IESO regulated market.

Chapter 3: Optimization Approach and Energy Hub Component Models

3.1 Introduction

As mentioned earlier under section 1.1, this thesis proposes to optimally size and operate power to gas energy hub components in order to form a seamless integrated energy system interlinking the power grid in Ontario with the natural gas and transportation sectors. The optimal design of the power to gas energy hub and how it operates depends on the mathematical formulation of an optimization problem. As with any optimization problem, there is/are objective functions and a set of constraints that they are subject to. In this thesis three multi-period optimization problems have been formulated (Chapters 4, 6, and 7). The premise of the optimization problems lie in presenting how these formulations can be used to determine what is 1) The cost optimal way to reduce emissions via repurposing excess electricity from the power grid into the natural gas sector (Chapter 4); 2) Assess how optimization problems can be used to analyze the interaction of the power to gas energy hub components with key parameteric inputs (Chapters 6, and 7, e.g., electricity price, natural gas flow, hydrogen demand, ancillary service requirement etc.), and 3) Analyze the impact of uncertainty in parameters on energy hub planning and operation (Chapter 7).

3.2 Optimization Approach

This section will give a brief overview of the optimization approaches presented in chapters 4, 6 and 7.

Chapter 4 presents a mixed integer linear programming problem (MILP). An optimization problem is called an MILP when 1) The objective function, the equality and inequality constraints are linear, and 2) There exist mix of decision variables characterized as integer and continuous variables.

The optimization approach adopted in chapter 4 is the trade-off based ε-constraint approach. The trade-off exists between minimizing the objective function total capital and operating cost (Total Cost) of the power to gas energy hub and maximizing the annual emissions offset by the energy

hub in the natural gas sector. The ε-constraint approach proposes to set one of the objectives as a primary objective and setting a limit (ε_m) on the other objectives by putting them in as a constraint. It is best suited for problems with two objectives. In chapter 4, minimizing total cost is set as the primary objective. A lower limit on the annual emissions offset objective is set through a constraint in the cost minimization problem. The solution set obtained from this approach is term as a set of pareto optimal solutions where value of one objective cannot be made better without sacrificing the value of the other objective. Chapter 4 further explains the solution steps and the results obtained for this study.

In chapter 6, a mixed integer non-linear program formulation has been proposed. The problem is non-linear due to the consideration of a non-linear constraint within the formulation. In chapter 6, this non-linearity is represented by estimating the unit cost of production of hydrogen through equation 6.7, which involves taking the ratio of two continuous decision variables. The challenge with non-linear optimization problems lie in whether the non-linear equation is a convex function. If it is a convex non-linear equation then a global optimum can be obtained. In chapter 6, the cost of production of hydrogen (equation 6.7) is estimated from the ratio of two linear functions. These types of equations in optimization problems are termed as linear fractional functions. Linear fractional functions are quasi-convex if one restricts the realm of possible values that the linear function in the denominator can take to be greater than zero. Therefore the optimization problem formulation in chapter 6 involves putting a lower bound the variable 'amount of hydrogen produced to a small value (0.00001) which is greater than zero. Other non-linear equations of the same form include equations 6.10 and 6.11 (refer to chapter 6 for description).

Chapter 7 presents a mixed integer linear programming problem. Chapter 4 presents a deterministic formulation for focus primarily on evaluating the effect of cost and emission offset trade-offs on power to gas energy hub configurations providing clean energy vectors to the natural gas sector. Chapter 7 on the other hand presents a 2-stage stochastic programming approach for optimally sizing and operating, a power to gas energy to provide multiple services including: 1) hydrogen for a refueling station, and natural gas end users, and 2) demand response ancillary service to the power grid operator. Uncertainty in electricity price, amount refueled, and number of refueling events has been considered. A 2-stage stochastic programming approach is a common way of solving such problems where decision variables are categorized in to 1st and 2nd stage

variables. 1st stage decision variables involve making a decision without having the knowledge of the realizations of the uncertain parameters. 2nd stage decision variables involve making decision once the knowledge of the realizations of the uncertain parameters are known.

Stochastic programming approaches involve putting realizations of uncertain parameters into sets/scenarios and then solving a deterministic equivalent optimization problem. The challenge with this approach lies in the number of set/scenarios created after creating possible combinations of the realizations of the uncertain parameters. Higher the number of scenarios greater is the computational time. In this thesis the primary goal of chapter 7 is to provide an initial insight into why accounting for uncertainty in power to gas energy hub modeling studies is important. Therefore, in order to not compromise the computation time of solving the problem, chapter 7 also gives a detailed description of how even with lesser number of generated scenarios, the value of stochastic solution shows the importance of accounting for uncertainty.

3.3 Energy Hub Component Models

In this chapter (3), the different baseline technological equations for a polymer electrolyte membrane (PEM) electrolyzer, compressed gas storage systems, compressor modules and a methanation reactor will be presented. The term 'baseline' mentioned above implies that these set of equations will remain consistent in chapters 4, 5, 6 and 7.

3.3.1 Electrolyzer model

Due to a higher efficiency, faster ramping rates and a lower 'minimum operating level' (see section 2.2.1), polymer electrolyte membrane (PEM) electrolyzers are chosen over alkaline electrolyzers for the power to gas energy hub models.

The operating characteristics associated with the PEM electrolyzer is based on data provided by Hydrogenics Inc. **[44]**. Although first-principle models for developing electrolyzers provide a more comprehensive understanding of electrolyzer operating principles, the modeling of the system will be based on empirical data provided by the industry. Upon consultation with technical staff at Hydrogenics, and their keenness in understanding the high level economics of the potential implementation of their electrolyzer stacks in large scale power to gas systems, it has been clarified and agreed upon that the empirical data prepared by the technical staff characterizes the

performance of the electrolyzer under changing load conditions well enough to discount adopting a first-principles model.

In this section, the constraints relating electrolyzer efficiency with electricity consumption and hydrogen production will be presented. In addition to this, the water consumption rate, operating level bounds and sizing constraints will also be shown.

Developing a complex model of an electrolyzer from first principles is out of the scope of this thesis. The goal is to utilize a black box model of the PEM electrolyzer to study how it could use clean electricity from the power grid to produce hydrogen. By taking the ratio of higher heating value of hydrogen (E_{HHV,H_2}, 3.55 kWh per m^3 of H_2) over the rated energy consumption by an electrolyzer module ($E_{Rated,Electrolyzer}$, 4.63 kWh per m^3 of H_2) **[44]** the energy conversion efficiency of the electrolyzer can be determined ($\eta_{Electrolyzer}$ %, see equation 3.1).

$$\eta_{Electrolyzer} = \frac{E_{HHV,H_2}}{E_{Rated,Electrolyzer}} \times 100 \tag{3.1}$$

The above equation yields an energy conversion efficiency ($\eta_{Electrolyzer}$) value of 76.67%. The hydrogen produced for the electricity consumed by the electrolyzer can now be estimated using equation 3.2. Throughout the thesis an hourly time index will be assumed and a subscript 'h' will be added to terms that can vary between consecutive hours. In equation 3.2, $H_{2,h}$ and E_h denote the hydrogen produced and the energy consumed in an hour.

$$H_{2,h} = \frac{\eta_{Electrolyzer} \times E_h}{E_{HHV,H_2}} \left(\frac{m^3}{h}\right) \tag{3.2}$$

The electrolyzer modules chosen for this study have a unit size of 1 MW or 1000 kW. Therefore the total electrolyzer system capacity chosen for a particular power to gas energy hub is sized in increments of 1000 kW. A single electrolyzer unit can operate between the maximum $E_{Electrolyzer,Max}$ (1000 kWh) and minimum $E_{Electrolyzer,Min}$ (0 kWh) energy consumption levels. The electrolyzers are allowed to be turned down due to fast ramping up rates within a matter of seconds (see section 2.2.6). The term $N_{Electrolyzer}$ in equation 3.3 denotes the optimal number of electrolyzers selected when used within an optimization formulation.

$$N_{Electrolyzer} \times E_{Electrolyzer,Min} \leq E_h \leq N_{Electrolyzer} \times E_{Electrolyzer,Max} \quad (3.3)$$

Equation 3.3 can be categorized as a constraint that bounds the variable hourly energy consumed by *N* electrolyzers.

$$W_h = WCR \times H_{2,h} \left(\frac{liter}{h}\right) \quad (3.4)$$

The product of water consumption rate specification for the electrolyzer modules (WCR, liter of H_2O per m^3 H_2) and the hourly hydrogen produced ($H_{2,h}$, m^3 per hour) is used to estimate the hourly water consumption (W_h, see equation 3.4).

3.3.2 Storage tank model

As the time index in the modeling study is considered to be on an hourly basis, there may be low electricity price time points when producing and storing excess hydrogen is more cost effective. This excess hydrogen can be withdrawn from storage at a later time point so that the electrolyzers can operate at a lower power level when electricity prices are high. This stored hydrogen can be used in meeting demand from the transportation sector, injecting hydrogen into the natural gas distribution/transmission pipelines and also direct it to methanation reactors for the production of renewable natural gas. Chapters 6 and 7 will highlight how the storage system will interact with these end uses. In this sub-section, the primary flow balance equality constraints and sizing constraints concerning a storage system have been outlined.

The equality constraint shown below (equation 3.5) splits the hydrogen flow coming from the electrolyzers into $H_{2,Direct,h}$(m^3 per hour) and $H_{2,In,h}$(m^3 per hour). The stream $H_{2,In,t}$ takes the portion of hydrogen produced by the electrolyzers into the storage tanks, while the $H_{2,Direct,h}$ stream bypasses injection into the storage tank and directs the flow of hydrogen coming from the electrolyzer to an end use (e.g.: hydrogen refueling station, natural gas pipeline, or methanation reactor)

$$H_{2,h} = H_{2,Direct,h} + H_{2,In,h} \quad (3.5)$$

In a particular hour, the end use application of hydrogen ($H_{2,End\ Use,h}$, e.g.: hydrogen refueling station, natural gas pipeline, or methanation reactor) can derive the gas from the flow directly coming from the electrolyzer ($H_{2,Direct,h}$, m^3 per hour) and the hydrogen withdrawn from the storage tank ($H_{2,Out,h}$, m^3 per hour). Equation 3.6 depicts this flow balance.

$$H_{2,End\ Use,h} = H_{2,Direct,h} + H_{2,Out,h} \tag{3.6}$$

The hydrogen inventory balance within the storage tank at the end of a particular hour is given by equation 3.7 below. The term $H_{2,Tank,h-1}$ in equation 3.7 denotes the amount of gas in place at the beginning of every hour.

$$H_{2,Tank,h} = H_{2,Tank,h-1} + H_{2,In,h} - H_{2,Out,h} \tag{3.7}$$

The type of hydrogen storage tank modules used in the case studies presented in chapters 6 and 7 have varying maximum storage capacities and pressures. In this sub-section, the focus will only be to highlight the formulation behind choosing the number of a specific type of storage tank module. This can be done by constraining the hourly hydrogen inventory variable ($H_{2,Tank,h}$, m^3 per hour) between the product of the integer variable denoting the number of tank modules (N_{Tank}) and the minimum ($H_{2,Tank,Min}$, m^3) and maximum ($H_{2,Tank,Max}$, m^3) capacities of the storage module.

$$N_{Tank} \times H_{2,Tank,Min} \leq H_{2,Tank,h} \leq N_{Tank} \times H_{2,Tank,Max} \tag{3.8}$$

The maximum capacity of storage tank modules in literature are in general specified in kilograms of hydrogen and at a certain pressure **[62]**. In order to convert it into cubic meter, the ideal gas equation adjusted with the compressibility factor for hydrogen has been used (see equation 3.9).

$$H_{2,Tank,Max} = \frac{R \times T \times n \times z}{P_{Tank,Max}} \tag{3.9}$$

In equation 3.9: 1) *R* is the ideal gas constant (m^3 bar per K mol), 2) *n* denotes the maximum moles of hydrogen that can be stored in a specific tank module; 3) *T* is the storage temperature; 4) *z* is the compressibility factor of hydrogen **[22]**, and 5) $P_{Tank,Max}$ (bar) is the specified maximum

storage pressure of the storage tank module. The minimum storage inventory level inside a tank can also be determined using equation 3.9. However, in this case, the value of pressure needs to be changed to the corresponding minimum pressure of the storage tank module ($P_{Tank,Min}$, bar).

3.3.3 Compressor model

A report of hydrogen refueling station compressor models prepared by the National Renewable Energy Laboratory (US) in collaboration with compressor developers **[91]** has been used as a basis for the compressor model developed in this section. The report **[91]** highlights that an accurate calculation of compressor power consumption would be achieved by accounting for 1) the enthalpy of gas as a function of temperature; 2) pressure losses occurring across each stage within a compressor; 3) assuming an effectiveness for intercooler so that gas temperature entering each stage is known, and 4) estimating the performance of each stage and adding over the total number of stages. This estimation is compared with assuming a perfect gas relationship to estimate power consumption. The analysis highlights that the low pressure ratios and outlet temperatures from each stage do not warrant rigorous calculations and the perfect gas relationship yields reasonable results. The H2A Delivery Models developed by the National Renewable Energy Laboratory in the US utilizes the perfect gas relationship to estimate compressor power consumption for hydrogen refueling station projects. Using this understanding for modeling hydrogen refueling stations, this thesis will not focus on developing a rigorous compressor model and use the relationship shown in equation 3.10 **[91]** below to estimate power consumption of compressors. The optimization studies presented in chapters 6 and 7 will utilize the methodology outlined below to estimate the electricity cost for compressing hydrogen. The goal is to control the decision variables associated with the flow of hydrogen directed to the compressor. Therefore developing a rigorous compressor model will not drastically improve the solution to the problem. This decision has been made based on a trade-off between model complexity and computational time with lowering computational time being the priority.

Hydrogen sent to the tank needs to be compressed to the maximum pressure level of the storage tank before injecting it. The energy required to compress a kilo mole of hydrogen can be estimated using equation 3.10 below.

$$\frac{P}{\dot{m}} = \frac{zRTN}{\eta_{isentropic}} \times \frac{k}{k-1} \times \left[\left(\frac{p_{outlet}}{p_{inlet}} \right)^{\left(\frac{k-1}{Nk}\right)} - 1 \right] \quad (3.10)$$

In the above equation (3.10), the term $\frac{P}{\dot{m}}$ denotes the ratio of power (kW) consumed and the molar flow rate of hydrogen (kmol per hour). This translates to the units of kilo-watthour per kilo mole of hydrogen. The terms on the right hand side of equation 3.10 include: 1) The compressibility factor of hydrogen (*z*) estimated at an average value between outlet and inlet pressures of the gas; 2) The ideal gas constant (*R*, kJ per kmol-K); 3) The inlet gas temperature (*T*, K); 4) The number of stages in a compressor (*N*); 5) The isentropic efficiency of the compressor ($\eta_{isentropic}$); 6) The ratio of specific heats for hydrogen (*k*), and 7) p_{outlet} and p_{inlet} are the outlet and inlet pressures of the gas. The value of the term $\frac{P}{\dot{m}}$ can then be converted from kWh per kmol of hydrogen to kWh per m^3 of hydrogen by multiplying it with the ratio of density and molecular weight of hydrogen.

$$H_{2,In,h} \leq N_{Compressor,Pre-Storage} \times F_{Max,Compressor,Pre-Storage} \quad (3.11)$$

Compressor specifications in the literature include the maximum flow handling capacity ($F_{Max,Compressor,Pre-Storage}$, m^3 per hour) and the required inlet pressures to it. The specifications also include the output pressure that it is capable of achieving. Therefore in order to constrain the flow of hydrogen directed towards the tank storage system ($H_{2,In,h}$, m^3 per hour), the bounding constraint shown in equation 3.11 has been used. This constraint also helps in sizing the compressor system by choosing the number of compressors ($N_{Compressor,Pre-Storage}$) required of a certain type.

3.3.4 Methanation reactor model

The operating principle of a methanation rector is based off of the well-known Sabatier reaction shown below (equation 3.12).

$$CO_2 + 4H_2 \leftrightarrow CH_4 + 2H_2O(g) \quad (3.12)$$

Hydrogen produced from the electrolyzer combines with carbon dioxide to produce methane and water vapor. The methane produced can then be upgraded to the specifications of the natural gas grid with the help of an upgrading equipment before being injected into the transmission/distribution pipelines. This sub-section will introduce the technological constraints used in an optimization formulation to optimally size and operate a methanation reactor.

Aicher et al. **[92]** in their work elaborate on the ramping rates of fixed bed and 3-phase methanation reactors. The former is known to have ramping rates between ± 1% per minute and needs to be at a minimum operating level of 40% load to achieve this ramp rate. The 3-phase methanation reactors are known to have a faster ramp rate which is closer to ± 3% per minute mark. Götz et al. **[71]** also highlight that the 3-phase methanation reactors can operate at lower loads of 10-20%. The 3-phase methanation reactor technology is chosen in this study for its better flexibility in the operating regime and faster ramping times.

The Sabatier reaction in equation 3.12 shows a 4:1 ratio ($\gamma_{H_2}:\gamma_{CH_4}$) of the amount of hydrogen required for methane production. Using this information, the efficiency of the methanation reactor is estimated from the ratio of energy content of methane produced by the reactor and the energy content of the input hydrogen fuel in equation 3.13.

$$\eta_{Reactor} = \frac{\gamma_{CH_4} \times HHV_{CH_4}}{\gamma_{H_2} \times HHV_{H_2}} = \frac{213.6\left(\frac{kcal}{g.mol}\right)}{4 \times 68.7\left(\frac{kcal}{g.mol}\right)} = 0.77 \tag{3.13}$$

The terms $\eta_{Reactor}$, HHV_{H_2}, and HHV_{CH_4} denote the efficiency of the methanation reactor, and the respective higher heating value of hydrogen and methane.

Since methane makes up almost 93% of natural gas sent to end users of Enbridge's natural gas fuel supply **[93]**, the ratio of renewable natural gas produced to hydrogen consumed is assumed to be 0.25 (π) in equation 3.14 and the efficiency of the reactor derived from equation 3.13 has been used below to estimate the hourly flow of renewable natural gas (RNG_h, m^3 per hour). The methanation reactor can have hydrogen coming to it either directly from the electrolyzers ($H_{2,direct,h}$, m^3 per hour) or from the storage tanks ($H_{2,out,h}$, m^3 per hour).

$$RNG_h \times HHV_{NG} = \eta_{Reactor} \times \left(H_{2,out,h} + H_{2,direct,h}\right) \times HHV_{H_2} \quad (3.14)$$

A 1:1 ratio is assumed to determine the carbon dioxide consumed for producing a cubic meter of renewable natural gas (equation 3.15).

$$CO_{2,h} = RNG_h \quad (3.15)$$

Since the hourly CO_2 consumption ($CO_{2,h}$, m^3 per hour) and renewable natural gas production (RNG_h, m^3 per hour) are related by the above equality constraint, the hourly flow of CO_2 available ($CO_{2,avialable,h}$) can be used to bound the maximum renewable natural gas production capacity for the methanation reactor. This is represented by equation 3.16 below.

$$RNG_{Max} \leq CO_{2,avialable,h} \quad (3.16)$$

Chapter 4 explains in more detail how the values for the parameter $CO_{2,avialable,h}$ (m^3 of CO_2 per hour) have been estimated.

$$RNG_h \leq RNG_{Max} \quad (3.17)$$

Equation 3.17 above is used to constrain the hourly flow of renewable natural gas produced by the reactor (RNG_h, m^3 per hour) to its maximum operating capacity (RNG_{Max}, m^3 per hour).

$$-RNG_{Max} \times \tau \leq RNG_h - RNG_{h-1} \leq RNG_{Max} \times \tau \quad (3.18)$$

The methanation reactor is assumed to ramp up from a shutdown state to full capacity in 2 hours **[94]**. Therefore, equation 3.18 is added as a constraint in the optimization problem to constrain the change in methane production output between two successive time points to ± 50% (denoted by 'τ') of the maximum reactor capacity (RNG_{Max}).

Chapters 4, 5, 6 and 7 will introduce the objective functions, modeling framework (including technological constraints) and the results behind the different services (energy recovery pathways, see section 2.2) that a power to gas energy hub can provide. Each of the above mentioned four chapters are listed below:

- Chapter 4: Comparing the investment required for offsetting a tonne of lifecycle emissions in the natural gas sector with the transportation sector in Ontario.
- Chapter 5: Estimating the scale of electrolyzer system required for absorbing all of the surplus electricity produced by Darlington and Pickering nuclear power stations.
- Chapter 6: Development of a pricing mechanism for valuing ancillary, transportation and environment services offered by a power to gas energy system.
- Chapter 7: A stochastic programming approach of for the planning and operation of a power to gas energy hub with multiple energy recovery pathways.

The technological equations presented within sections 3.1.1 to 3.1.4 in this chapter will be referred to in the above mentioned case studies.

Chapter 4: The Environmental Benefits and Economic Cost of Repurposing Surplus Electricity in Ontario: Natural Gas Sector vs. Transportation Sector

The following chapter is based on the premise of work presented in an article published in the International Journal of Hydrogen Energy in 2015. The title of the article is: '*Optimal sizing of an electrolytic hydrogen production system using an existing natural gas infrastructure*'. This has been authored by Ushnik Mukherjee, Mohamed Elsholkami, Sean Walker, Michael Fowler, Ali Elkamel, and Amir Hajimiragha.

The first author's primary contribution in both articles was to develop the formulation in GAMS, and writing the article. Sean Walker helped with developing some of the energy hub conceptual figures and writing parts of both articles. Mohamed Elsholkami helped with providing key insights in modeling formulation in the article. Amir Hajimiragha, Ali Elkamel and Michael Fowler provided helpful guidelines in preparing the article for publication.

4.1 Introduction

A power grid with a lower global warming impact has the potential to extend its benefits to energy systems that conventionally do not utilize electricity as their primary energy vector. A good example is the introduction of electric vehicles in the transportation sector all across the globe **[95]**. A new initiative almost always requires policies that help sustain its implementation. Similar to the feed-in-tariff programs for sustaining the growth of renewable generation portfolio, the introduction of incentive mechanisms for promoting the adoption of electric vehicles can be seen as a policy decision complementing the feed-in-tariff program. However, the cost-effectiveness of such complementing policies needs to be evaluated and compared with other potential technologies that can complement renewable energy generation policies. This study presents the case of Ontario and estimates the cost incurred (in incentives) by the provincial government to reduce emissions via the existing electric vehicles in Ontario over their lifetime. This is then compared with the potential cost incurred by two power to gas energy hubs that utilize clean

surplus electricity from the province to offset emissions within the natural gas sector. The use of hydrogen-enriched natural gas and renewable natural gas has been considered to offset emissions in the natural gas sector. To the best of the authors' knowledge, the cost of implementing such changes especially with respect to the implementation of power to gas, has not been explored in the literature. Therefore the analysis presented in this case study is of interest.

4.2 Methodology

At the end of 2016, there were 9178 registered electric vehicles on Ontario's roads **[19]**. Out of the 9178 electric vehicles, 4760 battery electric (BEV) and 4296 plug-in hybrid electric (PHEV) vehicles qualified for receiving incentives. The goal of this study is to establish the investment cost incurred by the government of Ontario to offset a unit (Tonne) of $CO_{2,e}$ emission via the electric vehicle incentive program. To be more specific, the study calculates the ratio of total incentives given and the lifetime $CO_{2,e}$ emission reduction achieved by the 9056 electric vehicles that exist in Ontario as of 31, December 2016. This value is compared to the investment cost per unit of $CO_{2,e}$ emissions offset value for installing power to gas energy hubs at a chosen pressure reduction station on Enbridge Inc.'s distribution pipeline network in the greater Toronto area. Two different types of power to gas energy hubs have been compared, one distributing hydrogen-enriched natural gas (HENG), and the other distributing renewable natural gas.

In order to be consistent, the metric of '*investment required to offset a tonne of $CO_{2,e}$ emissions*' will be referred to as the '*levelized cost of emissions reduced*' for both the electric vehicles and the power to gas energy hubs for the remainder of this chapter.

4.2.1 Lifecycle emissions analysis and estimating the levelized cost of emissions reduced by electric vehicle

The lifecycle $CO_{2,e}$ emissions of a vehicle can be segregated into three phases, namely, the production phase, the use phase and end of life treatment phase.

Work done by Requia et al., and Ellingsen et al. **[96,97]** are significant contributions to the literature that analyze the lifecycle emissions of electric vehicles.

Production and End of Life Treatment Emissions: In this work, the data associated with the production phase and end of life treatment emissions is taken from Ellingsen et al.'s work **[97]**. Table 4.1 lists the production phase emissions incurred (Tonnes of $CO_{2,e}$ per tonne of the car) and the end of life treatment emission (Tonnes of $CO_{2,e}$ per vehicle) for both gasoline and electric vehicles. The values of these two parameters are given for three different car size classifications, namely, a mini, medium and a large car.

Table 4.1: Electric and Gasoline Vehicle Production Phase and End of Life Treatment Emissions

Vehicle Size Class	Production Phase Emissions (Tonnes of $CO_{2,e}$ per tonne of the car)	End of Life Treatment Emissions (Tonnes of $CO_{2,e}$ per vehicle)
Mini – Electric Vehicle	6.3	0.5
Medium – Electric Vehicle	6.4	0.6
Large – Electric Vehicle	6.8	0.7
Mini – Gasoline Vehicle	3.9	0.3
Medium – Gasoline Vehicle	4.3	0.5
Large – Gasoline Vehicle	5.6	0.6

The US Department of Energy (US DOE) categorizes size classes based on a vehicle's passenger and cargo volume (ft^3) **[98]**. For the sake of simplicity, the electric vehicles considered for this case study that fall under the categories of mini-compact (<85 ft^3) and subcompact (85 to 99 ft^3) have been put under the minicar category. A vehicle classified by the US DOE under the compact and mid-size ranges are put in the medium car size (100-119 ft^3). Cars with passenger and cargo volumes greater than or equal to 120 ft^3 are put under the large car category.

The 9056 electric vehicles registered under the electric vehicle incentive program are listed in table 4.2. The table also shows the size category, vehicle weight, the total number of each type of electric vehicle existing on Ontario's roads and the reduction on manufacturer suggested retail price (MSRP) that these vehicles are eligible for.

Table 4.2: Electric vehicles (BEV/PHEV) existing in Ontario at the end of 31, December 2016 [18,19,99]

Vehicle model	Size class	Vehicle Weight (Tonnes)	The 2016 year-end numbers	Incentive per vehicle ($ per vehicle)	Electric Drive Range Efficiency (Wh per km)	Gasoline Drive Range Efficiency (liter per km)	Electric Range (km)
Nissan Leaf	Medium – BEV	1.55	986	$14,000	150	NA	160.9
Tesla Model S	Large – BEV	2.12	2300	$14,000	216		365
Smart Fortwo	Small – BEV	0.9	543	$13,000	151		119.2
Kia Soul	Medium – BEV	1.49	194	$14,000	147		183.7
Tesla Model X	Large – BEV	2.42	429	$14,000	227.8		356.7
Mitsubishi i-MiEV	Medium – BEV	1.11	123	$10,000	135		118.5
Ford Focus	Medium – BEV	1.62	96	$14,000	154		149.4
BMW i3	Medium – BEV	1.19	86	$13,000	129		170.5
Chevrolet Bolt	Medium – BEV	1.63	3	$14,000	173.9		344.9
Chevrolet Volt	Medium – PHEV	1.61	2416	$14,000	223.7	0.064	56.3
Ford C-Max	Medium – PHEV	1.77	360	$7730	251.8	0.06	32.2
BMW i3 REX	Medium – PHEV	1.43	236	$13,000	180.2		115.8
Ford Fusion Energi	Medium – PHEV	1.77	181	$7730	229.9		30.6
Porsche Cayenne	Medium – PHEV	3.05	254	$3000	428.7	0.106	22.5

Volvo XC90	Large – PHEV	2.34	212	$3000	360.4	0.0946	20.9
BMW i8	Medium – PHEV	1.58	177	$3000	267.2	0.0847	22.5
Audi A3 e tron	Medium – PHEV	1.54	167	$8095	242.3		25.7
Toyota Prius Prime	Medium – PHEV	2.29	94	$5000	155.3	0.0446	40.2
BMW X5 XDrive 40e	Large – PHEV	2.37	133	$8460	366.6	0.0988	20.9
Hyundai Sonata	Medium – PHEV	1.73	24	$8460	211.3	0.0586	43.4
Porsche Panamera	Medium – PHEV	2.80	12	$3000	316.9	0.0941	24.1
BMW 330e	Medium – PHEV	1.81	20	$7730	292	0.075	22.5
Mercedes S550E	Large – PHEV	2.40	4	$3000	366.6	0.0236	19.3
Mercedes GLE550	Large – PHEV	2.24	1	$3000	422.5	0.1128	16.1
BMW 740e	Large – PHEV	2.13	3	$3000	323.1	0.087	22.5
Chrysler Pacifica Hybrid	Large – PHEV	2.72	2	$14,000	248.5	0.073	53.1

The emissions incurred during the production phase of the electric vehicles (Tonnes of $CO_{2,e}$) listed in table 4.2 is estimated by equation 4.1.

$$Emissions_{Production\ Phase} = \sum_{v=1}^{26} W_{V,s} \times EMF_{EV,Production,v,s} \times N_V \quad (4.1)$$

'$W_{v,s}$' denotes the weight of each of the 26 electric vehicle models (Tonnes, see table 4.2). The subscript 'v' denotes the vehicle model number which ranges from 1 to 26. The subscript 's' represents the size category designated to the electric vehicle model 'V'. 's' can be mini, medium or large. The term '$EMF_{EV,Production,V,s}$' denotes the emission factor (Tonnes of $CO_{2,e}$ per tonne of car, see table 4.1) for the production of an electric vehicle in a particular size category 's'. The term 'N_V' denotes the number of each of the 26 electric vehicle models.

$$Emissions_{End\ of\ Life\ Treatment\ Phase} = \sum_{v=1}^{26} EMF_{EV,EOL,V,s} \times N_V \quad (4.2)$$

The term '$EMF_{EV,EOL,v,s}$' in equation 4.2 denotes the end of life treatment emission factor for an electric vehicle model 'v' (Tonnes of $CO_{2,e}$ per vehicle) based on the size category 's' that it has been designated.

Based on the number of mini, medium and large EVs listed in table 4.2, the end of life treatment and production phase emissions of an equivalent number of mini, medium and large gasoline vehicles have been estimated. This provides a baseline to compare the end of life and production phase emissions of gasoline and electric vehicles. Ellingsen et al. **[97]** assume the following average weights for gasoline vehicles: 1) Mini car: 0.935 tonnes; 2) Medium car: 1.259 tonnes and 3) Large car: 1.528 tonnes. These weight values combined with emission factor for production of gasoline vehicles from table 4.1 give their production phase emissions. The end of life treatment emissions has been estimated in a similar way.

Use Phase Emissions: Axsen et al. **[100]** carry out a detailed '*multi-method survey* and *interview process*', to highlight the potential of the electric vehicle market in Canada. Their work highlights how key parameters such as awareness of electric vehicle technology, consumer lifestyles, and life

values, vehicle travel behavior, interest in the purchase of electric vehicles etc. will lead to the formation of three potential electric vehicle consumer groups in Canada. The electric vehicle usage data collected through their surveys have been used to estimate the use phase emissions in this study.

A battery electric vehicle (BEV) will always run from charge obtained from an electricity source whereas a plug-in hybrid electric vehicle (PHEV) can utilize both its electric and gasoline range over the duration of a trip. Although there can be numerous different scenarios of how a plug-in hybrid electric vehicle runs, this study assumes two scenarios. In scenario 1, the plug-in hybrid electric vehicle initially uses up all of its electric range and then switches to using gasoline if its daily trip distance is not yet complete. In scenario 2, the plug-in hybrid electric vehicle is assumed to have a 100% utility factor. In other words, the PHEV completes the entirety of its daily trip distance by utilizing its electric drive range. However, in order to do so, the PHEV will have to charge its batteries at least twice (if not more) over the course of a day to complete its daily trip distance.

In this study, it is assumed that the average driving distance in Ontario is 61 km (Annual distance covered: 22,265 km). This value has been taken from the survey data collected by Axsen et al **[100]**. In terms of electric vehicle lifetime, Ellingsen et al. and Hawkins et al. assume values of 180,000 km, and 150,000 km, respectively **[97,101]**. Hawkins et al. also carry out a sensitivity analysis to determine how the lifecycle emissions per kilometer traveled changes with the lifetime of EVs. In this study, each of the vehicles listed in table 4.2 is assumed to have a baseline lifetime of 180,000 km. This translates to roughly 8 years of service life if a vehicle travels 61 km for each day of the year. A sensitivity analysis on the levelized cost of emission reduction is carried out by changing the vehicle lifetime mileage to 250,000 km.

Based on the assumed daily trip value of 61 km and the electric range of the PHEVs listed in table 4.2, the average utility factor of the PHEVs in scenario 1 described above is calculated to be 51.5%. Therefore, for consistency, scenario 1 will be termed as the case where PHEVs have a utility factor of 51.5% and scenario 2 will be termed as the case where they have a 100% utility factor.

The energy consumed by the electric vehicles in scenario 1 (PHEV Utility Factor: 51.5%) are estimated using equations 4.3 to 4.5.

$$E_{1,BEV_k} = D_{Daily} \times \eta_{BEV_k,El} \times N_{BEV_k} \quad (4.3)$$

Equation 4.3 estimates the total energy consumed by each battery electric vehicle (E_{1,BEV_k}, kWh) model over the course of a day. The subscripts '1' and 'BEV_k' denote scenario 1, and the battery electric vehicle model 'k', respectively. In this study 'k' ranges from 1 to 9, as there are 9 types of battery electric vehicles listed in table 4.2. The term 'D_{Daily}' is used to denote the daily trip distance of 61 km. '$\eta_{BEV_k,El}$' is the electric range efficiency in kWh per km (see table 4.2). The number of each of the 9 battery electric vehicle model is denoted by 'N_{BEV_k}' in equation 4.3.

$$E_{1,PHEV_n} = D_{PHEV,n} \times \eta_{PHEV_n,El} \times N_{PHEV_n} \quad (4.4)$$

Similarly, equation 4.4 estimates the total daily electrical energy consumed by the plug-in hybrid electric vehicles in scenario 1. The subscript '$PHEV_n$' in the above equation denotes the plug-in hybrid electric vehicle model 'n', where 'n' ranges from 1 to 17 as there exist 17 types PHEVs (see table 4.2). In the above equation 'D_{Daily}' is replaced by '$D_{PHEV,n}$', a term that is used to signify the electric range of the PHEVs. The terms '$\eta_{PHEV_n,El}$' and 'N_{PHEV_n}' denote the electric range efficiency (kWh per km) and the number of each type of 17 PHEV models.

$$G_{1,PHEV_n} = \left(D_{Daily} - D_{PHEV,n}\right) \times \eta_{PHEV_n,Gas} \times N_{PHEV_n} \quad (4.5)$$

Equation 4.5 estimates the daily gasoline consumed ($G_{1,PHEV_n}$, liters of gasoline) by the PHEVs in scenario 1. Note that in this case the gasoline consumption is estimated by calculating the difference between the terms 'D_{Daily}' and '$D_{PHEV,n}$'. The term '$\eta_{PHEV_n,Gas}$' in equation 4.5 denotes the gasoline drive cycle efficiency of the PHEVs (liters of gasoline per km, see table 4.2).

$$E_{2,V} = D_{Daily} \times \eta_{V,El} \times N_V \quad (4.6)$$

In scenario 2 (PHEV Utility Factor: 100%), the PHEVs cover the entirety of the daily driving distance by consuming electricity. Therefore, the daily electricity consumed by each type of electric vehicle is estimated by equation 4.6. The subscript '*2*' denotes the calculation is for scenario 2. Since all of the vehicles run on electricity, a common subscript '*V*' is used to denote both BEVs and PHEVs. Subscript '*V*' in equation 4.6 ranges from 1 to 26 as there are in total 26

types of electric vehicles listed in table 4.2. The electric range efficiency of each of the vehicle model is denoted by '$\eta_{V,El}$' in kWh per km and 'N_V' denotes the number of each of the 26 vehicle models.

In order to develop an hourly charging profile, the total daily electricity consumed by the electric vehicles in scenarios 1 and 2 have been split over the course of the day based on the location where the charging takes place and its duration. According to Axsen et al. **[100]**, 63% of all charging events occur at home, followed by 18% at public charging stations and 19% at work. These percentages are used to split the total daily consumption (kWh) in to amount of energy consumed at home and away from home. The hours during which charging occurs at home is taken to be 7 PM – 7 AM (12 hours). Charging at work and public stations are lumped together in periods between 9 AM – 12 PM and 2 PM – 5 PM (making up 6 hours).

Equation 4.7 is used to calculate the total energy consumed every hour ($E_{Home,i}$, kWh) at home by all the PHEVs and BEVs in both scenarios. 'i' is used to denote scenarios and can have values of 1, and 2.

$$E_{Home,i} = \frac{\left(E_{BEV,i} + E_{PHEV,i}\right) \times \emptyset_{Home}}{t_{Home}} \times 1hour \tag{4.7}$$

In the above equation '$E_{BEV,i}$' and '$E_{PHEV,i}$' are the total daily electrical energy consumed by all BEVs and PHEVs in scenarios 1 and 2 (denoted by the subscript i). These values as described earlier are derived from equations 4.3 to 4.6. 't_{Home}' denotes the time spent charging at home (12 hours). '$\emptyset_{Home}$' signifies the share of total energy consumed at home (63%) **[100]**.

$$E_{Public+Work,i} = \frac{\left(E_{BEV,i} + E_{PHEV,i}\right) \times \emptyset_{Public+Work}}{t_{Public+Work}} \times 1hour \tag{4.8}$$

Similarly, equation 4.8 calculates the total energy consumed every hour ($E_{Public+Work,i}$, kWh) at public and work charging stations by the BEVs and PHEVs. '$t_{Public+Work}$' denotes the aggregated time spent charging at public and work stations (6 hours). '$\emptyset_{Public+Work}$' signifies the share of total energy consumed at public and work charging station (37%) **[100]**. 'i' is used to denote scenarios and can have values of 1, and 2.

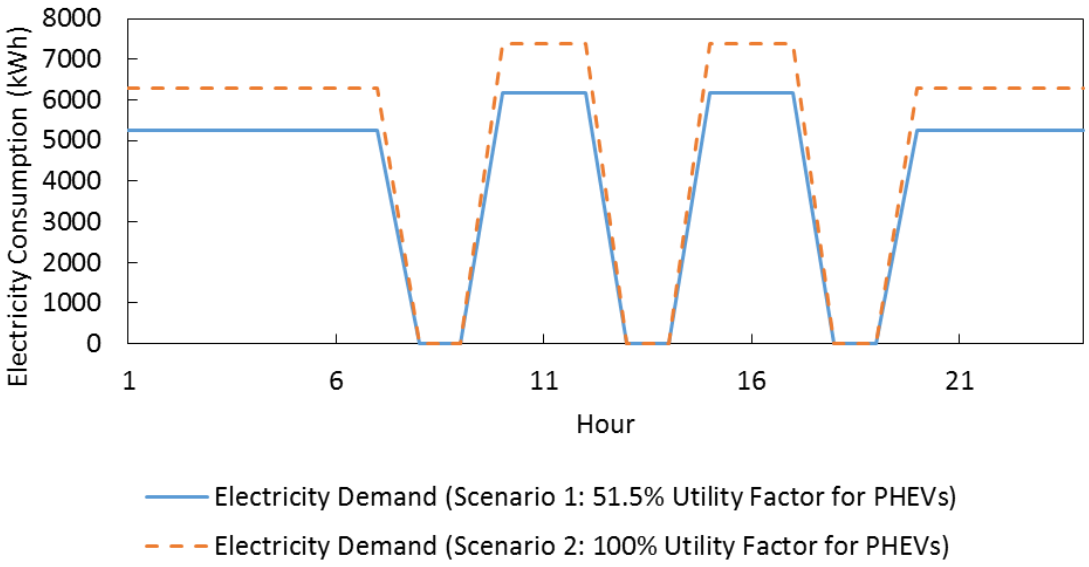

Figure 4.1: Charging pattern over the course of a day for scenario 1 (PHEV utility factor: 51.5%) and Scenario 2 (PHEV utility factor: 100%).

Figure 4.1 shows the electricity consumption profile for the electric vehicles in scenario 1 (PHEV utility factor: 51.5%) and scenario 2 (PHEV utility factor: 100%). The profile reflects the energy consumption periods over a day, with home charging starting at 7 PM – 7 AM and charging during the day occurs at work and public stations in hours between 9 AM – 12 AM and 2 PM – 5 PM. As PHEVs have a 100% utility factor in scenario 2, the overall energy consumption is higher in comparison to scenario 1 (51.5% utility factor for PHEVs). This profile is assumed to repeat for every day of the year, and the total annual energy consumption is multiplied by the service life of the electric vehicles to estimate the lifetime energy consumption. It should be noted that this study provides a baseline estimate for the cost paid in incentives by the provincial government to reduce emissions in the transportation sector. Therefore, considering complicated charging patterns is out of the scope of this work.

The annual use phase emissions associated with electricity consumption in scenarios 1 and 2 is estimated by summing the product of hourly electric vehicle energy consumption (kWh, figure 4.1) and hourly power grid emission factor (kg $CO_{2,e}$ per kWh). In order to determine the lifetime use phase emissions associated with electricity consumption, the annual use phase emissions (from electricity consumption) is multiplied by the service life of the vehicles.

The hourly emission factor of the grid is estimated by multiplying the hourly generation output by fuel type data for the year of 2016 in Ontario **[102]** and the lifecycle emission factor of individual generation sources **[103]**. Table 4.3 lists the annual average of hourly contributions from nuclear, gas-fired, hydroelectric, wind, solar and biofuel generators within the province. It also lists their respective lifecycle emission factor in kilogram of $CO_{2,e}$ per MWh of electricity generated.

Table 4.3: Lifecycle emission factor and generation output contribution by generator type

Type of Generator	Annual average of hourly generation output contribution (%)[102]	Lifecycle emission factor of electricity generated (kg $CO_{2,e}$ per MWh) [103]
Nuclear	61.6%	17
Natural gas-fired	8.4%	622
Hydroelectric	23.4%	18
Wind	6.1%	14
Solar	0.3%	39
Biofuel	0.2%	177

The PHEVs in scenario 1 consume gasoline fuel as well. The daily gasoline consumed ($G_{1,PHEV_k}$) by a PHEV is given by equation 4.3. This when summed over all PHEVs gives the total daily gasoline consumed in a day. Thus the annual gasoline consumption by all PHEVs is estimated by multiplying by the number of days in 2016 (366 days). The US environmental protection agency estimates the emission factor of motor gasoline to be 2.33 kg $CO_{2,e}$ per liter **[104]**. The product of annual gasoline consumption, the emission factor of gasoline and the service life of the vehicles gives the lifetime emissions associated with gasoline consumed by all PHEVs in scenario 1. Hence, the summation of emissions associated with gasoline (PHEVs) and electricity (PHEVs and BEVs) consumption for scenario 1 yields the total lifetime use phase emissions for the electric vehicles. For scenario 2, the lifetime use phase emissions of the electric vehicles will only be associated with electricity consumption as we assume that PHEVs have a 100% utility factor.

To serve as a baseline for comparison, the lifetime use phase emissions incurred from an equivalent number of mini, medium and large gasoline vehicles have been estimated. Table 4.4 lists the emission factor of the three gasoline vehicle size classes in kilogram $CO_{2,e}$ per km.

Table 4.4: Use phase emissions of conventional gasoline vehicles

Conventional Vehicle Size Class	Use Phase Emissions (kg $CO_{2,e}$ per km)
Mini	0.124
Medium	0.149
Large	0.166

The lifecycle emissions of the gasoline vehicles have also been estimated for vehicle service life of 180,000 km 250,000 km, respectively.

Incentives for electric vehicles: The electric vehicle incentive program also provides an incentive of $1000 to an electric vehicle owner or a business entity for installing a home/facility charging station **[18]**. The program also plans to provide free off-peak overnight charging to electric vehicles for a four year period starting in 2017 **[17]**.

The home charging station incentive is estimated by multiplying the incentive value $1000 per charging station and the total number of electric vehicles listed in table 4.2. The off-peak payments exempted is estimated from the product of the energy consumed by electric vehicles between 7 PM-7 AM and the off-peak residential hydro rate of $0.065 per kWh **[105]**.

4.2.2 Power to gas system sizing

This section presents a mixed integer linear programming problem (MILP). An optimization problem is called an MILP when 1) The objective function, the equality and inequality constraints are linear, and 2) There exist a mix of decision variables characterized as integer and continuous variables.

The optimization approach adopted in this chapter is the trade-off based ε-constraint approach. The trade-off exists between minimizing the objective function total capital and operating cost (Total Cost) of the power to gas energy hub and maximizing the annual emissions offset by the energy hub in the natural gas sector. The ε-constraint approach proposes to set one of the objectives as a primary objective and setting a limit (ε_m) on the other objectives by putting them in as a constraint **[106]**. It is best suited for problems with two objectives. In chapter 4, minimizing total

cost is set as the primary objective. A lower limit on the annual emissions offset objective is set through a constraint in the cost minimization problem. The solution set obtained from this approach is term as a set of pareto optimal solutions where value of one objective cannot be made better without sacrificing the value of the other objective.

This section describes the optimization problem formulation developed to determine and compare the costs incurred to achieve set emission offset targets via 1) A power to gas energy hub distributing renewable natural gas (Case 1: RNG/NG) and 2) A power to gas energy hub distributing hydrogen-enriched natural gas (Case 2: HENG) to natural gas end users within the greater Toronto area.

Electricity Source: The power to gas energy hubs in both cases are modeled to only run during periods of surplus baseload generation. Surplus baseload generation occurs when the total hourly electricity produced by the wind, nuclear, and hydroelectric generators exceeds Ontario's electricity demand **[107]**. The hourly generation output by fuel type and hourly demand data for Ontario have been taken from IESO's data directory to estimate the province's hourly surplus baseload generation in 2016. Since the power grid has ten different power zones, the contribution of each of these power zones towards surplus baseload generation varies. The generation output for each wind, nuclear and hydroelectric power plants in each of the 10 power zones were compiled. Using this information, the share that each power zone contributes towards surplus baseload generation has been estimated.

The power to gas energy hubs in both '*Case 1: RNG/NG*' and '*Case 2: HENG*' are located in the Toronto power zone. This power zone has 2 nuclear power stations which have a combined maximum capacity of 6600 MW. On annual average basis (2016), their contribution towards hours of surplus baseload generation in Ontario is ~34.57%. There are 4804 hours during the year when there is surplus baseload generation. The maximum value of hourly surplus baseload generation in the Toronto power zone in 2016 was 1095.24 MWh.

4.2.2.1 Case 1: Renewable natural gas (RNG/NG)

Figure 4.2 shows a flow chart of the energy hub producing and injecting renewable natural gas at a pressure reduction station. The primary components of this system include polymer electrolyte membrane (PEM) electrolyzers with a unit size of 1 MW **[44]**, a 3-phase methanation reactor and a methane upgrading equipment (incorporated within the pressure reduction station).

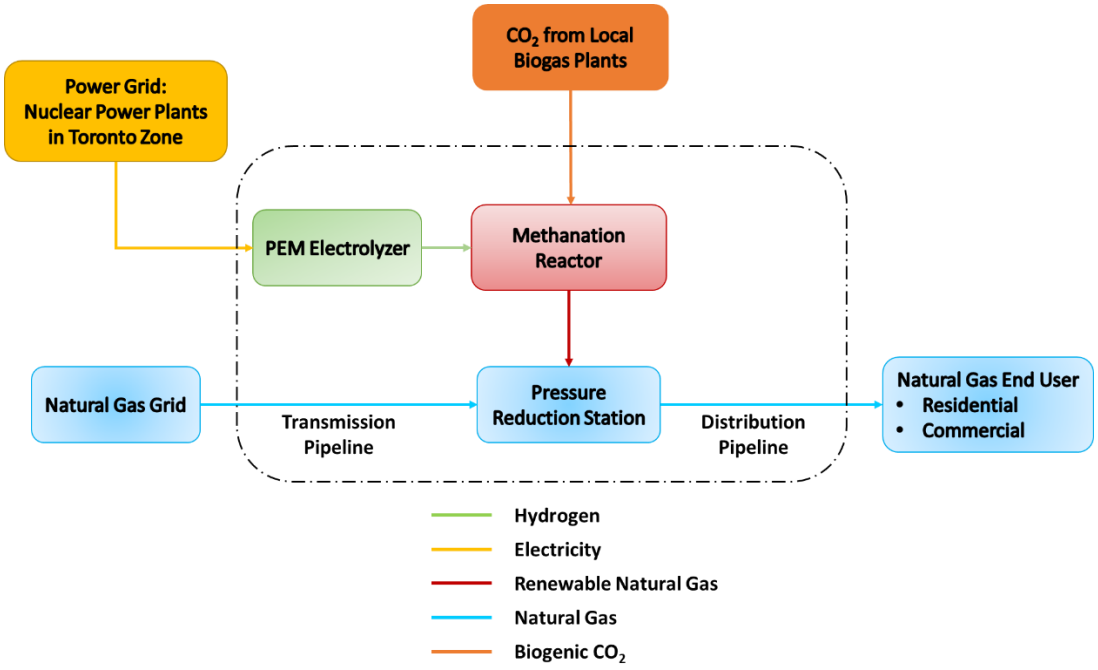

Figure 4.2: Flow diagram of power to gas energy hub for 'Case 1: RNG/NG'

The power to gas energy hubs are proposed to be collocated at a natural gas pressure reduction station along Enbridge's distribution network. The availability of hourly natural gas demand data for a period of a year is the primary reason behind this choice of location.

CO_2 Source: The CO_2 for producing renewable natural gas is considered to be biogenic due to the energy hub being located in close proximity to two organic waste processing plants (CCI Disco, and CCI Dufferin) and a digester within the Toronto zoo (ZOOSHARE) capable of decomposing animal waste.

The annual biogas production capacity of the CCI Disco and CCI Dufferin facilities are 11,250,000 and 6,050,000 Nm^3 **[108]**. The ZOOSHARE biogas digester has a production capacity of 260 m^3 per hour. Based on a 5 day per week, and an 8 hour per day run time, the total number of hours of

operation is estimated to be 6264 hours. In other words, ZOOSHARE is capable of producing 1,628,640 Nm^3 per year **[109]**. The biogas content for the three facilities is taken to be 67% CH_4 and 33% CO_2 **[110]**. Based on this assumption the total biogenic CO_2 available from the three plants is calculated to be 6,246,451 m^3.

4.2.2.2 Optimization Formulation (Case 1: RNG/NG)

In this section a mixed integer linear programming optimization formulation with the primary objective (Total Cost) and the constraints it is subject to have been shown. The second objective function (Annual Emissions Offset) is included as an ε-constraint among the list of constraints. The formulation is as follows:

$$Minimize: Total\ Cost_{Case\ 1} = CAPEX_{Case\ 1} + \left(OPEX_{Annual,Case\ 1} \times TVM\right)$$

s.t.

ε-constraint (Annual Emissions Offset):

$$Emissions\ Offset_{Case\ 1} \geq \emptyset \times Emissions\ Offset_{Case\ 1,Max} \mid \{\emptyset = 0.1,0.2, \dots ,1\}$$

Energy (Electrolyzer and Reactor) and H_2, CO_2 and RNG Flow Constraints:

$$H_{2,h} = \frac{\eta_{Electrolyzer} \times E_h}{E_{HHV,H_2}}$$

$$RNG_h \times HHV_{NG} = \eta_{Reactor} \times H_{2,h} \times HHV_{H_2}$$

$$CO_{2,h} = RNG_h$$

$$RNG_{Max} \leq CO_{2,avialable,h}$$

Energy (Natural Gas End User) Demand Constraint:

$$(RNG_h + NG_h) \times HHV_{NG} = D_h \tag{4.9}$$

Active Technological Constraints (Electrolyzer and Reactor):

$$N_{Electrolyzer} \times E_{Electrolyzer,Min} \leq E_h \leq N_{Electrolyzer} \times E_{Electrolyzer,Max}$$

$$E_h \leq SBG_{Toronto\ Zone,h}$$

$$RNG_h \leq RNG_{Max}$$

$$-RNG_{Max} \times \tau \leq RNG_h - RNG_{h-1} \leq RNG_{Max} \times \tau$$

$$N_{Electrolyzer} = \sum_{i=1}^{30} i \times \alpha_i$$

$$\sum_{i=1}^{30} \alpha_i \leq 1$$

The formulation consists of the integer variable $N_{Electrolyzer}$ (Number of electrolyzers) and the binary variables α_i. The problem also has continuous variables (e.g. E_h, RNG_h etc.) as well. Therefore the problem is a mixed integer linear programming problem. Appendix A.4.4 defines

the nomenclature of the different variables and parameters used in the above formulation in equation 4.9.

4.2.2.3 Objective Functions (Case 1: RNG/NG)

The environmental objective in '*Case 1: RNG/NG*' is denoted by the annual emission offset at the natural gas end user ('$Emissions\ Offset_{Case\ 1,Max}$', Tonnes of $CO_{2,e}$ per year) via a blend of conventional and renewable natural gas in equation 4.10 below. The value of '$Emissions\ Offset_{Case\ 1,Max}$' will help in determining the 10 emission offset targets for the cost optimization problem.

$$Emissions\ Offset_{Case\ 1,Max} = Emissions_{NG} - Emissions_{RNG,NG} \tag{4.10}$$

The term '$Emissions_{NG}$' (Tonnes of $CO_{2,e}$ per year) represents the annual emissions incurred when only conventional natural gas is used to meet the demand of natural gas placed at the pressure reduction station and is estimated by equation 4.11.

$$Emissions_{NG} = \delta \times \sum_{h=1}^{8784} \frac{EMF_{NG} \times D_h}{HHV_{NG}} \tag{4.11}$$

The terms 'EMF_{NG}' and 'HHV_{NG}' denote the lifecycle emission factor of conventional natural gas (kg $CO_{2,e}$ per m^3 of NG) and the higher heating value of natural gas (0.03623 MMBtu per m^3 of NG). 'D_h' denotes the hourly energy demand placed on the natural gas pressure reduction station. The subscript 'h' denotes the hourly time index and ranges from 1 to 8784 hours for the year of 2016. 'δ' is the coefficient used to convert kg $CO_{2,e}$ emissions to tonnes of $CO_{2,e}$ emissions.

The lifecycle emission factor of natural gas is estimated by the following equation.

$$\begin{aligned} EMF_{NG} = EMF_{WtP} + EMF_{CO_2,Combustion} + \left(EMF_{CH_4,Combustion} \times GWP_{CH_4}\right) \\ + \left(EMF_{N_2O} \times GWP_{N_2O}\right) \end{aligned} \tag{4.12}$$

The term 'EMF_{WtP}' denotes the well to pump emission factor or the emissions incurred during pre-production, processing, and transmission of natural gas (0.54 kg $CO_{2,e}$ per m^3 of NG, **[111]**). '$EMF_{CO_2,Combustion}$' signifies the kg of CO_2 emissions incurred when a cubic meter of natural gas

is combusted at the end user (1.863 kg CO_2 per m^3 NG, **[112]**). Similarly, the terms '$EMF_{CH_4,Combustion}$' (0.000037 kg CH_4 per m^3 of NG) and 'EMF_{N_2O}' (0.000035 kg N_2O per m^3 of NG) denote the kg of CH_4 and N_2O emissions occurring when a cubic meter of natural gas is combusted at either a residential, commercial, or manufacturing industry **[112]**. The global warming potential of CH_4 and N_2O are taken to be 25 (GWP_{CH_4}) and 298 (GWP_{N_2O}) for a 100 year time horizon or residence time within the atmosphere.

Equation 4.13 is used to estimate the annual lifecycle emissions incurred by natural gas end users when a blend of conventional and renewable natural gas is delivered to them ($Emissions_{RNG,NG}$, Tonnes of $CO_{2,e}$ per year).

$$
\begin{aligned}
Emissions_{RNG,NG} &= \left\{\delta \times \sum_{h=1}^{8784}\left[(EMF_{NG} \times NG_h) + \left(EMF_{Combustion,RNG} \times RNG_h\right)\right]\right\} \\
&+ \left\{\delta \times \sum_{h=1}^{8784}\left[EMF_{Nuclear} \times E_h\right]\right\} + \left\{\sum_{h=1}^{8784}\left[EMF_{Biogenic\,CO_2} \times CO_{2,h}\right]\right\} \\
&+ \left\{\sum_{h=1}^{8784}\left[EMF_{Electrolyzer} \times H_{2,h}\right]\right\} + \left\{\sum_{h=1}^{8784}\left[EMF_{Reactor} \times RNG_h\right]\right\}
\end{aligned}
\tag{4.13}
$$

The first term in equation 4.13 estimates the lifecycle $CO_{2,e}$ emissions occurring from conventional natural gas (NG_h, m^3 per hour) sent to the end user and the combustion associated $CO_{2,e}$ emissions ($EMF_{Combustion,RNG}$, kg $CO_{2,e}$ per m^3 of RNG) with renewable natural gas (RNG_h, m^3 per hour).

Cherubini et al. **[113]** estimate that the global warming potential of CO_2 released from combustion of renewable natural gas is zero or negligible (for a time horizon of 100 years) if the original biomass source has short rotation period ranging from 1 to 10 years. In this study, the biomass source utilized at the 2 organic waste processing facilities come from the residential green organic waste collection program in Toronto. This organic waste is assumed to comprise of vegetables that are short rotation crops (or annual crops) and meat products. The animal waste feed for the digester at ZOOSHARE is assumed to primarily originate from a farm feedstock fed to the animals at the zoo. The CO_2 released from the combustion of renewable natural gas produced from these biomass

sources are assumed to have a global warming potential of zero (over a 100-year time horizon). However, it is assumed that upon combustion, renewable natural gas produces CH_4 and N_2O emissions. Equation 4.14 shows the expression used to estimate the post-combustion emission factor of renewable natural gas.

$$EMF_{Combustion,RNG} = \left(EMF_{CH_4,Combustion} \times GWP_{CH_4}\right) + \left(EMF_{N_2O} \times GWP_{N_2O}\right) \qquad (4.14)$$

The terms '$EMF_{CH_4,Combustion}$', 'GWP_{CH_4}', 'EMF_{N_2O}', 'GWP_{N_2O}' in the above equation have already been described in equation 4.12.

Due to lack of information relating to the percentage breakdown of the different types of organic waste collected within Toronto, the CO_2 emissions incurred in processing and transportation of vegetable and meat products are not accounted for in this study.

The hourly energy consumed by the electrolyzers is denoted by the expression 'E_h' in equation 4.13. As the power to gas energy hub consumes surplus electricity produced by the 2 nuclear power plants in the Toronto power zone, the emissions associated with electricity consumption is associated with the emission factor of a nuclear power plant ('$EMF_{Nuclear}$', 0.017 kg $CO_{2,e}$ per kWh, see table 4.3).

The expressions '$EMF_{Biogenic\ CO_2}$' (Tonnes of $CO_{2,e}$ per m^3 of biogenic carbon dioxide produced) and '$CO_{2,h}$' (m^3 per hour of biogenic CO_2) in the third term of equation 4.13 denotes the emissions associated with the processing of organic waste and the hourly biogenic CO_2 consumed for producing renewable natural gas.

The processing associated emissions for organic waste include (see equation 4.15): 1) Garbage truck associated emissions during waste collection ($Emissions_{Waste\ Collection}$, Tonnes of $CO_{2,e}$ per year), 2) The emissions incurred during the operation of the CCI Dufferin and CCI Disco facilities ($Emissions_{Facility\ Operation}$, Tonnes of $CO_{2,e}$ per year) and 3) The emissions associated with truck transport of biogenic CO_2 to the power to gas energy hub.

$$EMF_{Biogenic\ CO_2} = \frac{Emissions_{Waste\ Collection} + Emissions_{Facility\ Operation}}{CO_{2,Total}} \qquad (4.15)$$

The expression '$CO_{2,\,Total}$' signifies the total annual CO_2 (6,246,451 m^3, see section 2.2.1) available from the three biogas producing facilities. The emissions associated with organic waste collection ($Emissions_{Waste\ Collection}$, 928 Tonnes of $CO_{2,e}$ emissions per year) is estimated by multiplying the emission factor data for garbage trucks (6.4 x 10^{-3} tonnes of $CO_{2,e}$ emitted per tonne of waste collected, **[114]**) and the total organic waste processed by the CCI Disco and CCI Dufferin facilities (145,000 tonnes per year, **[108]**).

The emissions associated with the operation of CCI Dufferin and CCI Disco has been estimated based on the facilities natural gas consumption and the values are provided in a report prepared by Golder Associates **[115]**. The value of '$Emissions_{Facility\ Operation}$' is estimated to be 481.4 tonnes of $CO_{2,e}$ per year. Therefore, this yields an emission factor value of 0.000226 tonnes of $CO_{2,e}$ emissions per cubic meter of biogenic CO_2 ($EMF_{Biogenic\ CO_2}$) consumed by the power to gas energy hub.

Note that the emissions associated with transportation of animal waste to ZOOSHARE's digester are negligible due to its location close to the zoo property. The scale of the biogas production facility at the zoo is much smaller in comparison to that of CCI Disco and CCI Dufferin, therefore the emissions associated with the operation of the zoo digester facility has been discounted. In addition to this, the emissions associated with diesel consumption in truck transportation of biogenic CO_2 from the three biogas plants to the power to gas energy hub has also been discounted. The rationale behind this comes from the estimation of diesel consumption based on a value of 1.06 kWh_{Diesel} per tonne of CO_2 transported per kilometer traveled given by McKenna et al. and Ausfelder et al. [**116,117**]. Based on the known distances and the amount of biogenic CO_2 available from each of the three plants, the emissions associated with transporting a total of 6,246,451 m^3 of biogenic CO_2 is calculated to be (a minimal value of) 0.123 tonnes. Hence, its contribution has been ignored.

The emissions associated with the construction and material acquisition for building electrolyzers, and methanation reactors are denoted by the expressions '$EMF_{Electrolyzer}$' (3.8x10^{-6} tonnes of $CO_{2,e}$ emissions per m^3 of hydrogen produced), and '$EMF_{Reactor}$' (1.53x10^{-4} tonnes of $CO_{2,e}$ emissions per m^3 of renewable natural gas produced), respectively **[118]**.

The total lifetime cost ($Total\ Cost_{Case\ 1}$, $) objective function in '*Case 1: RNG/NG*' is shown in equation 4.16 below.

$$Total\ Cost_{Case\ 1} = CAPEX_{Case\ 1} + \left(OPEX_{Annual,Case\ 1} \times TVM\right) \tag{4.16}$$

The '$Total\ Cost_{Case\ 1}$' is a function of the energy hubs lifetime capital cost (denoted by $CAPEX_{Case\ 1}$, $) and the product of annual operating cost of the energy hub ($OPEX_{Annual,Case\ 1}$) and the time value of money (*TVM*) coefficient. The time value of money is estimated based on an interest rate of 8% and a project lifetime of 20 years.

$$\begin{aligned} CAPEX_{Case\ 1} = &\left\{\beta \times \sum_{i=1}^{30}\left[C_{Electrolyzer,i} \times \alpha_i\right]\right\} + \{(\gamma \times RNG_{Max}) + k\} \\ &+ \left\{C_{Upgrading} \times RNG_{Max}\right\} \end{aligned} \tag{4.17}$$

Equation 4.17 shows the various cost constituents of '$CAPEX_{Case\ 1}$'. The first term is used to denote the electrolyzer system cost where the index 'i' denotes the system size (MW) of electrolyzer chosen by the optimization problem. The upper bound on 'i' is taken to be 30 MW based on market data suggestive of power to gas electrolyzer module sizes when they are commercially developed for large scale deployment **[44]**. Based on data published by Melaina et al. **[119]**, the unit cost of electrolyzers ($ per MW or $ per kW) reduces as the size of the installation increases (economics of scale). In this study the unit, costs have been estimated based on equation 4.18 below, where '*C**' is the updated unit cost of electrolyzers in $ per kW, 'C_o' is the base cost of a 1 MW (or 1000 kW) unit ($ per kW, **[44]**), '$\dot{V}_o$' is the base hydrogen production capacity of the 1 MW (or 1000 kW) unit (m^3 per hour), and '$\dot{V}$' is the production capacity of a unit larger than 1 MW (or 1000 kW). The superscript 'μ' is a scaling factor (0.707, **[119]**).

$$C^* = C_o\left(\frac{\dot{V}}{\dot{V}_o}\right)^{\mu} \tag{4.18}$$

Due to the non-linear nature of equation 4.18, the total cost of electrolyzer modules ranging from 1 MW to 30 MW has been pre-calculated and used as a parametric input in equation 4.17 above, '$C_{Electrolyzer,i}$' ($). The expression '$\alpha_i$' is used to denote the 30 binary variables that can either

have the value of 0 or 1. However, as will be described in section 4.2.3 (equations 4.21 and 4.22), only one of the 30 binary variables can have a value of 1. In this way the cost objective function remains a linear equation. The coefficient 'β' is used to account for the replacement cost (35% of capital cost) of the electrolyzer stacks. Therefore a value of β equal to 1.35 is assumed for this study.

Götz et al. provide unit costs of a 5000 kW (€400 per kW) and 110000 kW methanation reactor unit (€130 per kW) **[71]**. By converting this data to Canadian dollars, a linear trend line for cost is developed to account for economies of scale in methanation reactor size. The terms 'γ' ($1714.8 per m^3) and 'k' ($2,000,000) denote the slope and the intercept of this trend line and 'RNG_{Max}' is the variable that determines the maximum reactor capacity in equation 4.17.

The expression '$C_{Upgrading}$' ($ per methanation reactor capacity in cubic meter) is used to represent the total capital cost of a methane upgrading unit **[120]** in equation 4.17.

$$OPEX_{Annual,Case\ 1} = \left\{\sum_{h=1}^{8784}\left[C_{CO_2} \times CO_{2,h}\right]\right\} + \left\{\sum_{h=1}^{8784}\left[(HOEP_h + TC) \times E_h\right]\right\} + \left\{\sum_{h=1}^{8784}\left[C_{H_2O} \times WCR \times H_{2,h}\right]\right\} + \left[OPEX_{Annual,Upgrading} \times RNG_{Max}\right] \quad (4.19)$$

Equation 4.19 lists the operating expenditures incurred over the course of a year in '*Case 1: RNG/NG*'. The first term denotes the total annual cost associated with the biogenic CO_2 bought from the three biogas plants. Budzianowski et al. and Riva et al. report biogas production costs of €0.389 per m^3 (Application: Bio-methane and bioelectricity generation, **[121]**) and €0.355 per m^3 (Application: Electricity generation from biogas, [**122]**) from organic sources, respectively. In this study, the Canadian dollar equivalent average of the two reported costs is multiplied with the fractional CO_2 concentration in biogas (0.33 or 33%, **[110]** to determine the cost of biogenic CO_2 denoted by 'C_{CO_2}' ($0.172 per m^3) in equation 4.19. The term '$CO_{2,h}$' (m^3 per hour) denotes the hourly biogenic CO_2 flow directed to the methanation reactor.

The second term in equation 4.19 denotes the annual cost incurred from buying electricity for running the electrolyzers (E_h, kWh of energy consumed by electrolyzer) at the hourly Ontario electricity price ($HOEP_h$, $ per kWh **[123]**). An additional fixed transmission charge rate (TC $ per kWh) applied by Hydro One **[124]** is also considered in equation 4.19. The third term in equation 4.19 is used to estimate the annual expenditure associated with water consumption for electrolysis. The expressions 'C_{H_2O}' ($0.00314 per liter **[125]**), 'WCR' (liter per m^3 H_2, **[44]**) and '$H_{2,h}$' (m^3 per hour) denote the unit cost of water, the water consumption rate of the elctrolyzers and the hydrogen produced every hour. As shown in equation 4.19, the methane upgrading equipment has a fixed annual operating cost ($OPEX_{Annual,Upgrading}$, $ per m^3 **[120]**) and depends on the maximum capacity of the methanation reactor (RNG_{Max}, m^3 per hour).

4.2.2.4 Design Constraints (Case 1: RNG/NG)

Equations 3.2 and 3.3 shown under section 3.3.1 (Chapter 3) are used as design constraints for the electrolyzer model in this section. These equations will not be described again in this section. Since the main goal of the power to gas energy hub model is to run primarily during hours of surplus baseload generation, the hourly energy consumed by the electrolyzers (E_h, kWh) is constrained to not exceed the available hourly surplus baseload electricity in the Toronto power zone ($SBG_{Toronto\ Zone,h}$, equation 4.20).

$$E_h \leq SBG_{Toronto\ Zone,h} \tag{4.20}$$

As described earlier in equation 4.16, the maximum number of electrolyzers can't exceed 30. Equation 4.21 shows an equality constraint that used to constrain the number of electrolyzers ($N_{Electrolyzer}$) chosen by the solver between 1 and 30.

$$N_{Electrolyzer} = \sum_{i=1}^{30} i \times \alpha_i \tag{4.21}$$

The right-hand side of the above equation is the summation of the product between the parameter 'i' (also denoted as an index in equation 4.21) and the values taken by the 30 binary variables 'α_i'. Out of the 30 binary variables (α_i), only one of them can have a value of 1. Therefore, the summation of all 'α_i' for 'i= 1 to 30' is constrained to an upper bound of 1 in equation 4.22.

$$\sum_{i=1}^{30} \alpha_i \leq 1 \tag{4.22}$$

Equations 3.14-3.18 (under section 3.3.4, Chapter 3) are used as the design constraints for the methanation reactor in this case. These equation will not be explained again in this section as well. However, the parametric values of the hourly flow of CO_2 available ($CO_{2,avialable,h}$) used to constrain the maximum production capacity of the methanation rector (RNG_{Max}, m^3 per hour) in equation 3.16, is described as follows. The value of '$CO_{2,avialable,h}$' is determined from the ratio of total annual biogenic CO_2 available from the 3 biogas plants (6,246,451 m^3) and the total number of surplus baseload generation hours (4804 hours) in the Toronto power zone over the entire year.

From the above description, the hourly flow of biogenic CO_2 available throughout the year ($CO_{2,avialable,h}$, m^3 per hour) is estimated to be equal to 1300.26 m^3 of biogenic CO_2 per hour during the periods of surplus baseload generation and 0 otherwise (equation 3.16). This assumption enables all of the biogenic CO_2 to be available for producing renewable natural gas during surplus baseload generation hours.

$$(RNG_h + NG_h) \times HHV_{NG} = D_h \tag{4.23}$$

Equation 4.23 above shows the hourly energy demand balance at the pressure reduction station. The hourly demand 'D_h' (MMBtu per hour) is met by a combination of renewable and conventional natural gas. 'HHV_{NG}' (0.03623 MMBtu per m^3) is the higher heating value of natural gas **[93]**.

4.2.2.5 Case 2: Hydrogen Enriched Natural Gas (HENG)

Figure 4.3 below shows the flow diagram for the power to gas energy hub injecting hydrogen into the pressure reduction station. The end users, in this case, are supplied with a blend of hydrogen and natural gas (Hydrogen enriched natural gas: HENG).

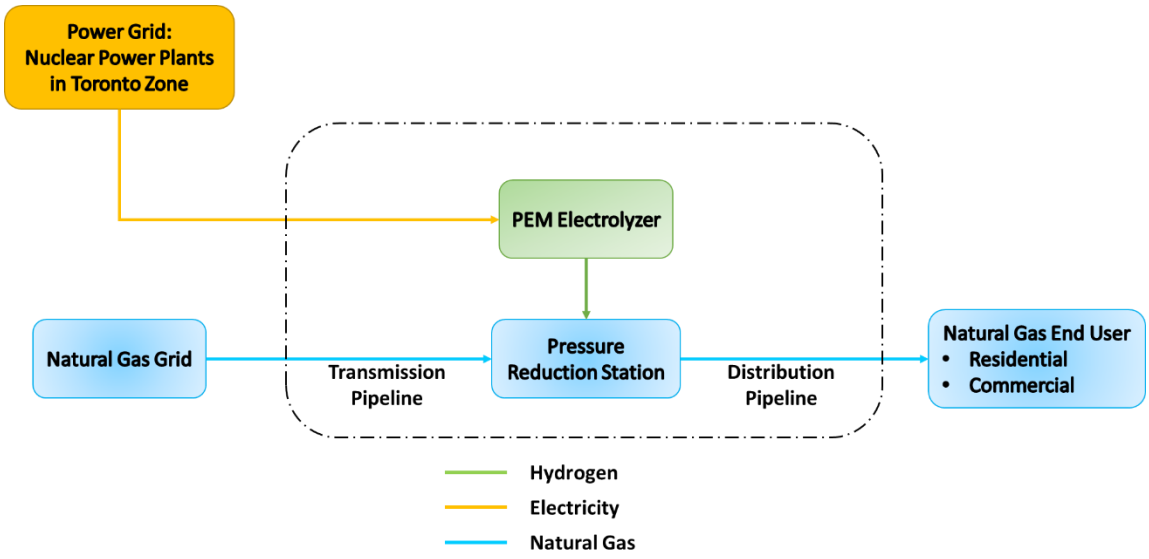

Figure 4.3: Flow diagram of power to gas energy hub for 'Case 2: HENG'

The methanation reactor and the associated upgrading equipment has been removed in figure 4.3.

4.2.2.6 Optimization Formulation (Case 2: HENG)

The formulation is as follows:

$$Minimize: Total\ Cost_{Case\ 2} = CAPEX_{Case\ 2} + \left(OPEX_{Annual,Case\ 2} \times TVM\right)$$

s.t.

ε-constraint (Annual Emissions Offset):

$$Emissions\ Offset_{Case\ 2} \geq \emptyset \times Emissions\ Offset_{Case\ 2,Max} \mid \{\emptyset = 0.1, 0.2, \dots, 1\}$$

Energy (Electrolyzer) and H_2, Flow Constraint:

$$H_{2,h} = \frac{\eta_{Electrolyzer} \times E_h}{E_{HHV,H_2}}$$

Energy (Natural Gas End User) Demand Constraint:

$$\left[H_{2,h} \times HHV_{H_2}\right] + \left[NG_h \times HHV_{NG}\right] = D_h$$

H_2 Concentration in Natural Gas Constraint and Electrolyzer Technological Specific (Active) Constraints: (4.24)

$$0.95 \times \left(H_{2,h}\right) \leq 0.05 \times NG_h$$

$$N_{Electrolyzer} \times E_{Electrolyzer,Min} \leq E_h \leq N_{Electrolyzer} \times E_{Electrolyzer,Max}$$

$$E_h \leq SBG_{Toronto\ Zone,h}$$

$$N_{Electrolyzer} = \sum_{i=1}^{30} i \times \alpha_i$$

$$\sum_{i=1}^{30} \alpha_i \leq 1$$

In this section a mixed integer linear programming optimization formulation with the primary objective (Total Cost) and the constraints it is subject to have been shown for the hydrogen

enriched natural gas case. The second objective function (Annual Emissions Offset) is included as an ε-constraint among the list of constraints.

The formulation consists of the integer variable $N_{Electrolyzer}$ (Number of electrolyzers) and the binary variables α_i. The problem also has continuous variables (e.g. E_h etc.) as well. Therefore the problem is a mixed integer linear programming problem. Appendix A.4.4 defines the nomenclature of the different variables and parameters used in the above formulation in equation 4.24.

4.2.2.7 Objective Functions (Case 2: HENG)

The environmental objective function in '*Case 2: HENG*' is given by equation 4.25. The expression '$Emissions\ Offset_{Case\ 2,Max}$' denotes the maximum annual lifecycle emissions offset (in Tonnes of $CO_{2,e}$) when HENG is used to meet the pressure reduction station demand.

$$Emissions\ Offset_{Case\ 2,Max} = Emissions_{NG} - Emissions_{HENG} \tag{4.25}$$

The estimation of '$Emissions_{NG}$' has already been explained in equation 4.11 (section 4.2.2.3).

$$\begin{aligned} Emissions_{HENG} &= \left\{\delta \times \sum_{h=1}^{8784} [(EMF_{NG} \times NG_h)]\right\} + \left\{\delta \times \sum_{h=1}^{8784} [EMF_{Nuclear} \times E_h]\right\} \\ &+ \left\{\sum_{h=1}^{8784} \left[EMF_{Electrolyzer} \times H_{2,h}\right]\right\} \end{aligned} \tag{4.26}$$

Equation 4.26 has been obtained from equation 4.13 (section 4.2.2.3) by omitting the factors contributing to emissions associated with renewable natural gas. The expressions in the above equation have been described in equations 4.13-4.15 within section 4.2.2.3.

$$Total\ Cost_{Case\ 2} = CAPEX_{Case\ 2} + \left(OPEX_{Annual,Case\ 2} \times TVM\right) \tag{4.27}$$

The cost objective function in '*Case 2: HENG*' is given by the total lifetime cost '$Total\ Cost_{Case\ 2}$' ($) in equation 4.27. The lifetime capital cost ($CAPEX_{Case\ 2}$, $) in case 2 (equation 4.28) is obtained by omitting the capital cost associated with the methanation reactor and upgrading equipment from equation 4.17 (section 4.2.2.3).

$$CAPEX_{Case\ 2} = \left\{\beta \times \sum_{i=1}^{30}\left[C_{Electrolyzer,i} \times \alpha_i\right]\right\} \quad (4.28)$$

Similarly, the annual operating cost ($) in case 2 ($OPEX_{Annual,Case\ 2}$, equation 4.29) has been obtained by omitting the cost associated with purchasing biogenic-CO_2 and the operating cost of the upgrading equipment from equation 4.19.

$$OPEX_{Annual,Case\ 2} = +\left\{\sum_{h=1}^{8784}\left[(HOEP_h + TC) \times E_h\right]\right\} + \left\{\sum_{h=1}^{8784}\left[C_{H_2O} \times WCR \times H_{2,h}\right]\right\} \quad (4.29)$$

4.2.2.8 Design Constraints (Case 2: HENG)

The energy demand constraint in case 2 is now as shown in equation 4.30 below, where, the demand is met by combination of conventional natural gas and hydrogen.

$$\left[H_{2,h} \times HHV_{H_2}\right] + \left[NG_h \times HHV_{NG}\right] = D_h \quad (4.30)$$

The amount of hydrogen that can injected within the natural gas pipelines are constrained to a 5 vol.% limit (equation 4.31). This assumption is taken from primarily from studies carried out by Melaina et al. **[40]** and after discussion with the natural gas utility operating the pressure reduction station.

$$0.95 \times \left(H_{2,h}\right) \leq 0.05 \times NG_h \quad (4.31)$$

The underlying optimization model constraints associated with the electrolyzer similar to what has been described in section 4.2.2.4 (Case 1: RNG/NG). The design constraints associated with the metanation reactor are not considered in this section as the energy hub in case 2 sends hydrogen-enriched natural gas to the end users.

4.3 Results

The mixed integer linear programming problems described in '*Case 1: RNG/NG*' and '*Case 2: HENG*' have been solved using the CPLEX solver in the 'General Algebraic Modeling System' software (version 22.6).

4.3.1 Power to Gas Energy Hub Configuration

Figure 4.4 below compares the annual $CO_{2,e}$ emissions offset achieved at each of the 10 emission offset targets when a blend of renewable and conventional natural gas (Case 1) and hydrogen enriched natural gas (Case 2) is sent to the end users.

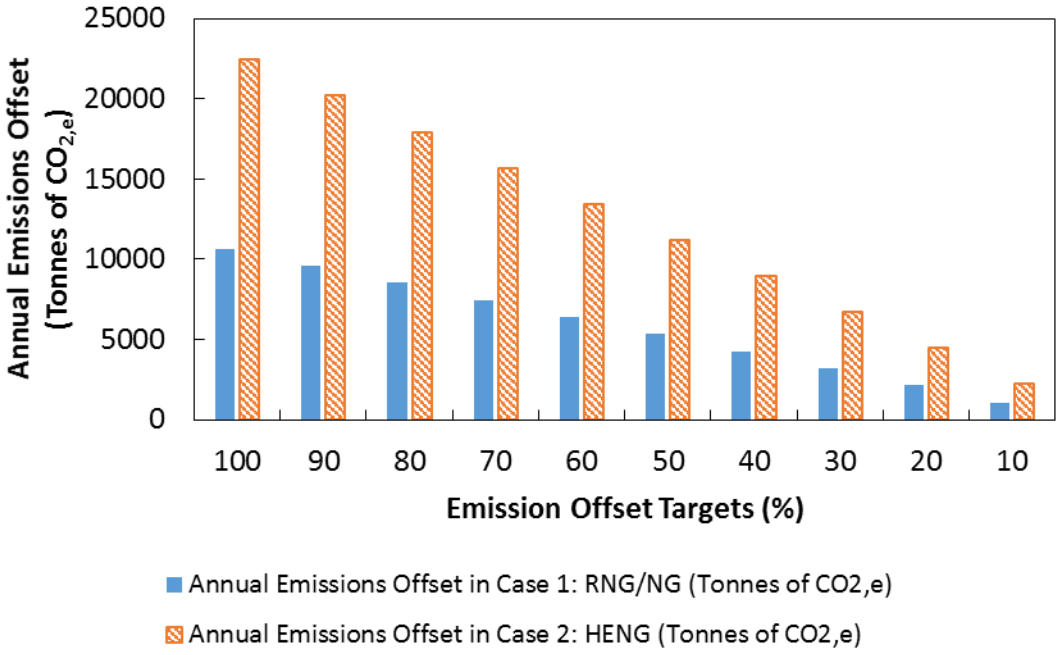

Figure 4.4: Annual CO2,e emission offset achieved for 'Case 1: RNG/NG' and 'Case 2: HENG'

The maximum annual $CO_{2,e}$ emission offset determined for cases 1 and 2 are 10,645.8 and 22,415.4 tonnes of $CO_{2,e}$. The x-axis in figure 4.4 is labelled as 'Emission Offset Targets (%)'. Each of the 10 targets represent a percentage of the maximum annual $CO_{2,e}$ emissions offset achieved in case 1 ($Emissions\ Offset_{Case\ 1,Max}$, equation 4.10) and case 2 ($Emissions\ Offset_{Case\ 2,Max}$, equation 4.25). The targets are set as a lower bound for the annual $CO_{2,e}$ emissions offset that need to be met for the total cost minimization problem in cases 1 ($Total\ Cost_{Case\ 1}$, equation 4.16) and 2 ($Total\ Cost_{Case\ 2}$, equation 4.27). From figure 4.4 it is seen that the solver chooses to meet the

emission offset targets exactly, as offsetting more emissions leads to increase in the total cost of the energy hub in both cases. Renewable natural gas and hydrogen both reduce emissions when blended with conventional natural gas. However, the emissions produced during the lifecycle of a cubic meter of renewable natural gas is higher due to:

- Every cubic meter of renewable natural gas requiring 4 m^3 of hydrogen. This increases the emissions associated with electricity consumption for hydrogen production.
- $CO_{2,e}$ emissions associated with CH_4 and N_2O released during its combustion
- Additional emissions associated with the collection and processing of organic waste.

The contribution of the above mentioned emissions have been detailed for the power to gas energy hub configurations with the lowest lifetime investment cost to lifetime emissions offset ratio in cases 1 (RNG/NG) and 2 (HENG) at the end of this sub-section.

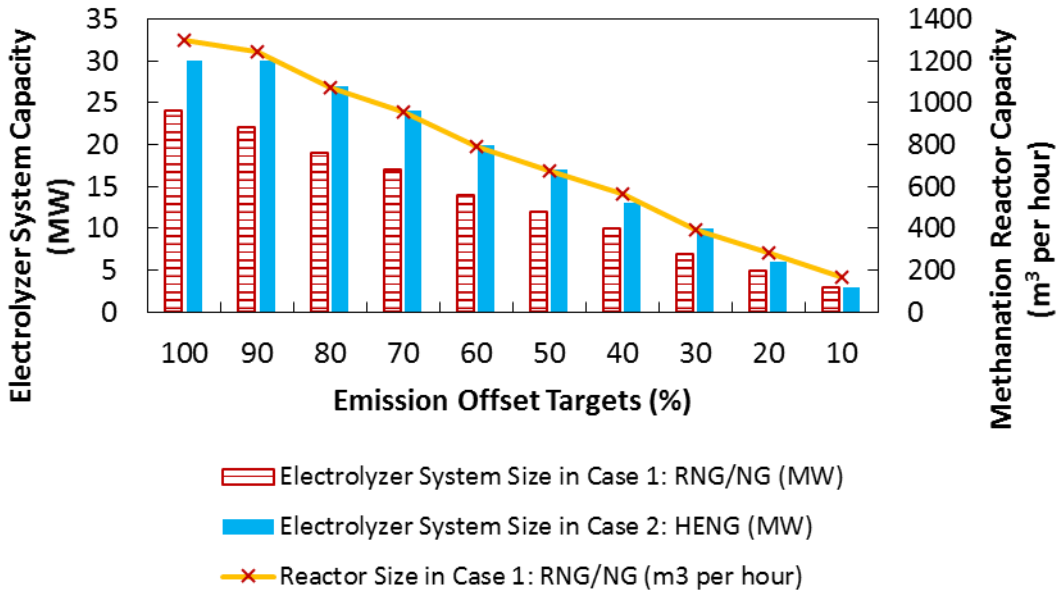

Figure 4.5: Electrolyzer and methanation reactor system size for Case 1: RNG/NG and Case 2: HENG

Figure 4.5 above shows the electrolyzer system size chosen to meet the 10 emission offset targets for '*Case 1: (RNG/NG)*' and '*Case 2: HENG*'. The figure also shows the corresponding methanation reactor capacities chosen for case 2 on the secondary vertical axis. As the strictness of the emission offset targets reduce from the 100% target to the 10% target, the electrolyzer system in both cases is seen to decrease. The maximum electrolyzer system sizes in cases 1 and 2

are 24 and 30 MW, respectively. As the higher heating value of hydrogen is one third of natural gas, a greater volume of hydrogen needs to be injected to make up for the same amount of energy content derived from natural gas. Therefore, the electrolyzer system size in case 2 (HENG) is higher in comparison to case 1 (RNG/NG) in figure 4.5.

The methanation reactor capacities shown in figure 4.5 are seen to decrease with the magnitude of the emission offset targets. The highest reactor capacity (for the 100% emission offset target) is seen to be 1300.3 m^3 of RNG per hour.

4.3.2 Operational Characteristics of Power to Gas Energy Hubs

The methanation reactor size to electrolyzer system hydrogen production capacity is seen to follow the stoichiometric ratios between H_2 and CH_4 from the Sabatier reaction (equation 3.12). This also implies that the capacity factor of the electrolyzer and methanation reactor in case 1 will be similar.

Table 4.5: Comparison of levelized cost of emission reduction in *Case 1* and *2*

Emission Offset Targets (%)	**Levelized Cost of Emission Reduction ($ Invested per Tonne of $CO_{2,e}$ Emissions Offset)**	
	Case 1: RNG/NG	**Case 2: HENG**
1	230.8	91.2
2	228.7	87.8
3	232.8	89.4
4	237.8	91.4
5	244.3	93.8
6	252	96.8
7	264.3	100.5
8	280	106
9	311.8	114.8
10	406.8	130.6

Table 4.5 above compares the levelized cost of emission reduction for the 10 emission offset targets in both case 1 (RNG/NG) and case 2 (HENG). The above values have been determined post-optimization. The levelized cost of emission reduction is the ratio of total lifetime cost and lifetime $CO_{2,e}$ emissions offset. The total lifetime cost corresponding to the 10 emission offset targets in cases 1 and 2 have been determined by the value of the objective functions $Total\ Cost_{Case\ 1}$ ($, equation 4.16) and $Total\ Cost_{Case\ 2}$ ($, equation 4.27). The 10 lifetime $CO_{2,e}$ emissions offset in both cases is determined by multiplying the values of

$Emissions\ Offset_{Case\ 1}$ (Tonnes of $CO_{2,e}$, equation 4.10) and $Emissions\ Offset_{Case\ 2}$ (Tonnes of $CO_{2,e}$, equation 4.25) by the 20 year lifetime of the project.

In both cases, the levelized cost of emission reduction is seen to initially decrease between emission offset targets 1 and 2 (table 4.5). For case 1 (RNG/NG), the electrolyzer system size and methanation reactor size decreases from emission offset target 1 to 2 (see figure 4.5). This leads to a slight increase in the unit cost paid for the electrolyzer ($ per kW) and methanation reactor systems ($ per m^3) as described by the economies of scale trend assumed in equation 4.17. Despite this fact, the lower levelized cost of emission reduction for emission offset target 2 ($228.7 per tonne of $CO_{2,e}$ emission offset) results from a greater operating cost decrease. The decrease in operating cost at target 2 here is a result of a lower annual average capacity factor (47.6%) for the 22 MW power to gas energy hub as compared to an annual average capacity factor of 48.5% for the 24 MW energy hub size for emission offset target 1.

In case 2 (HENG), the electrolyzer system size remains the same at 30 MW for emission offset targets 1 and 2. Therefore, the initial decrease in levelized cost of emission reduction between targets 1 and 2 is attributable to the decrease in the annual average capacity factor of the electrolyzer system from 53.5% at target 1 to 48.1% at target 2.

The increase in levelized cost of emission reduction post emission offset target 2 (table 4.5) in both cases is primarily attributable to the significant increase in the unit cost of electrloyzer and methanation reactors with the decrease in their size. The inference drawn from table 4.5 is that the emission offset target 2 in both cases 1 (RNG/NG) and 2 (HENG) results in the lowest levelized cost of emission reduction. The data can be interpreted as follows: '*For every $228.7 and $87.8 invested in power to gas energy hubs producing renewable natural gas and hydrogen enriched natural gas, 1 tonne of lifecycle $CO_{2,e}$ emissions is offset within the natural gas sector.*'

The best solutions for cases 1 (RNG/NG) and 2 (HENG) are able to consume only 1.73% and 2.38% of the total surplus baseload generation in Ontario for the year 2016. This implies that size of these power to gas units are not high enough to significantly reduce the exports of surplus baseload generation. Chapter 5 presents an analysis of the scale of power to gas system size required for consuming all of Ontario's surplus electricity.

Table 4.6 shows the contributors to the lifecycle emissions associated with the renewable natural gas sent to natural gas end users. The values shown are for the emission offset target 2 which achieves the lowest levelized cost of emission reduction in case 1 (RNG/NG).

Table 4.6: Contributors to lifecycle emissions of RNG for emission offset target 2 in Case 1 (RNG/NG)

Waste Collection and Biogas Facility Operation (over 20 years)	Production and End of Life – Electrolyzers and Reactor	Electricity Consumption (over 20 years)	Renewable Natural Gas Combustion (CH_4 and N_2O, over 20 years)
23434.5	3169.8	31281.7	1179322.6

Similarly, Table 4.7 shows the contributors to the lifecycle emissions associated with the hydrogen gas sent to natural gas end users. The values shown are for the emission offset target 2 which achieves the lowest levelized cost of emission reduction in case 2 (HENG).

Table 4.7: Contributors to lifecycle emissions of hydrogen for emission offset target 2 in Case 2 (HENG)

Production and End of Life – Electrolyzers	Electricity Consumption (over 20 years)
2178.9	43119.6

From the above two tables, it can be clearly seen that renewable natural gas has more contributors to emissions in comparison to hydrogen. Therefore, the emission offset target values seen in figure 4.4 are greater for case 2 (HENG) in comparison to case 1 (RNG/NG). From the analysis presented in this section it is seen that renewable natural gas production and distribution to end users leads to a lower value of lifecycle emissions offset and a higher investment and lifetime operating cost. This leads to it having a higher levelized cost of emission reduction (as seen in table 4.5) in comparison to hydrogen enriched natural gas being sent to the end user.

4.3.3 Electric Vehicle Lifecycle Emissions

This sub-section discusses the estimated levelized cost of emission reduction incurred by the Ontario government through the provincial electric vehicle incentive program. The 9056 registered electric vehicles (see table 4.2) at the end of 2016 form the basis of this analysis. The lowest levelized cost of emission reduction for case 1 (RNG/NG) and case 2 (HENG) are then compared to that of the electric vehicles.

Equations 4.1 and 4.2 are used to estimate the total emissions incurred during the production and end of life treatment of the electric vehicles. The emissions from the production of the 9056 electric vehicles is estimated to be 106,786 tonnes of $CO_{2,e}$. The end of life treatment of the electric vehicles has been estimated to be 5687 tonnes.

The annual electric charging associated emissions in scenario 1 (PHEV Utility Factor: 51.5%) for the electric vehicles is estimated from the charging profile developed in figure 4.1 and the emission factor of the grid at that time. The calculated value is 2430.5 tonnes of $CO_{2,e}$ emissions. Note that scenario 1 assumes that PHEVs (in table 4.2) initially run on their electric drivetrain until the range limit is hit. The PHEVs are then assumed to switch to the conventional gasoline powered drivetrain to complete the remainder of the assumed average 61 km daily trip distance for Ontario vehicles. Therefore, PHEVs in scenario 1 also emit 4457.2 tonnes of $CO_{2,e}$ emissions while running on gasoline over the course of a year. This value is estimated by determining the annual gasoline consumption from equation 4.5 and then multiplying it with the emission factor of gasoline (2.33 kg $CO_{2,e}$ per liter). Thus the total annual use phase emissions for electric vehicles in scenario 1 (PHEV Utility Factor: 51.5%) is 6887.7 tonnes of $CO_{2,e}$. This value translates to 55,101.6 tonnes of use phase lifecycle $CO_{2,e}$ emissions when multiplied with a vehicle lifetime of 8 years.

In scenario 2 (PHEV Utility Factor: 100%), the PHEVs are assumed to complete the entirety of the 61 km daily trip distance on the electric drivetrain. Therefore the total energy consumed by all the electric vehicles over the course of a day is higher in scenario 2 (figure 4.1). The annual use phase emissions is estimated to be 2909.3 tonnes of $CO_{2,e}$. This is equivalent to 23,274.4 tonnes of $CO_{2,e}$ emissions over the 8 year lifetime. This value is significantly lower than the annual emissions observed in scenario 1 (PHEV Utility Factor: 51.5%).

By adding the total emissions in the production, end of life treatment and use phases, the total lifecycle emissions in scenario 1 (PHEV Utility Factor: 51.5%) and scenario 2 (PHEV Utility Factor: 100%) are estimated to be 167,575.7 and 135,748.3 respectively.

In order to estimate the emissions offset by the electric vehicles, the lifecycle emissions associated with an equivalent number of gasoline vehicles has been estimated. The number of mini, medium, and large gasoline vehicles are determined based on the equivalent number of electric vehicles listed in those three size categories in table 4.2. The total production and end of life treatment phase emissions of all gasoline vehicles is estimated to be 57,760.2 and 4727.8 tonnes of $CO_{2,e}$. The lifecycle use phase $CO_{2,e}$ emissions has been estimated to be 249,875.5 tonnes for a 180,000 km lifetime mileage. The summation of the production, use and end of life treatment phases give a total lifecycle $CO_{2,e}$ emissions of 312,363.5 tonnes.

Table 4.8 summarizes the emissions incurred during each of the three phases for both electric and gasoline vehicles described above.

Table 4.8: Emissions breakdown and total lifecycle emissions offset by electric vehicles (8 year or 180,000 km lifetime)

Scenario	Production Phase Emissions (Tonnes of $CO_{2,e}$)	Use Phase Emissions (Tonnes of $CO_{2,e}$)	End of Life Treatment Emissions (Tonnes of $CO_{2,e}$)	Lifecycle Emissions (Tonnes of $CO_{2,e}$)	Lifecycle Emissions Offset (Tonnes of $CO_{2,e}$)
1 (PHEV Utility Factor: 51.5%)	106,786	55,101.6	5687	167,575.7	144,787.8
2 (PHEV Utility Factor: 100%)	106,786	23,274.4	5687	135,748.3	176,615.2
Gasoline Vehicles	57,760.2	249,875.5	4727.8	312,363.5	-

The lifecycle $CO_{2,e}$ emissions offset are estimated from the difference between gasoline vehicle lifecycle emissions and the lifecycle emissions of the electric vehicles under scenario 1 and 2 (table 4.8). The electric vehicles under scenario 2 (PHEV Utility Factor: 100%) are able to achieve a greater emission offset due to the lower use phase emissions while running entirely on their electric drivetrain.

4.3.4 Comparing Levelized Cost of Emission Reduction for Electric Vehicles and Power to Gas

The reduction on manufacture suggested retail price (MSRP) of an electric vehicle has been listed for the different models in table 4.2. The incentives associated with free off-peak charging (for a period of 4 years during a vehicle's lifetime, 2017-2020 **[**Error! Bookmark not defined.**]**) and i nstalling home/facility charging stations **[**Error! Bookmark not defined.**]** have been mentioned at the end of section 2.1. Table 4.9 provides a breakdown of the total incentive received by the electric vehicles listed in table 4.2.

Table 4.9: Breakdown of total monetary incentives given to electric vehicles existing at the end of 2016

Scenario #	Reduction on MSRP	Free off-peak charging (over 4 years)	Charging Station	Total Incentive
Scenario 1 (51.5% Utility Factor)	$111,914,615	$7,017,567.97	$9,056,000	$127,988,183
Scenario 2 (100% Utility Factor)	$111,914,615	$8,400,043.73	$9,056,000	$129,370,658.7

From the above table, it can be seen that the major portion of the incentives or the cost to the provincial government for promoting electric vehicles in Ontario go towards offering a reduction on the manufacture suggested retail price. Scenario 2 (100% Utility factor) has a greater total

incentive value due to a higher amount of electricity being consumed during off-peak hours to complete the entirety of the trip distance on the electric drivetrain.

Due to lack of data electric vehicle ownership, it is difficult to determine the number of charging stations to electric vehicles ratio for organizations/facilities owning multiple electric vehicles. Therefore, the total incentive given for helping electric vehicle owners install charging stations is estimated by a simplifying assumption of 1 charger per vehicle.

The data presented in table 4.9 can now be used to estimate the levelized cost of emission reduction incurred by the provincial government by using electric vehicles to offset $CO_{2,e}$ emissions. The ratio of total incentives (table 4.9) to lifecycle emissions offset (table 4.8) is estimated to be $883.9 per tonne of $CO_{2,e}$ emission offset for scenario 1 where both the gasoline and electric drivetrains are used in the PHEVs (from table 4.2) to complete the daily trip distances over their lifetime. Similarly, the ratio of total incentives to lifecycle emissions offset for scenario 2 where entirety of daily trip distances over the lifetime of the PHEVs are completed on the electric drivetrain is $732.5 per tonne of $CO_{2,e}$ emission offset.

The levelized cost of emission reduction for EVs under scenario 1 and 2 ($883.9 and $732.5 per tonne of $CO_{2,e}$ emission offset) is much higher in comparison to that of the best solution obtained from the optimal sizing of the power to gas energy hubs producing renewable natural gas and hydrogen enriched natural gas ($228.7 and $87.8 per tonne of $CO_{2,e}$ emission offset). The levelized cost of emission reduction for EVs under scenario 1 (51.5% Utility Factor) and 2 (100% Utility Factor) is seen to decrease to $578.4 and $488.1 per tonne of $CO_{2,e}$ emission offset when their lifetime mileage increases to 250,000 km. Therefore, current EV policies within the province will get more cost effective with further development of the electric vehicle technology.

4.3.5 Discussion on Policy Perspective

Power to gas energy hubs and electric vehicles offer the ability to use clean electricity from the power grid in Ontario. However, they differ in their

- Impact on the electricity grid,
- Effect on associated Canadian companies,
- Versatility,

- Infrastructural needs, and public acceptability

The above topics are briefly touched on in the following sections.

4.3.5.1 Comparing Impact of Pathways on the Power Grid

As consumers of electricity, power to gas and electric vehicles have different impacts on the grid. A power to gas system can act as a flexible load to the grid that can be operated to not act as a contributor to peak electricity demand. In this study the power to gas energy hubs only operate during periods of surplus baseload generation. The produced hydrogen has various energy recovery pathways that enable the repurposing of surplus electricity within Ontario rather than having to invest in costly transmission line upgrades to sell electricity to neighboring electricity markets **[126]**.

Although charging of electric vehicles may happen in times of surplus generation, this is not always the case. Electric vehicle owners may need to charge their vehicles in periods of peak demand which creates the need for further development of peak electricity generation capacity. These peak generation capacities are usually gas-fired plants (in Ontario) which will add to the charging associated emissions. Axsen et al. **[100]** mention the interest from vehicle owners to enroll in a 'utility controlled charging' program where the power utility controls the vehicle charging pattern when plugged in, to maintain grid reliability. However, they also highlight that not all vehicle owners will be willing to enroll in such a program due to concerns related to personal privacy and vehicle battery degradation. Canada's population in 2016 was roughly 36.2 million **[127]**. The number of passenger vehicles registered in Canada (2016) was approximately 22.4 million **[128]**. The ratio of vehicles to population is a high value of 0.62. Therefore, even if electric vehicles become the primary choice among vehicle owners in the future, the increase in electric vehicle numbers create the need for significant generation upgrades, and potential reinforcement for power transmission and distribution lines due to the increased demand. Even though electric vehicles provide one of the best alternative to reducing emissions in the transportation sector, there will still be a significant impact on how the power system in Ontario will be developed.

4.3.5.2 Versatility of Pathways

The goal of implementing support policies for electric vehicles is using the emission-free power available in the electricity sector to reduce emissions in the transportation sector.

In this work, power to gas energy hubs have been used to only produce renewable natural gas and hydrogen to increase the renewable content in the natural gas system. However, the hydrogen produced from surplus electricity can also provide:

- Fuel for transportation (for fuel cell vehicles)
- Hydrogen for industrial applications such as in oil refineries **[129]** and glass manufacturing, and
- Emission-free power via fuel cell modules.

Having multiple pathways means a power to gas system can contribute to emission reduction in the transportation sector, the residential sector, and the industrial sector. Thereby creating an efficient integrated energy system.

Sisternes et al. **[130]** show that energy storage systems not only increase the power factor of currently installed generation capacity but are also useful in increasing the implementation of new renewable generation resources in the electricity system. This means that incentivizing power to gas systems will also complement the incentives for renewable energy technologies (feed-in-tariffs).

4.4 Conclusion

Increasing penetration of intermittent renewable energy generators within electricity markets has its advantages if grid reliability is maintained. This study presents the case of Ontario, which plans to increase its wind generation portfolio to 23.8% of generation capacity by 2032. During the initial transition towards realizing this goal, the province of Ontario has experienced increased periods of surplus baseload generation. The contributors to surplus baseload generation within the province include its nuclear, wind and hydroelectric generation assets. In order to recover a share of the cost of this surplus electricity the province exports electricity to neighboring jurisdictions at a low price.

The issue of surplus baseload generation in Ontario provides an opportunity to use electricity in ways that could extend its environmental benefits to end users not constrained to the electricity sector. A good example of this is the transition towards the use of electric vehicles that can utilize

the clean electricity within the province. The implementation of such technologies requires effective energy policies that allow the transition towards their widespread adoption.

Through the electric vehicle incentive program, Ontario government promotes the purchase of electric vehicles and use of surplus electricity for vehicle charging. The climate change action plan of Ontario also cites power to gas as a viable option for consuming surplus electricity and produce hydrogen for use as an energy vector within the natural gas and transportation sector. However, current policy framework for technologies such as power to gas are in the developmental phase.

Through two mixed integer linear programming problems, this study presents optimal configurations for two power to gas energy hubs. The power to gas energy hubs are modeled to produce renewable natural gas and hydrogen enriched natural gas that is injected at a pressure reduction station and distributed to natural gas end users of Enbridge Inc.. The power to gas energy hubs run only during suplus baseload generation hours to produce hydrogen. Renewable natural gas is produced via the methanation process. The CO_2 source for methanation is biogenic in nature and is derived from 3 biogas producing plants in the greater Toronto area.

The key outputs of the optimization study are:

- The lifecycle emissions offset at the natural gas end users via renewable natural gas and hydrogen enriched natural gas, and
- Lifetime investment cost of the optimal power to gas energy hub configurations for renewable natural gas and hydrogen enriched natural gas.

These two key outputs are combined to derive the levelized cost of emission reduction or the dollar invested per tonne of $CO_{2,e}$ emissions offset. The values for the case of renewable natural gas and hydrogen enriched natural gas have been estimated to be $228.7 and $87.8 per tonne of $CO_{2,e}$ emission offset.

In order to compare these values with an existing policy, the cost incurred by the Ontario government to reduce a tonne of $CO_{2,e}$ emissions via the electric vehicle incentive program has been estimated. This calculation is based on a lifecycle emissions and emissions offset analysis carried out for the 9056 electric vehicles that existed in Ontario at the end of 2016. The analysis

presents two scenarios. Scenario 1 assumes that the 4296 plug in hybrid electric vehicles among the 9056 electric vehicles have a utility factor of 51.5% (or when they deplete their electric range before switching to gasoline range to complete daily trips of 61 km). In this scenario, the province invests $883.9 for every tonne of $CO_{2,e}$ emissions offset by all 9056 vehicles over their lifetime driving distance of 180,000 km. Scenario 2 assumes all plug in hybrid electric vehicles have a 100% utility factor. In this scenario, the province invests $732.5 for every tonne of $CO_{2,e}$ emission offset by the electric vehicles over a 180,000 km lifetime driving distance.

Through the results of this study, it can be seen that power to gas systems have the potential to repurpose surplus baseload electricity and produce hydrogen enriched natural gas and renewable natural gas for natural gas sector use within the province. The levelized cost of emission reduction for power to gas energy hubs is lower in comparison to the existing electric vehicle incentive program costs incurred by the government. Ontario requires energy technologies that complement and enable the effective utilization of clean electricity generators. The levelized cost of emission reduction presented in this study can serve as a metric towards shaping policies for technologies such as power to gas for their widespread implementation.

Chapter 5: Scale of Power to Gas System Size Required to Absorb Ontario's Surplus Electricity

The work presented in this chapter is based on a collaboration between Ehsan Haghi and Ushnik Mukherjee. The analysis presented here has been carried out by Ushnik Mukherjee, while Ehsan Haghi contributed with providing key insights on writing about the potential use of hydrogen within the province.

5.1 Introduction

In chapter 4, the optimally sized power to gas energy hubs were constrained to not exceed the 30 MW electrolyzer capacity. This was done because the maximum size of commercially available PEM electrolyzers were 30 MW **[44]**. The 22 MW and 30 MW electrolyzer system designed in chapter 4 for producing renewable natural gas (Case 1) and hydrogen enriched natural gas (Case 2), respectively were only able to consumed 1.73% and 2.38% of the total surplus baseload electricity generated in Ontario at the end of 2016. Therefore, it is of interest to understand the potential size of electrolyzer systems required to absorb all of Ontario's surplus electricity.

In this chapter a brief overview of the Independent Electricity System Operator's (IESO's) definition of deploying different types of energy storage systems used to store surplus electricity will be presented. This chapter will also highlight briefly what could be the best power zones where power to gas energy hubs can be deployed. Our focus will only be limited to the power to gas energy recovery pathways that involve converting electricity to produce hydrogen, and renewable natural gas for the natural gas and transportation sectors. Finally, the chapter will also highlight the electrolyzer system size required to consume all of Ontario's surplus electricity. This analysis will be based off of the year 2016.

The IESO in its 2016 energy storage report categorizes energy storage technologies depending on how they use electricity after connecting with the power grid. There are broadly three categories, namely, type 1, 2, and 3 **[131]**. Type 1 energy storage technologies store electricity for a short period of time (maximum over few days) and then re-inject it back to the grid when required (e.g.:

batteries, flywheels, compressed air etc.). Type 2 energy storage technologies use electricity from the grid to store and then displace on-site electricity consumption at a later time point. Examples of this category can include heat storage units or ice production plants **[131]**. Type 3 energy storage technologies are systems that repurpose electricity in a different energy sector by converting electricity in to another energy vector. Power to gas, and electric vehicles can be an example for type 3 categories.

According to the IESO, energy storage technologies (Type 1) that store electricity for a short period of time will only be able to provide limited benefits **[131]** as the power grid will continue to experience limited periods of non-surplus generation until 2024 **[13]**. The auditor general report released in 2015 predicts that surplus generation will drop down to ~1-2% of net demand from current levels of 6-7% post 2024 due to the shutting down of Pickering nuclear generation station. Therefore, the IESO highlights that technologies that can store electricity over longer durations (months, seasonally) and ones that can repurpose electricity in another energy sector will be most beneficial for managing surplus baseload generation **[131]**.

5.2 Favorable power zones in Ontario to install power to gas energy hubs

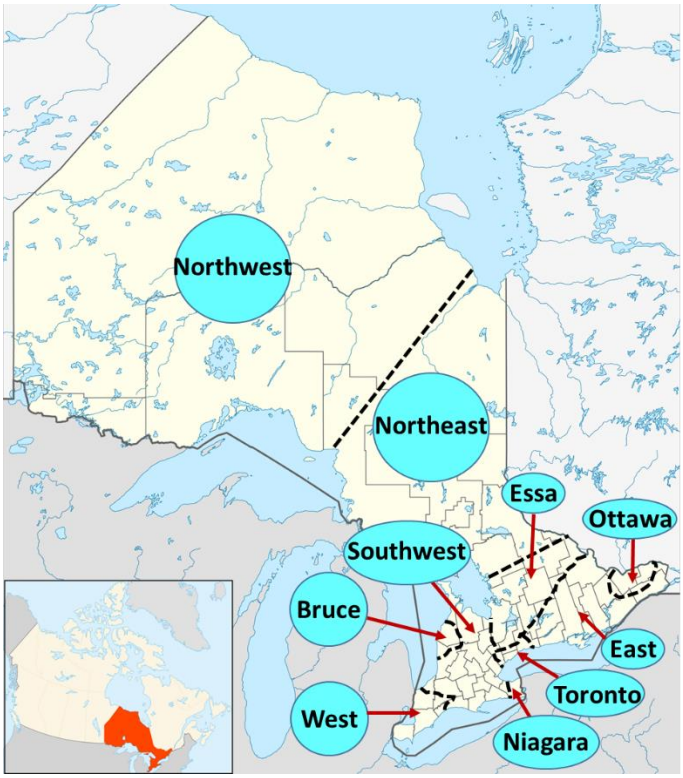

Figure 5.1: An overview of the boundaries separating the 10 different power zones in Ontario

Figure 5.1 above shows the 10 different power zones that exist in Ontario. Table 5.1 below shows contribution of the 9 power zones towards total generation output in 2016. Note that total generation output in this case only includes the sum of electricity generated by wind, nuclear and hydroelectric power plants in Ontario. The Ottawa power zone does not have either of three electricity generators used to estimate surplus baseload generation (wind, nuclear and hydroelectric power plants) and therefore has not be included in table 5.1.

Table 5.1: Contribution of power zones towards total wind, nuclear and hydroelectric generation output in 2016

Power Zone	**Contribution (%)**
Bruce	36%
Toronto	34.8%
Niagara	8.5%
East	6.8%
Northeast	4.7%
Southwest	2.7%
Northwest	2.6%
West	2.6%
Essa	1.3%

The IESO's report on energy storage **[131]** lists the power zones favorable for type 1, 2, and 3 storage technologies. However, in this chapter our focus will primarily be on highlighting the favorable power zones where type 3 (power to gas energy hubs) storage technologies can be installed.

East and Southwest: The East and Southwest power zones (see figure 5.1) in most parts are neither capacity nor load congested. This will allow power to gas energy hubs to draw from power grid at any time point over the course of a day. The only region within the Southwest power zone where power to gas will be restricted from operating during peak load hours is the Kitchener-Waterloo-Cambridge-Guelph (KWCG) area. The KWCG area is load congested during periods of peak demand. Hydrogen refueling stations in populous areas such as the KWCG could benefit from utilizing surplus electricity to produce and store hydrogen for fuel cell vehicles. Hydrogen and renewable natural gas can also be produced in these areas while using surplus electricity to directly inject it at natural gas distribution pipelines for space heating. The source of CO_2 from local biogas farms within the Southwest and East power zones could be a potential way of producing renewable natural gas **[132]**.

West: Since the West power zone (see figure 5.1) at times only gets capacity congested when the natural gas fired generation stations within the zone are operating, power to gas energy hubs will be able to withdraw electricity from the grid without any restriction in this zone. The West power zone also houses the Dawn hub's underground natural gas storage infrastructure. Hydrogen produced within this zone could be stored seasonally in underground storage sites at the Dawn hub. The West and Southwest power zones are well connected by big transmission pipelines (see figure 5.1 and figure 2.4 in section 2.2.2) with bi-directional flow. Since, the Southwest power zone houses a greater number of biogas plants in Ontario **[132]**, renewable natural gas produced in this zone can then be transported via Union Gas's transmission line capacity to Dawn hub's underground storage infrastructure.

Northwest, Northeast, Bruce, Niagara: The Northwest, Northeast, Bruce and Niagara power zones are capacity congested **[131]**. Therefore a power to gas energy hub acting as a load, can draw electricity at any time without being limited. The Bruce power zone especially is a good site for large scale hydrogen production because of the power zones massive nuclear generation

capacity. The Niagara power zone has hydroelectric power plants with energy storage capacity, therefore electricity excess to its storage capacity can be directed to electrolyzers for hydrogen production and injection into the natural gas transmission pipelines coming into the Niagara power zone from the US (see figure 2.4 in section 2,2,2). The Northwest and Northeast power zones primarily have hydroelectric power plants with lower or no water storage capacity, therefore this makes it ideal for power to gas energy hubs to produce hydrogen and inject it along different points of the TransCanada transmission pipeline bringing natural gas from western Canada. Hydrogen can also serve as a transportation fuel in each of these zone in fuel cell vehicle refueling stations.

Toronto and Essa: The Toronto and Essa power zones are load congested, especially the highly populous greater Toronto-Hamilton area (GTHA) **[131]**. Therefore power to gas energy hubs within these zones will be constrained to primarily operate during non-peak hours. Similar to the KWCG area in the Southwest power zone, the GTHA area within the Toronto power zone have the potential to utilize surplus electricity for hydrogen production and use at fuel cell vehicle refueling station. The well connected natural gas distribution and transmission pipelines going through these zones can enable hydrogen injection within them for space heating purposes. The production of renewable natural gas in these power zones will be limited due to lower number of biogas plants existing within them **[132]**.

5.3 Required hydrogen production capacity for absorbing surplus electricity

This section presents a simple analysis where the size of the electrolyzer system is iteratively increased to assess: 1) The fraction of total surplus baseload generation it is capable of consuming in (Ontario) 2016; 2) The average operating level of the electrolyzer during hours when hydrogen is being produced, and 3) The levelized production cost of hydrogen for a 20 year project lifetime.

The data of hourly surplus baseload generation occurring in Ontario for the year 2016 has been used. It is assumed that in hours when surplus baseload generation (MWh) is greater than the electrolyzer system size, the electrolyzers run at full capacity. Otherwise, the electrolyzers run at a value equal to the amount of surplus baseload generation available. The levelized cost of hydrogen includes the capital and replacement cost of the electrolyzers, the cost of water to produce hydrogen, and the cost of buying electricity at the hourly Ontario electricity price. The

unit cost ($ per MW) of the electrolyzer system has been modified with the increase in system size to account for economies of scale (see equation 4.17, section 4.2.2). Water consumption rate is based on values provided by Hydrogenics **[44]**. All calculations mentioned above have been carried out in Microsoft Excel (Version 2013).

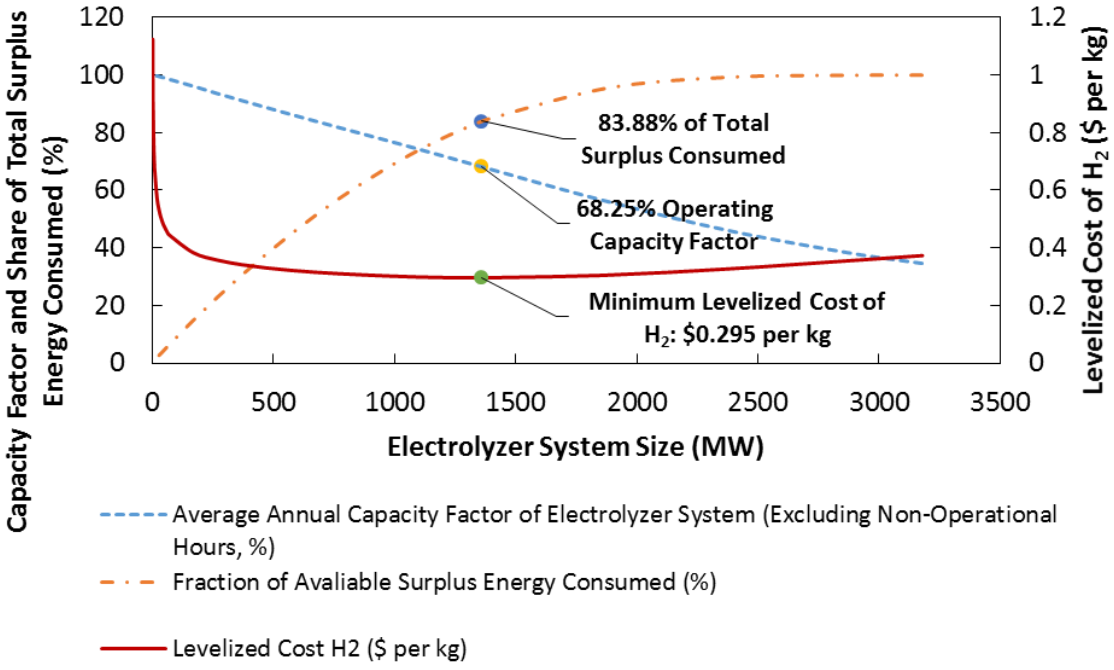

Figure 5.2: A plot showing the variation in capacity factor, total amount of surplus electricity consumed and the levelized cost of hydrogen with the change in electrolyzer system size

Figure 5.2 shows a plot of how the change in electrolyzer system size effects: 1) The annual average operating level of the electrolyzer in hours when it is consuming surplus electricity (or capacity factor); 2) The fraction of annual available surplus energy consumed; and 3) The levelized cost of hydrogen. As the electrolyzer system size is increased, it is able to consume a greater portion of the surplus electricity available. However, since all the hours throughout a year do not have the same surplus electricity generation, the annual average capacity factor (or operating level) of the electrolyzer is seen to decrease with increase in system size. The levelized cost of hydrogen is seen to be high at smaller electrolyzer system size due to a higher unit cost of the system. As electrolyzer system size increases, economies of scale lowers the unit cost of electrolyzers, thereby enabling hydrogen to be produced at lower cost. The three points highlighted in figure 5.2 are used to denote the lowest levelized cost of hydrogen achievable ($0.295 per kg). The corresponding electrolyzer system size for this is 1359 MW. The capacity factor and the percentage of annual

surplus electricity consumed by 1359 MW electrolyzer system is 68.25%, and 83.88% (or ~4.45 TWh of surplus electricity consumed), respectively. An electrolyzer system ~3179 MW can consume all of Ontario's surplus electricity produced in 2016. The total surplus baseload generation in Ontario at the end of 2016 was ~5.3 TWh. The auditor general of Ontario projects average surplus baseload generation (including wind, and nuclear curtailment, solar shutoff and hydro spill off) between 2017 and 2032 to be close to 4.03 TWh **[13]**. The 1359 MW electrolyzer system size that is able to achieve the lowest levelized hydrogen cost in figure 5.2, will be able to absorb most of the surplus electricity between 2017 and 2032.

However, this analysis only tries to highlight the potential of power to gas energy hub to absorb surplus electricity. This chapter only tries to highlight the fact that as the market for technologies that can form an interlink between clean electricity generation and different energy sectors (such as natural gas and transportation sector: battery electric and fuel cell electric vehicles) grows, power to gas will certainly be a relevant option for the future.

Chapter 6: Development of a Pricing Mechanism for Valuing Ancillary, Transportation and Environmental Services Offered by a Power to Gas Energy System

The following chapter is based on two articles. The first article has been published in the International Journal of Environmental Studies under the name: '*Power to Gas in a Demand Response Market*' in 2016. This has been authored by Ushnik Mukherjee, Sean Walker, Michael Fowler and Ali Elkamel. The second article is work published in the journal called Energy in 2017. The title of the work is '*Development of a Pricing Mechanism for Valuing Ancillary, Transportation and Environmental Services Offered by a Power to Gas Energy System*'. It has been authored by Ushnik Mukherjee, Sean Walker, Azadeh Maroufmashat, Michael Fowler and Ali Elkamel.

The first author's primary contribution in both articles was to develop the formulation in GAMS, and writing the article. Sean Walker helped with developing some of the energy hub conceptual figures and writing parts of both articles. Azadeh Marourmashat helped with providing key insights in modeling formulation in the second article. Ali Elkamel and Michael Fowler provided helpful guidelines in preparing the two articles for publication.

6.1 Introduction

In this chapter an optimization model of a power to gas energy hub having a hydrogen production module capacity of 2 MW has been developed. The goal of the optimization study is to carry out an economic feasibility of the energy hub under existing pricing mechanisms for the three primary services that it provides, namely: 1) Offsetting CO_2 emissions at natural gas end users by providing hydrogen enriched natural gas; 2) Providing demand response when directed by the Independent Electricity System Operator of the province, and 3) Providing pure hydrogen to a fuel cell vehicle refueling station. It is observed that current pricing mechanisms are not valued high enough for the power to gas energy hub to be economically feasible and payback period longer than the project lifetime (20 years) has been observed. Therefore, through a post-processing economic calculation, the additional monetary incentive required for the energy hub to achieve a NPV equal to zero for

shorter project lifetimes of 8, 9 and 10 years have been calculated. The required additional monetary incentives (for the new project lifetimes) have then been split proportionally to the share of the revenues earned by the energy hub while providing each of the three services. Through this, the existing pricing mechanisms have been scaled up and a new pricing mechanism has been developed that highlights the monetary requirements of a power to gas energy hub to be economically feasible. To the best of the author's knowledge, pricing mechanism for valuing the services offered by the energy hub in this study have not been reported in the literature.

6.2 Methodology: Parametric data development

The methodology section presents the steps taken to develop the parametric data associated with hydrogen demand and the demand response ancillary service provided by the power to gas energy hub. This section also highlights the power to gas energy hub components considered in this study.

6.2.1 Hydrogen demand data

The characteristic shape of the hydrogen demand curve used in this paper is based off of the '100 kg per day default Chevron Demand Profile' from the Hydrogen Refueling Station Analysis Model (HRSAM) developed by the National Renewable Energy Laboratory (NREL) **[91]**. In order to account for variations in the total daily demand placed on the station over a period of one week, variability data from a feasibility analysis of a hydrogen fueling station in Honolulu is considered **[133]**.

Pratt et al. **[134]** highlight three near-term hydrogen filling station capacities: 100 kg per day, 200 kg per day, and 300 kg per day. The filling stations having a capacity of 100 and 200 kg are suitable for large city centers where the demand fits the 'low use commuter or intermittent station classifications' **[135]**. The 300 kg per filling station is better suited for an urban market with high demand, and can be categorized as a 'High Use Commuter' fueling station. However, the 2 MW PEM electrolyzer systems can meet a daily hydrogen demand of 300 kg with sufficient capacity to spare. Therefore a scaled up hydrogen demand curve based off of Mukherjee et al.'s **[136]** previous work has been used here.

In their work, Mukherjee et al. **[136]** develop a linear programming optimization problem to size the on-site tank storage and compression capacity for a 2 MW power to gas plant. The size of the electrolyzer system in their work is fixed as it is based off of a real life demonstration project being developed in the greater Toronto area. The purpose of the work was to assess the maximum daily hydrogen demand that can be supplied by the 2 MW system while providing demand response service to the power grid. The hydrogen demand profile of the 100 kg per day refueling station is scaled up manually until the optimization problem gives an infeasible solution. In other words this implies that the hydrogen demand placed on the energy hub goes unsatisfied. The conclusion of their work shows that the 2 MW power to gas energy hub can meet a maximum daily hydrogen demand of 670 kg from a refueling station while also satisfying demand response requirements placed on it by the power grid. The 670 kg per day hydrogen demand value in **[136]** is used in this study as well.

6.2.2 Energy hub configuration

The final configuration of the energy hub proposed by Mukherjee et al. **[136]** includes:

- 2 x 1 MW PEM electrolyzers **[44]** for producing hydrogen;
- 1 storage tank with a maximum capacity of 89 kg at 172 bar (ASME Steel) **[62]**;
- A three stage reciprocating booster compressor capable of handling inlet pressures as low as 20 bar (compression ratio ~ 21) and has a capacity of 87 kg per h; and,
- A pre-storage reciprocating compressor developed by RIX Industries **[91]** that has a maximum flow handling capacity of 42 kg per h and can compress hydrogen gas from 3 bar to 310 bar.

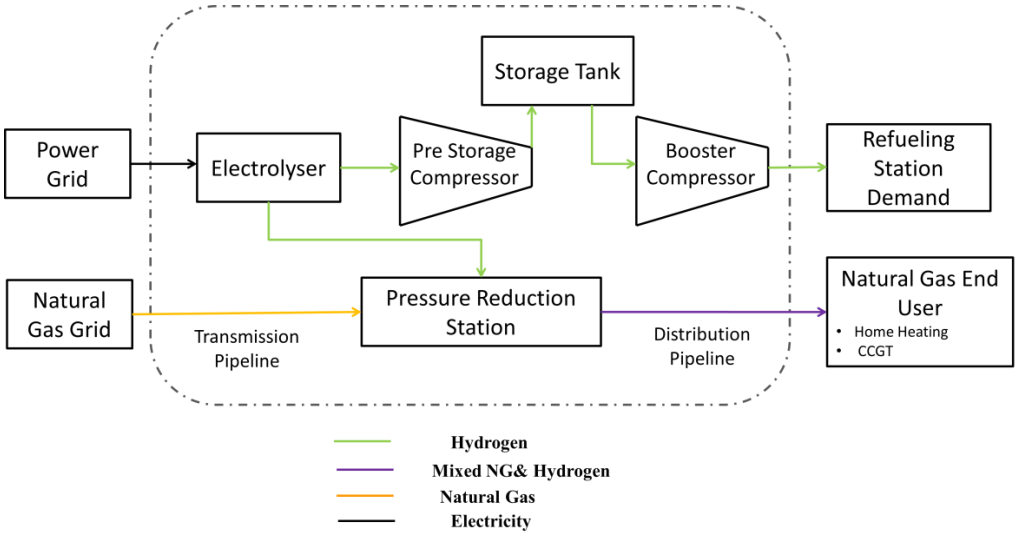

Figure 6.1: Conceptual overview of the energy hub

The component sizes outlined above will be utilized in this study as well. Figure 6.1 shows the overall conceptual diagram of the 2 MW power to gas energy hub proposed in the study. The difference between this work and **[136]** is that the energy hub is co-located at a natural gas pressure reduction station.

As shown in Figure 6.1, a fraction of the hydrogen produced by the electrolyzer is sent directly to the pressure reduction station where the gas is mixed with natural gas to form HENG and injected in to low pressure distribution lines. The compressors and storage tank unit are a part of an integrated system that provides pure hydrogen to a hydrogen refueling station. Hydrogen produced for satisfying fuel cell vehicle (FCV) fuel demand passes through a pre-storage reciprocating

compressor that compresses gas coming in at 30 bar and 21°C to the storage tank pressure of 172 bar. The booster compressor placed outside the tank is used to compress hydrogen gas coming out of the tank to 350 bar, which is considered to be the storage pressure of hydrogen gas on board fuel cell vehicles **[91]**. The temperature assumed for calculating the properties of hydrogen is taken to be 21°C which is temperature at which hydrogen is stored on board fuel cell vehicles **[91]**.

6.2.2 Demand response data

The energy hub provides hourly load following demand response services through load reductions, as directed by the IESO. The hourly load-following requirement of the grid is calculated via the schematic shown in Figure 6.2.

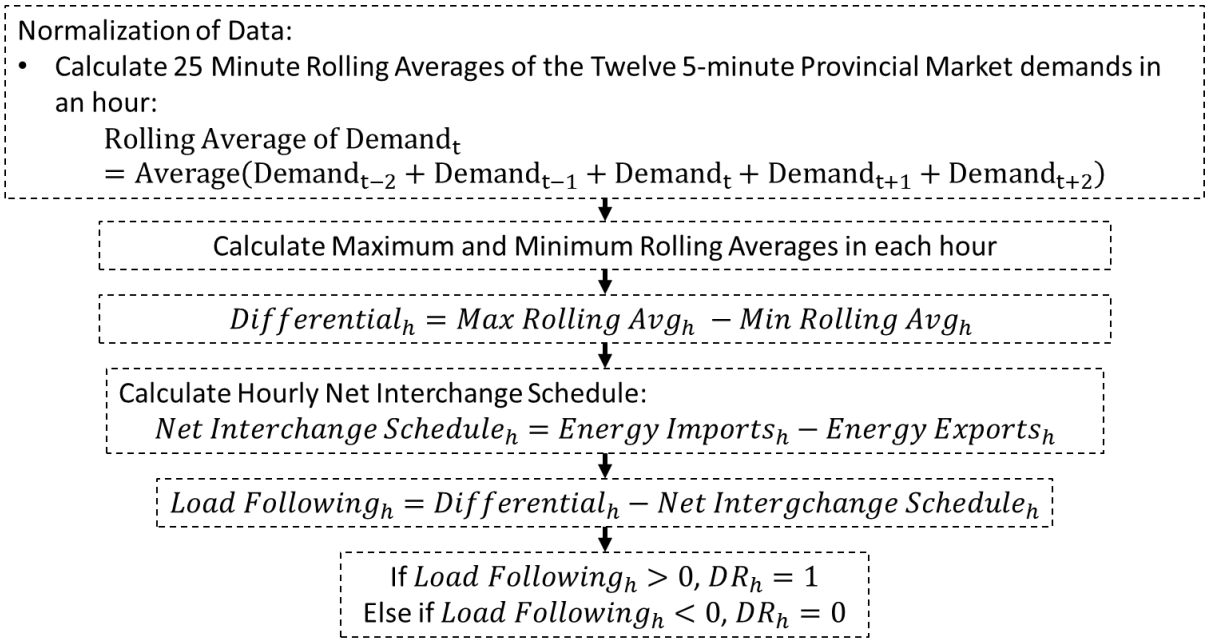

Figure 6.2: Schematic showing the development of the demand response data

The hourly load following requirement helps establish the hours in which a positive load following service needs to be provided by ramping up contracted generators. The demand response service provided by the power to gas energy hub can offset a share of the total positive load following requirement in a particular hour.

The first step in developing the demand response data used in this study involves normalizing the twelve 5-minute provincial market energy demands in an hour. The historical 5 minute market demand data has been provided by the IESO. The normalization is done by calculating the 25

minute rolling averages of each of the twelve 5-minute market demands. Subsequently, the maximum and minimum rolling averages occurring in an hour are estimated. Following this the difference between the maximum and minimum rolling average is also determined ($Differential_h$).

Since the market demand data includes energy exchanges between the neighboring jurisdictions, the provincial imports and exports of energy occurring in an hour need to be accounted for. The hourly net interchange schedule is estimated by calculating the difference between the hourly imports and exports of energy to and from the province **[137]**. Upon the determination of the hourly net interchange schedule the hourly load following is calculated by calculating the difference between the terms $Differential_h$ and $Net\ Interchange\ Schedule_h$ **[138]**. The binary parameter 'DR' is '1' when the electrolyzers need to provide demand response and it is set as '0' when there is no demand response action required.

6.3 Methodology: Optimization problem formulation

In this section, a mixed integer non-linear program formulation has been proposed. The problem is non-linear due to the consideration of a non-linear constraint within the formulation. This non-linearity is represented by estimating the unit cost of production of hydrogen through equation 6.7, which involves taking the ratio of two continuous decision variables. The challenge with non-linear optimization problems lie in whether the non-linear equation is a convex function. If it is a convex non-linear equation then a global optimum can be obtained. The cost of production of hydrogen (equation 6.7) is estimated from the ratio of two linear functions. These types of equations in optimization problems are termed as linear fractional functions. Linear fractional functions are quasi-convex if one restricts the realm of possible values that the linear function in the denominator can take to be greater than zero. Therefore the optimization problem formulation involves putting a lower bound the variable ‘amount of hydrogen produced to a small value (0.00001) which is greater than zero. Other non-linear equations of the same form include equations 6.10 and 6.11.

The formulation for mixed integer non-linear optimization problem is presented in this section.

$$Maximize: CF = -C_{Capital,Annual} + NR$$

s.t.

Energy (Electrical) and Hydrogen Flow Balances in Energy Hub:

$$F_{H_2,h} = \frac{\eta_{Electrolyzer} \times E_h}{E_{HHV,H_2}}$$

$$F_{H_2,h} = F_{H_2,Pipe,h} + F_{H_2,In,Tank,h}$$

$$I_{H_2,h} = I_{H_2,h-1} + F_{H_2,In,Tank,h} - F_{H_2,Out,Tank,h}$$

Energy (Natural Gas End User) and Hydrogen Fuel Demand Constraints:

$$D_{H_2,h} = F_{H_2,Out,Tank,h}$$

$$\left(F_{H_2,Pipe,h} \times HHV_{H_2}\right) + \left(F_{NG,Pipe,h} \times HHV_{NG}\right) = D_{NG,h}$$

(Technological) Active Constraints:

$$I_{Min} \leq I_{H_2,h} \leq I_{Max}$$

$$F_{H_2,In,Tank,h} \leq N_{Compressor,Pre-Storage} \times F_{Max,Compressor,Pre-Storage}$$

$$F_{H_2,Out,Tank,h} \leq N_{Booster\ Compressor} \times F_{Max,Booster\ compressor}$$

$$N_{Electrolyzer} \times E_{Electrolyzer,Min} \leq E_h \leq N_{Electrolyzer} \times E_{Electrolyzer,Max}$$

$$E_h \leq E_{max} - LR_h$$

$$1000 \times DR_h \times \alpha_h \leq LR_h \leq CCA \times DR_h \times \alpha_h$$

$$F_{H_2,Pipe,h} \leq \theta \times F_{NG,Pipe,h}$$

Demand Response Ancillary Service Constraints:

$$UF_h = \frac{CCA - LR_h}{CCA} \times DR_h$$

$$C_{DR,h} = (UF_h \times R_{Load\ Reduction} \times CCA) \quad (6.1)$$

Additional Equality Constraints:

$$T_{H_2} = \sum_{h=1}^{H} F_{H_2,h}$$

$$L = \{UPC_{H_2} - \sum_{h=1}^{H} \left(HHV_{H_2} \times R_{NG,h}\right)\} \times F_{H_2,Pipe,h}$$

$$T_{H_2,FCV} = \sum_{h=1}^{H} F_{H_2,Out,Tank,h}$$

$$O_h = \frac{D_{NG,h}}{HHV_{NG}} - F_{NG,Pipe,h}$$

$$EO_{NG} = \sum_{h=1}^{H} \left[O_h \times \left(EMF_{NG} + EMF_{NG,production}\right) - \left(F_{H_2,Pipe,h} \times EMF_{H_2}\right)\right]$$

Non-Linear Constraints:

$$\frac{C_{H_2}}{T_{H_2}} = UPC_{H_2}$$

$$R_{H_2,FCV} = T_{H_2,FCV} \times UPC_{H_2}$$

$$ASP_{H_2} = \frac{(L + R_{H_2,FCV})}{T_{H_2,FCV}}$$

The problem has a mix of binary and continuous variables, and has linear fractional functions as non-linear constraints. Therefore it is a mixed integer non-linear programming problem. Linear fractional functions are a type of non-linear equation in optimization formulations that are represented by a ratio of two linear functions. These non-linear constraints in the study are made quasi-convex by restricting the realm of possible values that the linear function in the denominator can take to be greater than zero.

The following sections describe the objective function and its corresponding constraints. The list of symbols for parameters and variables in the following section have been shown in appendix A.6.1 and A.6.2.

6.3.1 Objective function

The primary objective function of the problem is to maximize the annual cash flow earned. Equation 6.2, below describes the different components of the cash flow function.

$$Maximize: CF = -C_{Capital,Annual} + NR \tag{6.2}$$

The term $C_{Capital,Annual}$ ($) denotes the annual cash outflow associated with the capital cost of individual energy hub components which includes the amortized capital costs of: 1) The 2 MW polymer electrolyte membrane electrolyzer; 2) The three stage reciprocating booster compressor (used for FCV refueling); 3) The pre-storage reciprocating compressor, and 4) The on-site ASME Steel hydrogen storage tank. Another term also included within the term $C_{Capital,Annual}$ is the annual operating and maintenance cost of the electrolyzers. Since the energy hub configuration is fixed, the term $C_{Capital,Annual}$ is a fixed quantity (parameter) in equation 6.2. The capital cost of the energy hub components have been amortized based on an interest rate of 8% and project lifetime of 20 years.

The term NR in equation 6.2 denotes the difference between the revenue earned and the operating cost of the power to gas energy hub over a year. Equation 6.3 further expands on the different variables that make up NR ($).

$$NR = \sum_{h=1}^{H} \Big[-\big(F_{H_2,h} \times CR_{Water} \times UC_{Water} \big) - \Big[\big\{ E_h + (ECF_{Booster\ compressor,h} \times F_{H_2,Out,Tank,h}) + \big(F_{H_2,In,Tank,h} \times ECF_{Compressor,Pre-Storage} \big) \big\} \times \big(C_{Electricity,h} + TC_h \big) \Big] + \Big(F_{H_2,Pipe,h} \times HHV_{H_2} \times \big(R_{NG,h} - [\gamma \times \delta] \big) \Big) + \big(F_{H_2,Out,Tank,h} \times ASP_{H_2} \big) - C_{DR,h} + (LR_h \times R_{Load\ Reduction} \times DR_h) \Big] + (EO_{NG} \times R_{CO_2}) \quad (6.3)$$

In addition to the operating and maintenance costs of the PEM electrolyzers, the system also incurs the following operating costs:

- $CR_{Water} \times UC_{Water}$, accounts for the cost ($) of water per kmol of hydrogen produced;
- $C_{Electricity}$, helps in estimating the cost incurred to run the two compressors and the PEM electrolyzers installed in the energy hub;
- E is denoted as the energy (kWh) consumed by the PEM electrolyzers;
- The terms $ECF_{Compressor,Pre-Storage}$, and $ECF_{Booster\ compressor}$ denote the energy (kWh) consumed by the pre-storage and booster compressor per kmol of hydrogen fed to it. The terms are pre-calculated (using equation 3.11).
- TC ($), is a fixed charge added to the total operating cost for using the power transmission lines. It is calculated by multiplying a set cost factor ($ per kWh) by the energy (kWh) consumed by the electrolyzers, and the two compressors;
- γ ($\$\ per\ MMBtu$) is the rate charged by natural gas distribution utility to supply fuel for compressors located along their pipelines that help in maintaining the pressure of the flow within the pipelines **[139]**;
- δ (%) is the amount of natural gas fuel required by natural gas distribution utility to run their pipeline compressors, on top of the gas is being transported. The requirement is expressed as a percentage of gas to be transported **[139]**, and
- C_{DR} is a term defined to calculate the money owed by the energy hub to the IESO at times when the system is actually scheduled to provide its entire contracted capacity for demand

response but chooses to offer a demand response curtailment lower than the contracted amount. This term is calculated using equation 6.17.

The terms that represents the revenue earned by the energy hub (in equation 6.3) include:

- R_{NG} ($\$\ per\ MMBtu$) is the Henry Hub Natural Gas Spot Price that is used as the selling price of hydrogen supplied to the natural gas end users;
- HHV_{H_2} ($MMBtu\ per\ kmol$) is the higher heating value of hydrogen used in the study;
- ASP_{H_2}($\$\ per\ kmol$) is the marked up or adjusted selling price at which the hydrogen produced by the electrolyzers is sold to the fuel cell vehicle end users and it is a variable that is calculated using equation 6.12.
- $R_{Load\ Reduction}$ ($\$\ per\ kWh$) is the incentive that the power to gas energy hub receives for reducing its load and provide the demand response services to the grid **[86]**;
- DR is a binary parameter which takes a value of '1' when the power to gas system is contracted to provide the demand response service to the grid, and '0' when it does not have to provide the demand response service;
- LR (kWh) is the actual amount of curtailment provided by the PEM electrolyzers at a particular hour;
- EO_{NG} is the amount of CO_2 emissions offset (kg) by sending HENG in place of pure natural gas to the end users. Equation 6.13 shows how the term is calculated;
- R_{CO_2} is the existing emission credit incentive given to services that reduce their CO_2 emissions. For this study this value has been set at the $ 15 per tonne of CO_2 emissions carbon tax value used in Alberta, Canada **[140]**. Note that at the time of this publication, Ontario did not have a price on carbon.

6.3.2 Energy hub design constraints

The design constraints associated with the production of hydrogen, the maximum and minimum operating levels of the electrolyzer, hydrogen storage inventory balance, hydrogen flow balance within the energy hub, storage and compressor capacity constraints, will not be shown in this section. These equations have been shown in sections 3.3.1, 3.3.2 and 3.3.3 (refer to chapter 3). Note that in this chapter, the various hydrogen flows have slightly different nomenclature and are

represented in kilo moles instead of cubic meter. Therefore each of them have been described below:

- $F_{H_2,h}$ (kmol per hour) is the hourly hydrogen flow coming out of the 2 MW electrolyzer.
- $F_{H_2,In,Tank}$ (kmol per hour) is the flow of hydrogen directed through the pre-storage compressor and then sent to the tank storage unit.
- $F_{H_2,Pipe}$ (kmol per hour) is the hydrogen flow sent to the pressure reduction station where it mixes with natural gas and is then injected into the distribution pipelines supplying HENG to the natural gas end users.
- $F_{H_2,Out,Tank}$ (kmol per hour) is the amount of hydrogen taken out of the tank and sent to the booster compressor before being sent to the refueling station.
- The maximum and minimum amount of hydrogen that can be stored in the tank at any instant is set by the upper and lower bounds I_{Max} (kmol) and I_{Min} (kmol).

6.3.2.1 Demand constraints

The pure hydrogen demand constraint coming from the refueling station is shown using Equation 6.4, where the flow of hydrogen coming out the tank storage unit ($F_{H_2,Out,Tank}$, kmol per hour) should be equal to the pure hydrogen demand parameter (D_{H_2}, kmol per hour).

$$D_{H_2,h} = F_{H_2,Out,Tank,h} \tag{6.4}$$

The energy demand placed at the pressure reduction station is denoted by D_{NG} $(MMBtu)$. The sum of energy content of hydrogen and natural gas injected into the distribution lines should be equal to D_{NG}, as illustrated in equation 6.5.

$$\left(F_{H_2,Pipe,h} \times HHV_{H_2}\right) + \left(F_{NG,Pipe,h} \times HHV_{NG}\right) = D_{NG,h} \tag{6.5}$$

Since natural gas pipelines can be subjected to hydrogen embrittlement at high concentrations of hydrogen, a safe upper limit on the hydrogen injectability has been set with the help of Equation 6.6.

$$F_{H_2,Pipe,h} \leq \theta \times F_{NG,Pipe,h} \tag{6.5}$$

The upper bound on hydrogen concentration in natural gas is set based on the analysis published in a report by Melaina et al. on blending hydrogen in natural gas pipelines **[40]**. The term θ in equation 6.6 is a constant that makes sure that flow units in kilo moles are converted to cubic meter to make sure the 5 vol.% level is not exceeded.

6.3.2.2 Adjusted selling price (of H_2) estimation equations

The annual hydrogen production of the energy hub can be calculated by summing the hourly hydrogen flow ($F_{H_2,h}$, kmol per hour) over the entire year (Nov, 2012-Oct, 2013) or 8760 hours (H), as seen in equation 6.7 below.

$$T_{H_2} = \sum_{h=1}^{H} F_{H_2,h} \tag{6.7}$$

Now, by taking the ratio of total annual cost (C_{H_2}, \$) over total annual hydrogen production, the unit cost of hydrogen can be estimated in \$ per kmol of H_2 (UPC_{H_2}, see equation 6.8). The total annual cost term (C_{H_2}, \$) involves paying for the amortized cost of equipment and annual operational cost of electrolyzer. The factors contributing to this cost have been described in equations 6.2 and 6.3. These types of equations in optimization problems are termed as linear fractional functions. Linear fractional functions are quasi-convex if one restricts the realm of possible values that the linear function in the denominator can take to be greater than zero. Therefore the optimization problem formulation in chapter 6 involves putting a lower bound the variable 'amount of hydrogen produced to a small value (0.00001) which is greater than zero.

$$\frac{C_{H_2}}{T_{H_2}} = UPC_{H_2} \tag{6.8}$$

As the higher heating value of hydrogen is three times lower than the higher heating value of natural gas, it is intuitive that selling hydrogen to natural gas end user at a price set at the natural gas energy value is going to be less economical. Also, since the unit hydrogen production cost calculated in equation 6.8 accounts for both the hydrogen produced for the natural gas end user and the refueling station, hydrogen sold to the pipeline is undervalued. Therefore, the monetary loss in selling hydrogen at a lower price to the natural gas end user is used to adjust the selling price of hydrogen to fuel cell vehicles.

The monetary loss (L) while selling hydrogen to the natural gas end user on an energy basis by using the Henry Hub Natural Gas Spot Price ($R_{NG,h}$, $ per MMBtu) is calculated from the difference between the unit production cost (UPC_{H_2}, equation 6.8) and the hourly spot price ($R_{NG,h}$, $ per MMBtu) as seen in equation 6.9 below.

$$L = \{UPC_{H_2} - \sum_{h=1}^{H} (HHV_{H_2} \times R_{NG,h})\} \times F_{H_2,Pipe,h} \quad (6.9)$$

The summation of all of the hydrogen sold to the fuel cell vehicle over the course of a year ($T_{H_2,FCV}$, kmol) is estimated by summing hydrogen withdrawn from the tank storage as seen in equation 6.10.

$$T_{H_2,FCV} = \sum_{h=1}^{H} F_{H_2,Out,Tank,h} \quad (6.10)$$

The variable $R_{H_2,FCV}$ in equation 6.11, is used to estimate the revenue earned if the hydrogen sent to the refueling station is sold at unit production cost determined from equation 6.8.

$$R_{H_2,FCV} = T_{H_2,FCV} \times UPC_{H_2} \quad (6.11)$$

Using the values of $T_{H_2,FCV}$ (kmol) and $R_{H_2,FCV}$ ($) from equations 6.10 and 6.11, the adjusted selling price of hydrogen sold to the refueling station has been estimated in equation 6.12, below.

$$ASP_{H_2} = \frac{(L + R_{H_2,FCV})}{T_{H_2,FCV}} \quad (6.12)$$

Equations 6.11 and 6.12 also represent linear fractional functions which are made quasi-convex by setting a lower bound on the variables in their respective denominators ($T_{H_2,FCV}$: Total hydrogen sold to fuel cell vehicles in both equations 6.11 and 6.12) to a small value greater than zero (0.00001).

6.3.2.3 Emission offset equations

The total CO_2 emissions offset is calculated by estimating the emissions reduced at natural gas end users (EO_{NG}).

$$EO_{NG} = \sum_{h=1}^{H} \left[O_h \times \left(EMF_{NG} + EMF_{NG,production} \right) - \left(F_{H_2,Pipe,h} \times EMF_{H_2} \right) \right] \quad (6.13)$$

The term $'O'$ in the above equation (6.13) denotes the amount of natural gas displaced with hydrogen and is calculated by taking the difference of natural gas flow when energy demand placed at the pressure reduction is satisfied solely with natural gas $\left(\frac{D_{NG}}{HHV_{NG}}\right)$ and natural gas flow ($F_{NG,Pipe}$) when HENG is used to satisfy the energy demand (see equation 6.14).

$$O_h = \frac{D_{NG,h}}{HHV_{NG}} - F_{NG,Pipe,h} \quad (6.14)$$

The calculated offset is then multiplied by the sum of the emission factors when natural gas combusts ($EMF_{NG}, kg\ of\ CO_{2,e}\ per\ kmol\ of\ NG\ burnt$) **[112]** and when it is produced and processed ($EMF_{NG,production}\ kg\ CO_{2,e}\ per\ kmol\ of\ NG\ produced$) **[111]**.

The emission factor associated with using grid electricity in the electrolyzers is available as a parametric data in kg of CO_2 per kWh of electricity produced. Using this value and multiplying it with the efficiency factor (kWh of electricity consumed per kmol of hydrogen produced) of the PEM electrolyzers gives the value for EMF_{H_2} in kg of $CO_{2,e}$ emissions per kmol of hydrogen. The product of EMF_{H_2} and $F_{H_2,Pipe,h}$ (kmol per hour) yields emissions incurred from electrolysis.

6.3.2.4 Demand response service constraints

The variable LR in Equation 6.15 denotes the amount of load reduction offered in hours when the electrolyzers are required to reduce their energy consumption based on the load following demand response logic described in section 6.2.2 (figure 6.2).

$$E_h \leq E_{max} - LR_h \quad (6.15)$$

The contracted curtailment amount (CCA) of the electrolyzers to offer demand response is set at 2000 kW in an hour. The Independent Electricity System Operator (IESO) sets the minimum amount of demand response offered by a contracted facility to be 1000 kW in an hour **[141]**. Equation 6.16 is used to limit the amount of load reduction offered by the electrolyzers in a given hour to 1000-2000 kW (CCA).

$$1000 \times DR_h \times \alpha_h \leq LR_h \leq CCA \times DR_h \times \alpha_h \tag{6.16}$$

The term α is used as a binary variable that gives the optimization problem the flexibility to choose between either offering or not offering the demand response service at time points it is scheduled to provide the service. The term DR as described in earlier in section 6.2.2 (figure 6.2) and 6.3.1 (equation 6.3) is the parameter signal which has a value of '1' in hours when there is a potential for loads to provide demand response service to the IESO.

The IESO administers a clawback (C_{DR}) charge in hours where a facility cannot provide the entire contracted curtailment amount. Equation 6.17 is used to take into account this clawback charge when the electrolyzers are not able to offer a demand response of 2000 kWh (CCA).

$$C_{DR,h} = (UF_h \times R_{Load\ Reduction} \times CCA) \tag{6.17}$$

The clawback charge is calculated by initially multiplying the unavailability factor (UF) with the contracted curtailment amount. This product can also be defined as the difference between the contracted curtailment amount and the actual load reduction provided by the electrolyzers. The original incentive offered by the IESO for providing the demand response service ($R_{Load\ Reduction}$, \$ per kWh) is then multiplied to this difference to calculate the clawback charge. The unavailability factor is an estimate of the fractional decrease in demand response offered and is calculated by Equation 6.18.

$$UF_h = \frac{CCA - LR_h}{CCA} \times DR_h \tag{6.18}$$

6.4 Results

The results from the mixed integer non-linear optimization model formulated in the previous section are presented here. The model is run for the electricity pricing in the time period November, 2012 – October, 2013. Solutions to the problem have been obtained by using the mixed integer

non-linear programming (MINLP) solver DICOPT available in Version 22.6 of the General Algebraic Modeling System (GAMS) software.

The results and discussion section here in are split into 3 sections. Section 6.4.1 discusses the baseline pricing mechanism for the services provided by the energy hub. Section 6.4.2 talks about the observed operating characteristics of the energy hub, and section 6.4.3 presents the premium pricing mechanisms for the three services offered by the energy hub.

6.4.1 Baseline pricing mechanism

The unit production cost of hydrogen estimated from equation 6.7 is $5.47 per kmol or $2.74 per kg. Similarly, the total hydrogen produced over the course of the year is estimated to be 160,121 kmol or 320,242 kg (using equation 6.6). The annual monteary loss of selling hydrogen at the natural gas energy value has been calculated to be $210,269 using equation 6.8. This value is used in adjusting the selling price of hydrogen to fuel cell vehicles. As seen in table 2, the adjusted selling price of hydrogen is estimated to be $3.665 per kg of hydrogen produced.

Tabe 6.1: Baseline pricing mechanism

H_2 Selling Price to Refueling Station ($ per kg)	**H_2 Selling Price to Natural Gas End User ($ per MMBtu)**	**Demand Response Incentive ($ per kWh)**	**$CO_{2,e}$ Emissions Offset Benefit ($ per kg)**
3.665	Hourly Henry Hub Spot Price	0.0215	0.015

The values of demand response incentive and $CO_{2,e}$ emissions offset benefit are $0.0215 per kWh and $0.015 per kg of $CO_{2,e}$ emissions.

6.4.2 Operating regime of energy hub

Analyzing the variation in hourly energy consumption by the electrolyzer system and the hourly hydrogen concentration levels maintained within the natural distribution pipeline system are of interest. However, the sheer size of the data makes it difficult to capture the variations of these primary decision variables. Therefore, to better analyze this data, their weekly averages have been calculated and shown in Figures 6.3 and 6.4.

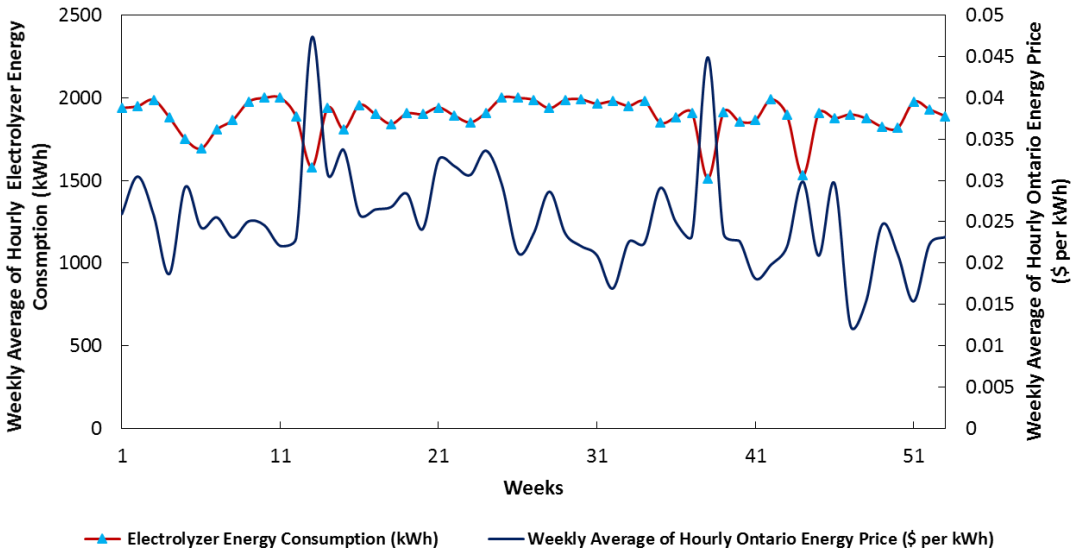

Figure 6.3: Variation in weekly average: 1) hourly energy consumption of electrolyzers and, 2) hourly Ontario electricity price

From figure 6.3, it can be concluded that the weekly average of the hourly Ontario electricity price is the primary parameter that influences the energy consumption profiles for the electrolyzers in the energy hub. An inverse relationship between the electricity price and the energy consumption profile has been observed. This phenomena can be termed as energy arbitrage where the electrolyzers run at maximum capacity and produce excess hydrogen that is stored in the on-site storage tank during low electricity prices. This enables the system to lower its energy consumption during hours of high electricity price and withdraw excess gas stored in the tank to meet refueling station demands. Thereby, helping in lowering operating cost of the energy hub.

Since the energy consumption profile has been averaged over a period of a week and there are only 801 hours spread across the year when the electrolyzer provides demand response, the drop in energy consumption while providing demand response is not seen in figure 6.3.

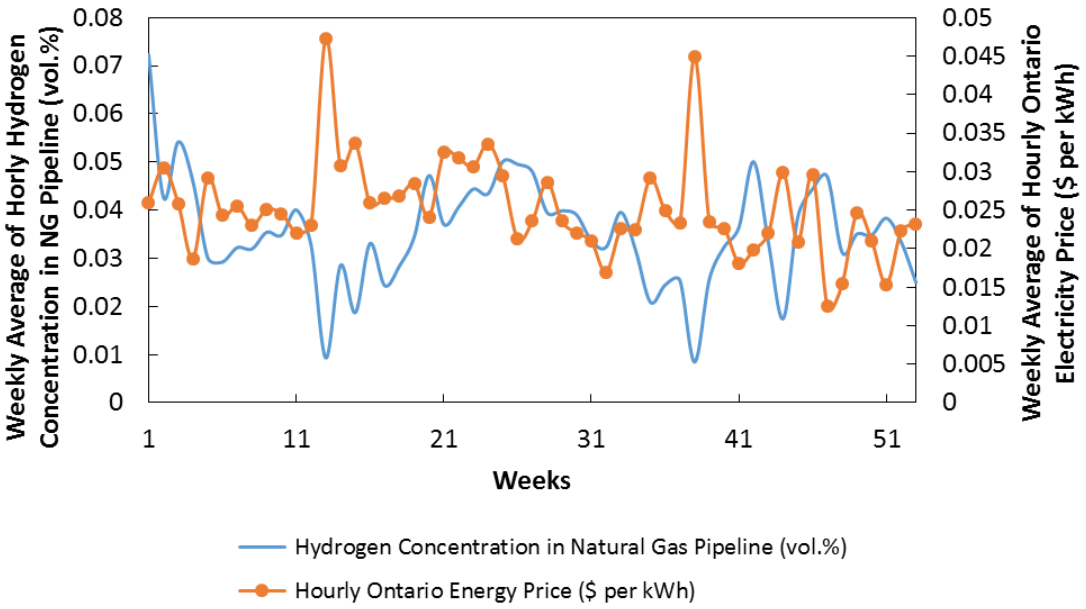

Figure 6.4: Variation in weekly average: 1) Hourly hydrogen concentration (vol.%) in natural gas distribution pipeline, and 2) Hourly Ontario electricity price ($ per kWh)

The variation in weekly average of hourly hydrogen concentration within the natural gas pipeline has been plotted and shown in figure 6.4. The hydrogen produced by the electrolyzer module changes with the variation in energy consumed by the system. Hydrogen is sold on an energy value basis (Henry Hub Spot Price, $ per MMBtu) to the natural gas end user. Since hydrogen has a lower energy content in comparison to natural gas, more hydrogen needs to be injected to make up for the energy loss. In order to maximize the primary cash flow objective (equation 6.1), the energy hub tries to achieve energy arbitrage in this case by making use of the price differential that exists between the cost of electricity ($ per kWh) and the selling price of natural gas ($ per MMBtu). The system reduces the amount of hydrogen injected in to the pipeline when this price differential is not favorable.

It is seen in figure 6.4 that the maximum weekly average of hourly hydrogen concentration is 0.0723 vol%. The maximum hydrogen concentration from all of the hours in a year is calculated to be 0.511 vol%. This maximum concentration is well below the 5 vol% safety limit.

Since a blend of HENG is sent to the natural gas end user, there can be potential $CO_{2,e}$ emissions offset at the end user. The system achieves a maximum $CO_{2,e}$ emissions offset of 427 tonnes at the natural gas end user.

6.4.3 Development of premium pricing mechanisms

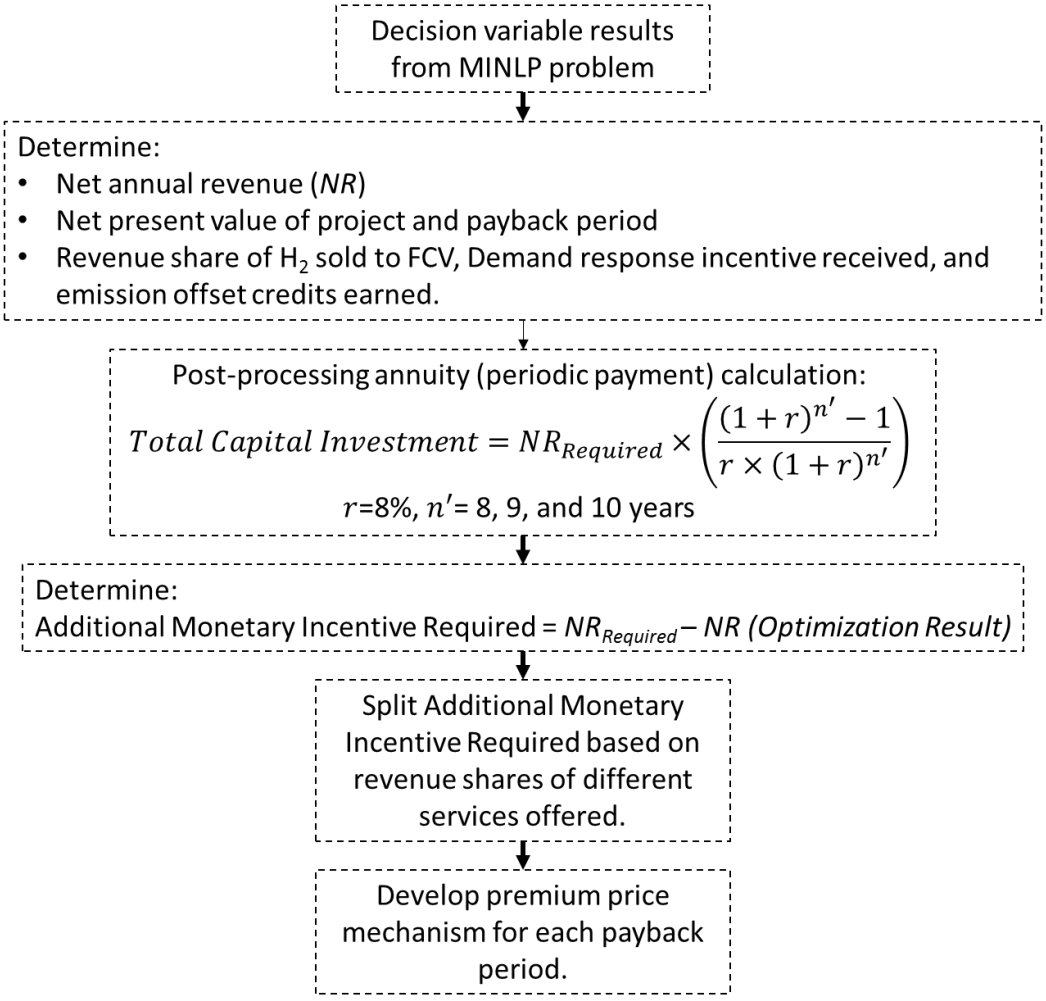

Figure 6.5: Process schematic for determining premium pricing mechanism

Figure 6.5 shows the step by step procedure of determining the new pricing mechanism for each of the three individual services that the energy hub is designed to provide in this study. The energy hub earns its revenue from providing: 1) Hydrogen to fuel cell vehicles; 2) Demand response; 3) Hydrogen enriched natural gas to natural gas end users, and 4) Offsetting $CO_{2,e}$ emissions at natural gas end users. The following paragraphs describe this post-processing calculation in more detail.

The first step (second bubble) in the schematic in figure 6.5 shows the estimation of the net present value and the payback period for the optimization problem. The net present value of the energy hub at the end of its 20 year lifetime is estimated to be -$213,883. Upon projecting the calculation beyond the twenty year time period, it is seen that the project has a payback period of 24 years.

Selling hydrogen to fuel cell vehicles represents the highest revenue share for the energy hub (92.4%). This is followed by a 1.7% and 0.7% contribution from providing demand response and offsetting $CO_{2,e}$ emissions, respectively. The remaining 5.2% of the revenue share is from selling hydrogen to natural gas end users. This implies that a slight increase in the selling price of hydrogen from its unit production cost of $2.74 per kg (see equation 6.7) to $3.665 per kg (see equation 6.11) obtained after accounting for the monetary loss incurred in hydrogen injection to the natural gas pipeline is not high enough to drive a positive net present value at the end of the projects 20 year lifetime. The incentive received for each of the three revenue streams will have to be adjusted further with selling price of hydrogen requiring a greater increase due to its higher share in contributing towards total revenue.

The sum of the amortized capital costs of the individual energy hub components is $302,024 ($C_{Capital,Annual}$, see equation 6.1). This value when multiplied by 20, gives the total investment ($6,040,478) over the course of 20 years. The term '*Total Capital Investment'* used in the equation shown in the third bubble in figure 6.5 denotes this value. The term '$NR_{Required}$' in the third bubble in figure 6.5 denotes the net annual revenue required for the energy hub to have a NPV equal to zero at the end of shorter project payback periods of 8, 9 and 10 years, respectively. r and n' denotes the discount rate (8%) and the project payback periods (n'), 8, 9 and 10 years, respectively.

Current net annual revenue (*NR*) obtained from equation 6.2 is $304,401. The required net annual revenue ($NR_{Required}$) values for project payback periods of 8, 9 and 10 years are $1,05,1132, $966,958, and $900,209, respectively. The difference between $NR_{Required}$ and *NR* is termed as the additional monetary incentive required (see bubble 4 in figure 6.5). Based on this logic, it has been estimated that additional monetary incentives of $746,731, $662,557, and $595,808 are required for project payback periods of 8, 9 and 10 years, respectively.

As mentioned earlier, the revenue shares earned via 1) selling hydrogen to fuel cell vehicles; 2) providing demand response service and 3) offsetting $CO_{2,e}$ emissions at natural gas end users, were 92.4%, 1.7%, and 0.7%, respectively. The selling price of the hydrogen sold in the natural gas market will not be changed in the model, and therefore its contribution to total revenue share will not be considered. Therefore, the percentage contributions of the first three revenue streams, are used to proportionately split the additional monetary incentive requirements into the new: 1)

hydrogen selling price, 2) demand response incentive, and 3) $CO_{2,e}$ emissions offset credit (refer to bubbles 5 and 6 in figure 6.5).

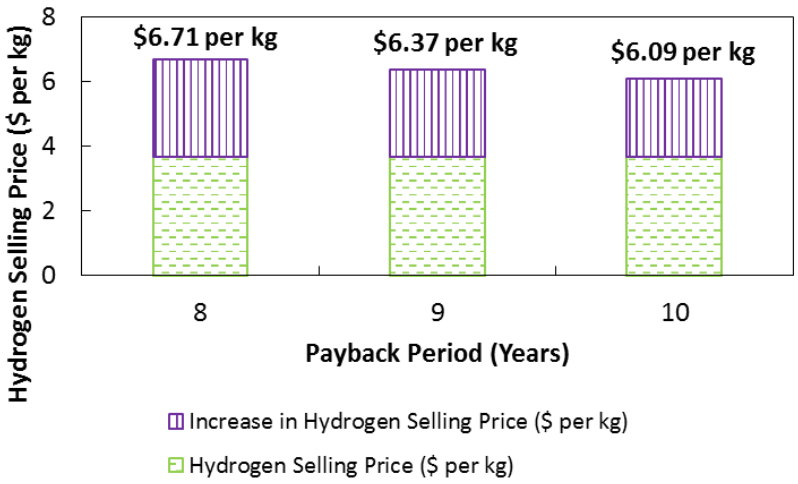

Figure 6.6: Premium pricing for hydrogen sold to fuel cell vehicles for project payback periods of 8, 9 and 10 years.

Figure 6.6 shows the required selling price of hydrogen to the fuel cell vehicles to achieve the project payback periods of 8, 9 and 10 years, respectively. In each of the three project payback periods, a base selling price of $3.66 per kg of hydrogen has been used (table 6.1). Based on this, a simple percentage increase in required selling price of hydrogen shows that a project payback periods of 8 years requires the maximum percentage increase of 83% followed by 74% and 66% increase for project payback periods of 9 and 10 years, respectively. Currently, the selling price of hydrogen in the US ranges between $5-10 per kg of hydrogen as illustrated by the National Hydrogen Association **[142]**. The maximum price of hydrogen ($6.71 per kg) from the results presented in figure 6.6 is therefore well within the price range existing in the North American market.

The IESO in its auction report **[86]** sets a demand response incentive of $0.0215 per kWh or $516 per MW-day. This price is used as a basis upon which the projected increase in the demand response incentive has been estimated for each of the three project payback periods as seen in Figure 6.7.

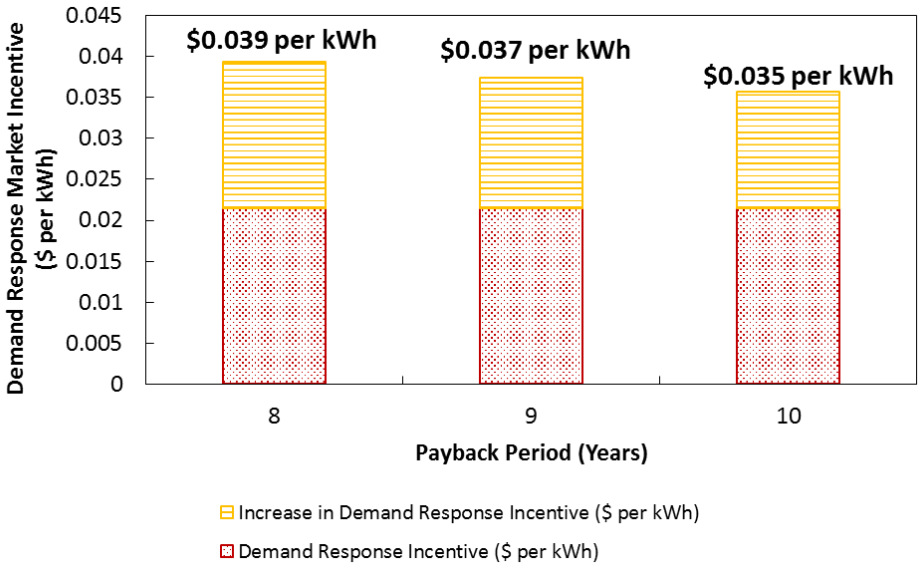

Figure 6.7: Demand response incentive for project payback period of 8, 9 and 10 years.

A maximum demand response incentive of $0.039 per kWh ($936 per MW-day) is required for the energy hub to achieve a project payback period of 8 years. The power to gas energy hub is considered to be a novel concept and in future markets the introduction of innovative technologies to provide grid support will require a higher incentive price for them to be economically feasible.

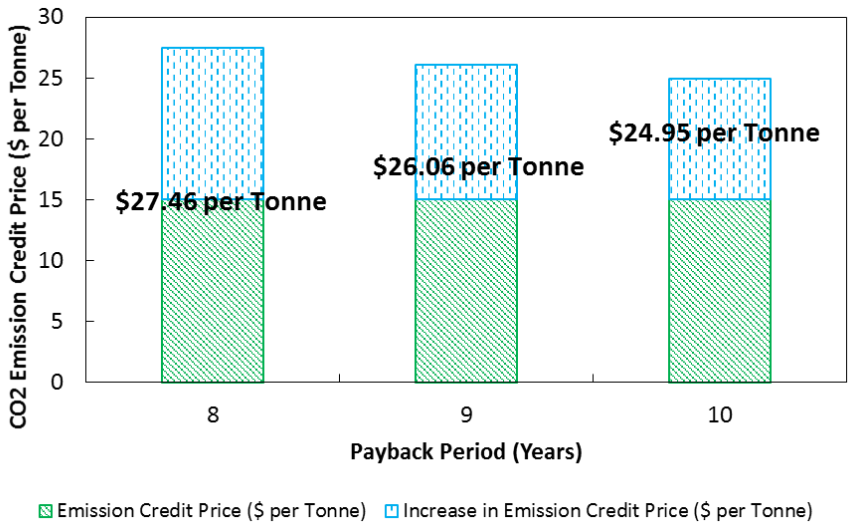

Figure 6.8: CO_2 emission offset credit for project payback periods of 8, 9 and 10 years.

At the time of writing this article, a preliminary emission offset credit value of $15 per tonne of $CO_{2,e}$ emissions existed as a carbon tax in Alberta (2014). This is used as a basis in figure 6.8. The calculated emission credit values in figure 6.8 range from $27.5 to $24.95 per tonne of $CO2_{,e}$. The monetary value associated with offsetting $CO_{2,e}$ emissions and earning credits supports the industries making a financial case for the use of green technology. The province of Alberta planned to increase the carbon tax it charges to emitters to $ 20 per tonne of $CO_{2,e}$ at the beginning of 2017 and increase it further to $30 per tonne of $CO_{2,e}$ in 2018 **[143]**. In Ontario since the beginning of the cap and trade program (in 2017) the allowance price for carbon has stayed around $17-18 per tonne of $CO_{2,e}$. Higher $CO_{2,e}$ emission offset incentive values will be required in power to gas projects which do not have the option of selling hydrogen as a high value fuel to the transportation sector. This was evident in the result presented for larger scale power to gas energy hubs modeled to only provide renewable natural gas ($228.7 per tonne of $CO_{2,e}$) and hydrogen enriched natural gas ($87.8 per tonne of $CO_{2,e}$) in chapter 4.

The economics of the 2 MW plant modeled and optimized in this study looks promising considering the fact that some of the premium pricing mechanisms shown lie within the ranges of studies carried out internationally (e.g.: Hydrogen fueling price analysis done by National Hydrogen Association, USA **[142]**). On the other hand premium pricing structures for carbon emissions adopted across the world have been variable. A 2013 report published by 'The Climate Group' shows a wide variety of carbon prices adopted across the world with values ranging from

as high as $615 per tonne of $CO_{2,e}$ to as low as $3 per tonne of $CO_{2,e}$ **[144]**. As more countries adopt either strict carbon taxes or a cap and trade mechanism, the experience of operating such programs might lead to a standardization on the carbon pricing.

The pricing structure for energy storage systems capable of providing ancillary services such as demand response to the power grid in Ontario is relatively new and it will take more time to account for power to gas systems to be able to compete in the provincial demand response market. Demand response service for power to gas units can also be utilized as an incentive to ramp up their operating levels to absorb surplus electricity. In this way the hourly electricity price paid by the energy hub during surplus generation hours will be slightly discounted by the demand response incentive price. However, this has not been considered in this work and is a suggestion for future work.

6.5 Conclusions

In this study, the potential benefits of the energy recovery pathways of a power to gas energy hub of predetermined size has been demonstrated through the development of a mixed integer nonlinear programming (MINLP) problems. The 2 MW energy hub modeled in this study earns revenue from providing: 1) Hydrogen to 254 fuel cell vehicles on a daily basis; 2) Demand response ancillary service to the power grid; 3) Hydrogen enriched natural gas to the natural gas end user, and 4) Emission reduction service credit at the natural gas end user from burning hydrogen enriched natural gas, which is a cleaner fuel.

In the MINLP problem, the selling price of hydrogen to the fuel cell vehicle is adjusted to account for the loss in selling hydrogen to natural gas end user at the natural gas spot price, which is lower than the cost incurred in producing that hydrogen. The energy consumption profile of the electrolyzers is sensitive to the hourly Ontario electricity price. When the price of electricity increases, the electricity consumption of the electrolyzers decreases. This occurs in order to minimize the cost incurred in producing hydrogen for both the fuel cell vehicle and natural gas end users. The unit production cost of all hydrogen produced is estimated to be $2.74 per kg. This selling price is then adjusted for hydrogen sold to the fuel cell vehicles at $3.66 per kg. It is seen that the incentive mechanism used in the MINLP problem are not high enough for the power to gas energy hub to have a positive net present value by the end of its 20 year lifetime.

Thus, via a post processing annuity calculation, the annual net revenues required for energy hub to have an NPV equal to zero for a discount rate of 8% and project payback periods of 8, 9 and 10 years, have been determined. The net annual revenue of the energy hub from the optimization results is chosen as a basis to determine the additional revenues required for each of the three project lifetimes. The revenue share from selling hydrogen to the fuel cell vehicles, providing demand response and earning emission offset credits have been estimated to be 92.4%, 1.7%, and 0.7%, respectively. Based on these revenue shares, the additional revenue required for each of the three project lifetimes has been split among these three concerned revenue streams to develop the premium price mechanisms required. The hydrogen selling price to fuel cell vehicles is estimated to be between $6.09-6.71 per kg for the project payback period range considered in the study. The power to gas energy hub requires a maximum demand response incentive of $0.039 per kWh ($936 per MW-day) for a project lifetime of 8 years. A maximum $CO_{2,e}$ emission credit incentive of $27 per tonne of $CO_{2,e}$ emissions is required for the shortest project payback period of 8 years.

From the results of the study it can be concluded that selling hydrogen as a high value fuel is the most economical pathway for a power to gas energy hub. Energy hubs that do not focus on providing this service will require higher $CO_{2,e}$ emission offset incentive values as seen from results in chapter 4. Demand response service to reduce electricity consumption is not highly lucrative as Ontario experiences greater periods of surplus electricity generation than peaks in electricity demand. Therefore, future demand response markets could also account for power to gas energy hubs to act as responsive loads that increase consumption to absorb surplus electricity. By receiving a demand response incentive on consuming surplus electricity, the energy hub can in other words pay a reduced price to what the hourly Ontario electricity price is during surplus generation hours.

Chapter 7: A Stochastic Programming Approach for the Planning and Operation of a Power to Gas Energy Hub with Multiple Energy Recovery Pathways

The following chapter is based on the work published in the journal called Energies in 2017. The title of the work is '*A Stochastic Programming Approach for the Planning and Operation of a Power to Gas Energy Hub with Multiple Energy Recovery Pathways*'. It has been authored by Ushnik Mukherjee, Azadeh Maroufmashat, Apurva Narayan, Ali Elkamel and Michael Fowler.

The first author's primary contribution was to develop the formulation in GAMS, and writing the article. Azadeh Marourmashat helped with providing key insights in modeling formulation. Apurva Narayan helped with charactering uncertainty associated with the uncertain parameters considered in this study. Ali Elkamel and Michael Fowler provided helpful guidelines in preparing the article for publication.

7.1 Introduction

This study focusses on accounting for uncertainty in input parametric data that can influence the sizing and operation of a large scale hydrogen production center co-located at a natural gas pressure reduction station in the greater Toronto area. The services provided by the energy hub in this study will again include: 1) hydrogen as a fuel for the transportation and natural gas sector, and 2) providing demand response ancillary service. However, the novelty of this study lies in associating uncertainty in the following three key parameters: 1) hourly electricity price; 2) the number of fuel cell vehicles serviced; and 3) the amount of hydrogen refueled during a single refueling event. An hourly time index for each of the uncertain parameters is adopted to analyze how the operation of the energy hub is impacted under different realizations of the uncertain parameters mentioned above. The analysis presented in this chapter will also focus on assessing whether there is a potential economic benefit for the power-to-gas system if it is modeled using the two-stage stochastic programming approach in comparison to a deterministic optimization

study. A short note on the potential environmental benefits both from the perspective of the producer and end user of hydrogen will also be presented.

7.2 Literature review

Of late, maximizing the effective utilization of renewables has led to them being utilized to produce hydrogen for the transportation sector. Juan et al. **[145]** review the challenges (both strategic and operational) and potential environmental benefits of implementing the use of hydrogen and battery powered electric vehicles in urban communities. Franzitta et al., and Blanco-Fernández et al. **[146,147]** highlight the benefits of harnessing wind and wave energy for the production of hydrogen. This hydrogen can then be utilized for fueling fuel cell vehicles. Liu et al. **[24]** carry out an economic analysis on the hydrogen economy infrastructure required to sustain the introduction of hydrogen fuel cell vehicles in Ontario. They consider three scenarios each for the years 2015, 2025 and 2050 that represents the percentage share of fuel cell vehicles among all new vehicles sold in Ontario. Each of the three scenarios have different rates at which fuel cell vehicles are introduced in the market. In order to account for uncertainty in their economic analysis, they carry out a sensitivity analysis on the electricity price, water price, efficiency of the electrolysis process and the lifetime of the hydrogen production plant. Their uncertainty/sensitivity analysis shows that variability in electricity price can significantly impact the hydrogen system cost. Change in efficiency of electrolyzers although does effect the system economics, however it is seen that its impact is lower in comparison to variability in electricity price. The sensitivity analysis on price of water and the project lifetime are deemed to have insignificant impact on system economics, according to Liu et al. **[24]**.

Kim et al. **[148]** carry out an optimization study to determine the optimal hydrogen supply chain technologies for the year of 2044 in different regions of South Korea. The estimated hydrogen demands for each region is used as a base (average) value around which two more scenarios are developed to account for uncertainty in hydrogen demand. The two scenarios considered assume that the demand varies by −20% of the average values for a ‘below average’ scenario, and +20% of the average values for an ‘above average’ scenario. The third scenario comprises of the average values itself. The problem is solved as a two-stage stochastic programming problem. However it

should be noted that one of the assumptions of their study is that the hydrogen demand scenarios for each region is time invariant.

Almansoori et al. **[149]** develop a long-term hydrogen supply chain model for Great Britain that accounts for uncertainty in hydrogen demand through a scenario tree approach. They develop a multi-stage stochastic MILP problem. The time horizon considered in their work includes three time periods (each of 6 years) ranging from 2005–2022. Each time period has 9 scenarios. Their modeling study analyzes the effect of uncertainty on three different liquid hydrogen supply chain configuration cases where the hydrogen transportation mode has been varied. Dayhim et al. **[150]** develop a hydrogen supply chain for the state of New Jersey by implementing the two-stage stochastic programming approach. The uncertainty in their study is associated with the market penetration rate of fuel cell vehicles in the state. A total of 10 scenarios have been considered. The market penetration of fuel cell vehicles has been varied between 5–100%. The computational intensity is reduced as only 4 time periods have been considered.

Nunes et al. develop a two-stage stochastic optimization problem to design and plan a liquid hydrogen supply chain for Great Britain **[151]**. They account for the uncertainty in hydrogen demand by generating scenarios via a first order autoregressive model (which includes a random error element following a normal distribution). The modeling time horizon spans a period of 18 years which is split into three periods comprising of six years each. They determine that 15 scenarios is a good limit to account for the uncertainty in hydrogen demand for a supply-chain planning study, without compromising computational time of solving the optimization problem.

Taljan et al. **[152]** develop a model to optimally operate and assess the economic viability of a hydrogen production, storage and fuel cell subsystem of fixed capacities in Ontario. Their work focusses on assessing the viability of running the hydrogen production subsystem solely on power available from a nuclear power plant and a wind farm in Ontario. The uncertain parameters include electricity price and wind farm output. Each time point in their study has 30 electricity price scenarios (generated from a normal distribution), and only one wind scenario. Their analysis shows that electricity from the power grid when utilized for providing hydrogen to the transportation sector rather than providing energy storage, is an economically viable option.

The stochastic analysis presented in this chapter tries to address the uncertainty in dynamic (hourly) electricity pricing by developing 5 possible electricity pricing scenarios for each hour

over the course of a year. This is different from Liu et al.'s **[24]** assumption of three different static electricity pricing scenarios for the entire period of 2015–2050. The uncertainty in hydrogen demand accounted by Kim et al. **[148]** is also static whereas in this study uncertainty in hourly (dynamic) hydrogen demand has been conside with respect to time in their red providing for a unique result.

There are two major points of difference when the work presented in this study is compared to work done by Almansoori et al., Dayhim et al., and Nunes et al. **[149,150,151]**. Firstly, this study focusses more on the effect of uncertainty in electricity pricing, and hydrogen demand on the sizing and dynamic (hourly) operation of an energy hub. Secondly, the two-stage stochastic optimization problem developed in this study is more focused towards developing an energy hub system that can satisfy gaseous hydrogen demand for a local region within the province of Ontario, and not the entire country or an entire state. Due to a finer time resolution of the optimization study used in this work the problem is more computationally intensive. Therefore, the number of scenarios considered here are lower in comparison to Almansoori et al., Dayhim et al., and Nunes et al.'s work **[149,150,151]**. Considering more scenarios leads to an increase in the number of variables and that in turn increases the convergence time to the solution. Also in this stochastic study it is assumed that the energy hub is co-located at the refueling station, therefore there is no exchange of hydrogen between production centers as shown in each of Almansoori et al., Dayhim et al., and Nunes et al.'s work, and distributed hydrogen generation is thus examined in this work **[149,150,151]**.

In comparison to Taljan et al.'s **[152]** work where electricity pricing scenarios were obtained from a normal distribution, this study carries out a more rigorous probability distribution fitting analysis for electricity pricing. Different probability distribution functions have been fitted to historical electricity pricing for a period of 10 years (2003–2013) in Ontario (Section 7.3.1). Taljan et al. **[152]** do not consider uncertainty and variability in hydrogen demand with respect to time in their study. The uncertainty in hydrogen demand on an hourly basis has been accounted for through the development of five potential demand scenarios each hour (Section 7.3.2). In addition to providing hydrogen to the transportation sector, this modeling study also looks into the potential of hydrogen to be supplied to natural gas end users as hydrogen enriched natural gas and for the electrolyzers to provide ancillary services to the power grid.

7.3 Methodology

Techno-economic optimization models of power to gas energy hubs involve the use of data signals or data sets that can be categorized under the term 'random'. From wind speed, to electricity demand, there exist many such data sets that have an associated randomness with them. Such data sets/signals could have 'n' number of potential values at any given instant. In other words, there can be 'n' number of scenarios. Deterministic techno-economic optimization approaches look at solving the problem by considering expected values of such data signals (or sets). However, by taking the expected value, the accuracy of the physical system can be compromised. Another approach could be to solve numerous deterministic optimization problems for each of the possible scenarios of the random data sets **[153]**. The results obtained could then be used to draw inferences from the results from each of the deterministic runs. However, this approach can be time consuming. Considering the randomness associated with these data sets is important as they can influence the operation of the energy hubs. Therefore, developing a stochastic optimization problem could be an alternative.

7.3.1 Stochastic hourly Ontario electricity price data

In this study, the historical electricity price data in Ontario has been used in order to develop potential electricity prices that can occur in an hour. Information for this has been gathered from the Independent Electricity System Operator's (IESO) historical data archives **[154]**.

Historical Hourly Ontario Electricity Price for the period of 2003–2013 has been considered for this study. The gathered data for each of the years have been first reoriented from an 8760 (h) × 1 (year) or 8784 (h) × 1 (year) matrix to a 365 (days) × 24 (h) or 366 (days) × 24 (h) matrix. This is done so that one can better analyze the trends in how the electricity price for each hour of the 365 days in a year looks like. However, before starting to carry out the fit test, the entire year's data is segregated into 4 seasons, namely winter (91 days), spring (91 days), summer (91 days), and fall (92 days).

After segregating each of the years (2003–2013) in the order described above, the data for winter, spring, summer and fall seasons were aggregated and arranged into 4 separate data sets with each having values from the period of 2003–2013 for the respective season.

In order to describe how the fitting tests are carried out, the fitting test on the winter season has been described. The fitting tests were carried out using the EasyFIT XL software (MathWave Technologies, Dnepropetrovsk, Ukraine) which is an add-on in Microsoft Excel. The software is used for each of the 24 h. To begin with, we select the column having hour 1's data and fit the distribution and check the fit rank (based on the chi squared test). The fit rank helps to determine the best probability distribution that fits the histogram plot of the column data. Upon fitting the different distributions available in the EasyFIT XL software to each of the 24 h in the accumulated data for every the winter season from 2003–2013, it is seen that the log-logistic (3P) distribution is the best fit. Similarly, after carrying out the same steps for the other three seasons, it is seen that log-logistic (3P) is the best fit. 96 (24 h × 4 seasons) fit tests have been carried out to develop the stochastic data for the hourly Ontario electricity price. In order to give the reader an idea of the values that the fit parameters can take on, Table 7.1 lists values obtained for hour '1' from each of the four seasons. The symbols α, β, and γ are called the shape, scale and location parameters, respectively.

Table 7.1: Values of fit parameters for hour '1' in each of the four seasons

Probability Density Function	Fall	Winter	Spring	Summer
$f(x)=\frac{\alpha}{\beta}\left(\frac{x-\gamma}{\beta}\right)^{\alpha-1}\left(1+\left(\frac{x-\gamma}{\beta}\right)^{\alpha}\right)^{-2}$	$\alpha = 4.5 \times 10^8$, $\beta = 4.04 \times 10^6$, $\gamma = -4.04 \times 10^6$	$\alpha = 25.88$, $\beta = 0.26$, $\gamma = -0.22$	$\alpha = 3.88 \times 10^8$, $\beta = 3.3 \times 10^6$, $\gamma = -3.3 \times 10^6$	$\alpha = 104.4$, $\beta = 0.86$, $\gamma = -0.83$

Using the distributions obtained for electricity price for every hour of winter, fall, spring and summer day, a time series data for a year has been developed. This is done by sampling 5 values or realizations for each hour for all 91 days in a year for the winter, spring, and summer, and for 92 days in the fall season. This data set is now combined and rearranged to develop a year worth of data with each hour in the year having 5 realizations of electricity prices with equal probability associated with it.

7.3.2 Stochastic hourly hydrogen demand data

In this study the power to gas energy hub proposes to meet hourly demand at a hydrogen refueling station located in the greater Toronto area (this is a large urban area with about 6 million people). The first step in preparing the stochastic hydrogen demand data includes setting an estimate on potential fuel cell vehicle market penetration. Oak Ridge National Laboratory carry out a cost and benefit analysis of ramping up fuel cell vehicle market penetration in the US **[155]**. They propose

3 market penetration scenarios, where the number of hydrogen vehicles deployed starting from 2012 to 2025 have been reported. According to the report, scenarios 1 and 2 have been developed such that they follow a market penetration trend similar to what has been observed for the increase in the share of hybrid electric vehicles in North America in the past. The only difference between scenario 1 and 2 is that, scenario 2 assumed an earlier ramp up in market penetration beginning in 2015, whereas scenario 1 assumes a later ramp up in the year 2018. Scenario 3 is defined as an optimistic scenario, and it assumed that availability of refueling infrastructure will not be a constraining factor for the deployment of the fuel cell vehicles in the market. This study uses the market penetration scenario 2 projection for the year 2016. As the Oak Ridge National Laboratory Report presents scenarios for the US market, this study scales the figures down to a value for the greater Toronto area. This is done by initially converting the per capita fuel cell vehicle car ownership in the US to per capita fuel cell vehicle ownership in Canada (based on population data obtained via **[127,156]**). The per capita fuel cell vehicle ownership in Canada is then further scaled down to the per capita fuel cell vehicle ownership for the greater Toronto area **[157]**. The total fuel cell vehicles in the greater Toronto area at the end of 2016 is calculated to be 1766. This value was used in this study to have an estimate of the size of the power to gas energy hub required to meet demands from a large fleet. Figure 7.1 below shows the planning region within which the 1766 fuel cell vehicles are going to be serviced.

Figure 7.1: Ontario Planning Region Map denoting the fuel cell vehicle service area covered by the power to gas energy system.

It is important for a supply chain system to be able to account for the uncertainty in the demand that it is catering to. This study tries to account for the uncertainty in the hydrogen demand on an hourly basis over the course of a year by developing probability distribution functions of two essential factors to account for at a refueling station, namely: (1) The percentage of total number of refueling events over the course of a 24 h period at a refueling station; and (2) The different fueling amounts a station can encounter for a single refueling cycle.

The data for the percentage of total number of refueling events for a 24 h period at a refueling station has been obtained from a presentation prepared by the National Renewable Energy Laboratory (NREL) on the "Performance Status of Hydrogen Stations and Fuel Cell Vehicles" **[158]**.

Figure 7.2 represents the data gathered from the presentation.

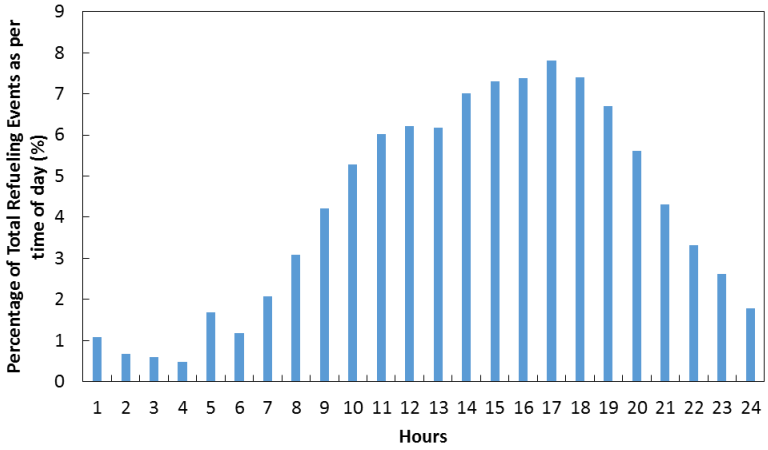

Figure 7.2: Variation in number of refueling events over the course of a day. Data is presented as a percentage of total number of refueling events occurring in a day.

The data taken from the presentation has been segregated into two time frames: (1) 9 AM to 9 PM; and (2) 10 PM to 8 AM. In order to have a less complicated distribution function, the data was fit to two normal distribution functions. The distribution for the time period of 9 AM to 9 PM has a mean of 6.26% and standard deviation of 1.12, respectively. Similarly, for the time period of 10 PM to 8 AM, the distribution has a mean of 1.7% and a standard deviation of 0.9, respectively. Upon generating data from the two normal distributions, they have been combined to form data for a 24 h period for each of the days in a single year. Five different realizations have been sampled for the percentage of total number of refueling events occurring every hour with each realization

having an equal probability of 1/5 associated to them. Note that the total number of refueling events is dependent on the total number of cars that has been estimated above to be 1766.

As mentioned earlier, the second essential factor considered in the study is the different fueling amounts in kg of H_2 that a refueling station can encounter. The range of the data has been taken from NREL's data archive **[159]**. To maintain the simplicity in the distribution considered, a normal distribution has been fitted to the data having a mean and standard deviation of 3.45 and 1.9, respectively. The amount of hydrogen refueled for a single refueling event ranges from 0.7–6.95 kg. The final data was converted to kmol by dividing the realizations sampled with the molecular weight of H_2 (2 kg per kmol). Figure 7.3 shows the normal distribution plot used for the uncertain parameter 'amount of hydrogen refueled'.

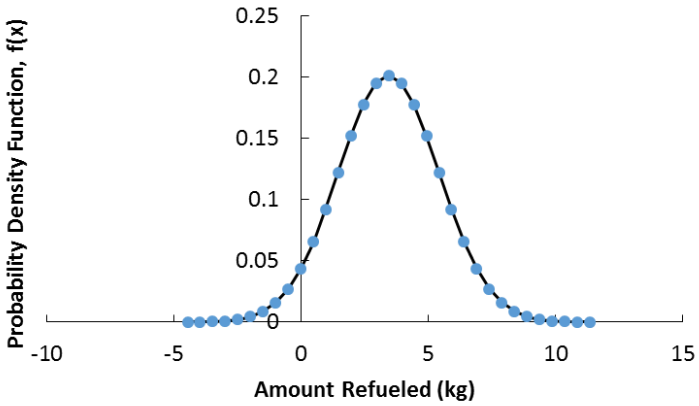

Figure 7.3: Normal distribution plot for the uncertain parameter 'Amount Refueled'.

Note that the number of refueling events data set is time dependent. However, since the data for the amount refueled was only a range, it is assumed for the sake of simplicity to be time independent for each of its five realizations sampled for every hour in a year. The probability of the 5 realizations in every hour is assumed to be equal (=1/5).

7.3.3 Two-Stage stochastic optimization formulation

This sub-section describes the constraints and the objective function of the mixed integer stochastic linear programming problem. The optimization problem has been formulated in the general algebraic modeling system software (GAMS, Version 22.6 (GAMS Software GmbH, Frechen, Germany)).

As mentioned earlier, the services provided by the energy hub in this study include: 1) hydrogen as a fuel for the transportation and natural gas sector, and 2) providing demand response ancillary service.

Figure 7.4 below shows a block diagram layout of the power to gas energy hub modeled in this study.

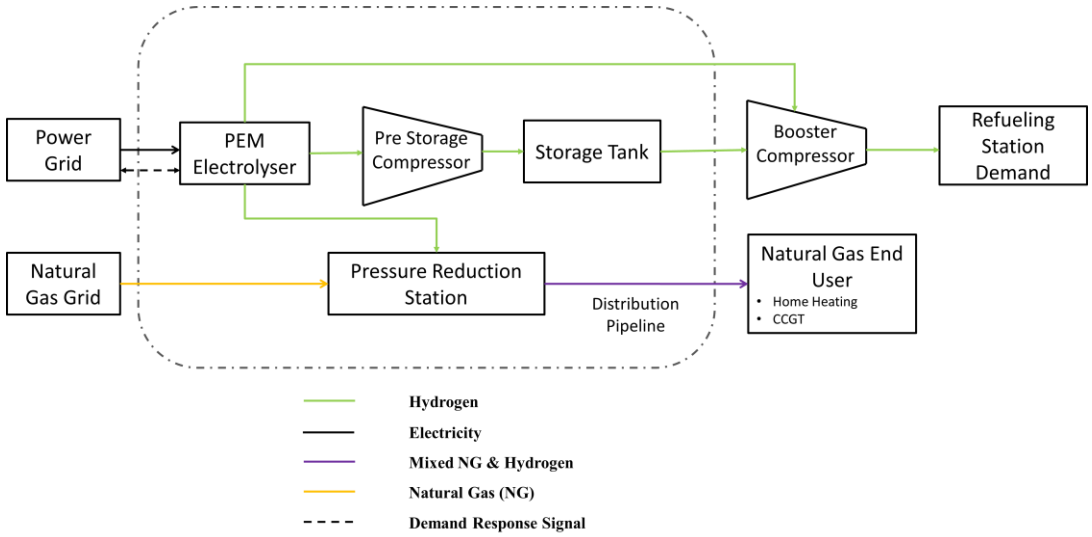

Figure 7.4: Power to gas energy hub system block diagram.

As mentioned earlier in section 7.3.2, the fuel cell vehicle projection used in the study was for the year 2016. However, the data pertaining to the demand response service requirement from the power grid and natural gas flow in the distribution pipelines is only available for the period of November 2012–October 2013. Therefore, the modeling study assumes the November 2012–October 2013 timeframe and looks at the economics of a power to gas energy hub that can meet fuel demand from a high penetration of fuel cell vehicles (ahead of time in the market).

The two stage stochastic programming problem employs two types of decision variables, namely: (1) the first stage decision variables; and (2) the second stage decision variables. The first stage decision variables are assigned values before having known the actual values of the random parameters. Second stage decision variables involve recourse actions taken once the knowledge of the realization of the uncertain parameters is known. Therefore the probability of the realization of the uncertain parameter is also now associated to the corresponding second stage decision variable used to take a recourse action in response to it.

The first stage decision variables in this study determine the size of both the electrolyzer system, and the compressed hydrogen storage system. The second stage decision variables determine how the power to gas energy hub operates. Some examples of the second stage variables include: amount of hydrogen produced, stored, withdrawn or purchased, amount of hydrogen injected in to the pipeline, and amount of load curtailment (demand response) offered.

Stochastic programming approaches involve putting realizations of uncertain parameters into sets/scenarios and then solving a deterministic equivalent optimization problem. The challenge with this approach lies in the number of set/scenarios created after creating possible combinations of the realizations of the uncertain parameters. Higher the number of scenarios greater is the computational time. In this thesis the primary goal of chapter 7 is to provide an initial insight into why accounting for uncertainty in power to gas energy hub modeling studies is important. Therefore, in order to not compromise the computation time of solving the problem, this chapter also gives a detailed description of how even with lesser number of generated scenarios, the value of stochastic solution shows the importance of accounting for uncertainty.

Equation 7.1 presents the formulation of the stochastic optimization problem developed for this study.

$$Minimize: Net\ Cost = C - R$$

s.t.

Energy (Electrolyzer) and H_2 Flow Constraints in Energy Hub:

$$E_{h,s} = (N_{Ele} \times E_{Max}) - ER_{h,s} - DR_{h,s}$$
$$G_{H_2,h,s} = \eta_{El} \times E_{h,s}$$
$$G_{H_2,h,s} = I_{H_2,h,s} + PRS_{H_2,h,s} + B_{H_{2,h,s}}$$
$$Inv_{H_2,h,s} = Inv_{H_2,h-1,s} + I_{H_2,h,s} - O_{H_2,h,s}$$

Energy Demand and H_2 for FCV Demand Constraints:

$$\left(PRS_{H_2,h,s} \times HHV_{H_2}\right) + (PRS_{NG,h,s} \times HHV_{NG}) = ED_h$$
$$RE_{H_2,h,s} \times RA_{H_2,h,s} \times N_{Car} = B_{H_{2,h,s}} + O_{H_2,h,s} + P_{H_2,h,s} \quad (7.1)$$

Technological (Including Active) Constraints:

$$N_{Ele} \times E_{Min} \leq E_{h,s} \leq N_{Ele} \times E_{Max}$$
$$ER_{h,s} \leq N_{Ele} \times E_{Max} \times (1 - \alpha_h)$$
$$PRS_{H_2,h,s} \leq \theta \times (PRS_{NG,h,s} + PRS_{H_2,h,s})$$
$$St_{max} \leq 10000$$
$$N_{Tank} \times C_{Min} \leq St_{max} \leq N_{Tank} \times C_{Max}$$
$$Inv_{H_2,h,s} \leq St_{max}$$
$$\varepsilon \times N_{C_1} \leq I_{H_2,h,s} \leq F_{Max,C} \times N_C$$

Demand Response Ancillary Service (Including Active) Constraints:

$$\alpha_h \times DR_{min} \leq DR_{h,s} \leq N_{Ele} \times E_{Max} \times \alpha_h$$
$$X_{h,s} = \left[(N_{Ele} \times E_{Max}) - DR_{h,s}\right] \times \alpha_h \times Y_{DR}$$

Additional Constraints:

$$NG_{Offset,h,s} = \frac{ED_h}{HHV_{NG}} - PRS_{NG,h,s}$$
$$Net_{CO_2,Offset} = S_{CO_2} - A_{CO_2}$$
$$S_{CO_2} = \left[\frac{1}{p_s} \times \sum_s \sum_h NG_{Offset,h,s} \times EF_{NG}\right] + \left[\frac{1}{p_s} \times \sum_s \sum_h G_{H_2,h,s} \times EF_{SMR}\right]$$
$$A_{CO_2} = \left[\frac{1}{p_s} \times \sum_s \sum_h G_{H_2,h,s} \times \frac{EF_{Grid,h}}{\eta_{El}}\right] + \left[\frac{1}{p_s} \times \sum_s \sum_h P_{H_2,h,s} \times EF_{SMR}\right]$$
$$RL_{PRS,H_2} = \left[SP_{H_2} \times \frac{1}{p_s} \times \sum_s \sum_h PRS_{NG,h,s}\right] - \left[HHV_{H_2} \times \frac{1}{p_s} \times \sum_s \sum_h (PRS_{NG,h,s} \times MP_{NG,h})\right]$$
$$R_{FCV,H_2} = \left[SP_{H_2} \times \frac{1}{p_s} \times \sum_s \sum_h (O_{H_2,h,s} + B_{H_{2,h,s}} + P_{H_2,h,s})\right]$$
$$\Delta_{low} = \left[(SP_{H_2} + 1) \times \frac{1}{p_s} \times \sum_s \sum_h (O_{H_2,h,s} + B_{H_{2,h,s}} + P_{H_2,h,s})\right] - R_{FCV,H_2}$$
$$\Delta_{up} = \left[(SP_{H_2} + 4) \times \frac{1}{p_s} \times \sum_s \sum_h (O_{H_2,h,s} + B_{H_{2,h,s}} + P_{H_2,h,s})\right] - R_{FCV,H_2}$$
$$\Delta_{low} \leq RL_{PRS,H_2} \leq \Delta_{up}$$

The nomenclature associated with the expressions shown in equation 7.1 are described in the following sections and also in Appendix A.7.1-A.7.3.

7.3.3.1 Scenario Definition

The deterministic optimization formulations shown in chapters 4 and 6, had dynamic decision variables (e.g.: energy consumed by electrolyzer E_h) with a subscript 'h' indicating the time index. In this chapter an additional subscript 's' has been defined for the dynamic second stage decision variables. For example, the energy consumed by the electrolyzers will now be denoted as $E_{h,s}$.

One individual combination of the 3 uncertain parameters is defined as a single scenario 's'. Since there are 5 realizations sampled for each of the 3 uncertain parameters, we can hypothetically have 125 combinations which can be assumed to be scenarios. 125 scenarios multiplied by the number of hours in a year (8760) leads to the computation time increasing drastically. The goal of the study

lies in giving an initial insight into the role of uncertainty in power to gas energy hub modeling. Therefore, in order to reduce computational time, the realization values of the 3 uncertain parameters have been aggregated into two categories, namely a high realization value and a low realization value. Then the 5 most probable combinations of the 2 realization categories for each of the 3 uncertain parameters have been created to form 5 most probable scenarios. The probability associated with each of the 5 scenarios has been considered to be 0.2.

The most probable combinations that is assumed in this study include:

- A scenario with high electricity price realization, low amount refueled realization, and low number of refueling events realization;
- A scenario with low electricity price realization, high amount refueled realization and high number of refueling events realization;
- A scenario with low electricity price realization, low amount refueled realization and high number of refueling events realization;
- A scenario with high electricity price realization, low amount refueled realization and high number of refueling events realization, and
- A scenario with high electricity price realization, high amount refueled realization and high number of refueling events realization.

High electricity price realizations are assumed to include values greater than or equal to 6.5 cents per kWh, whereas values of realization below that are considered to be low electricity price realizations. High amount refueled realizations include values greater than or equal to 2.5 kg (or 1.25 kmol), whereas values less than that are taken to be low amount refueled realizations. Number of refueling event realizations above 4% of 1766 total fuel cell vehicles are considered high number of refueling events, while realization values less than or equal to 4% of 1766 total fuel cell vehicles are considered low number of refueling events.

Due to the new notation style, all of the energy hub design constraints will be explained again to maintain clarity. The nomenclature for this chapter has been shown in Appendix A.7.1 to A.7.3.

7.3.3.2 Energy hub design constraints

Equation 7.2 is used to estimate the hydrogen produced ($G_{H_2,h,s}$) by polymer electrolyte membrane (PEM) electrolyzers which are the chosen technology for this study. The electrolyzer efficiency is denoted by η_{El} in kmol per kWh. The amount of energy consumed by the electrolyzers is denoted by $E_{h,s}$, kWh.

$$G_{H_2,h,s} = \eta_{El} \times E_{h,s} \tag{7.2}$$

The hydrogen produced by the electrolyzer can be broken down in to three streams (see equation 7.3), namely: 1) hydrogen injected into the on-site compressed storage system ($I_{H_2,h,s}$, kmol); 2) hydrogen sent to the pressure reduction station for injection in to the natural gas distribution pipelines ($PRS_{H_2,h,s}$, kmol); and 3) the stream that bypasses storage in the on-site tanks and is sent directly to the fuel cell vehicle refueling station dispenser ($B_{H_{2,h,s}}$, kmol):

$$G_{H_2,h,s} = I_{H_2,h,s} + PRS_{H_2,h,s} + B_{H_{2,h,s}} \tag{7.3}$$

The product of number of cars (N_{Car}), with both stochastic parameters, namely, the percentage of total number of refueling events ($RE_{H_2,h,s}$), and the amount fueled ($RA_{H_2,h,s}$) can be interpreted as the hourly hydrogen demand:

$$RE_{H_2,h,s} \times RA_{H_2,h,s} \times N_{Car} = B_{H_{2,h,s}} + O_{H_2,h,s} + P_{H_2,h,s} \tag{7.4}$$

Equation 7.4 shows the flow balance at the hydrogen dispensing point. A combination of hydrogen coming directly from: 1) the electrolyzers (storage bypass stream, $B_{H_{2,h,s}}$, kmol); 2) the storage tank ($O_{H_2,h,s}$, kmol); and 3) industrial producer (hydrogen purchased, $P_{H_2,h,s}$, kmol) can be used to meet hydrogen demand.

The rated energy consumption capacity of the PEM electrolyzers used in the study is 1000 kWh (E_{Max}). Due to the fast ramping capabilities of the electrolyzers it is assumed that they can be turned off and restarted fairly quickly. Therefore, the lower operating limit (E_{Min}, kWh) is set at 0

kWh. The constraint shown in equation 7.5 is used to determine the number of PEM electrolyzers to be installed at the energy hub (N_{Ele}):

$$N_{Ele} \times E_{Min} \leq E_{h,s} \leq N_{Ele} \times E_{Max} \tag{7.5}$$

The energy consumed by the electrolyzers is one of the second stage variables of the stochastic optimization problem. It can be regulated according the change in electricity price, the demand response required and the hydrogen demand placed on the energy hub. Equation 7.6 shows two variables that are used in order to denote the reduction in energy consumption by the electrolyzers. During hours when demand response is to be offered, the variable $DR_{h,s}$ (kWh) is used to denote the reduction in energy consumption. Consequently, the variable $ER_{h,s}$ (kWh) is used to denote the amount by which energy consumption is reduced when there is no demand response service that needs to be offered to the power grid. These two variables are subtracted from the maximum energy consumption limit of the electrolyzer system, denoted by the product of the number of electrolyzers (N_{Ele}) in the energy hub and the maximum energy consumption rating (E_{Max}, kWh) of a single electrolyzer unit:

$$E_{h.s} = (N_{Ele} \times E_{Max}) - ER_{h.s} - DR_{h.s} \tag{7.6}$$

The usage of the two variables $ER_{h,s}$ and $DR_{h,s}$ to denote energy consumption reduction will also require one to create a clear distinction between the hours in which demand response needs to be offered and the hours in which it does not have to be offered. The binary parameter α_h (Equation 7.7) is used to denote hours when demand response is required and it takes a value of 1 during these hours. There is no subscript 's' associated with α as demand response is not considered to be a stochastic random parameter in this study. Equation 7.7 is used to set an upper and lower bound on the demand response capacity offered by the energy hub. As mentioned earlier in section 6.3.2.4, when participating in the demand response market, a load has to provide a minimum of 1000 kWh when it has been contracted to provide the service. The maximum reduction in load that the system can offer is its rated capacity. In other words the electrolyzers can be completely turned off. This upper bound is shown by the right hand side of the inequality constraint in Equation 7.7:

$$\alpha_h \times DR_{min} \leq DR_{h,s} \leq N_{Ele} \times E_{Max} \times \alpha_h \tag{7.7}$$

Similarly, during the hours when no demand response is required (denoted by the term $1 - \alpha_h$ in Equation 7.8), the variable $ER_{h,s}$ (kWh) can have a maximum value equivalent to the rated capacity of the electrolyzer system:

$$ER_{h,s} \leq N_{Ele} \times E_{Max} \times (1 - \alpha_h) \tag{7.8}$$

The demand response service provider is issued a clawback cost by the IESO in hours when the entire contracted demand response capacity is not offered. The unit clawback cost ($ per kWh) is the same as the unit price offered to the load to provide demand response. The notation Y_{DR} ($ per kWh) is defined to denote this unit price. The contracted capacity of the power to gas energy hub is taken to be equal to the rated capacity ($N_{Ele} \times E_{Max}$, kWh) of the electrolyzer system as shown in equation 7.9. The clawback ($X_{h,s}$, $) is estimated by multiplying the difference between the rated capacity and the demand response offered with the demand response incentive (Y_{DR}, $ per kWh):

$$X_{h,s} = \left[(N_{Ele} \times E_{Max}) - DR_{h,s}\right] \times \alpha_h \times Y_{DR} \tag{7.9}$$

Equation 7.10 is used in the model to constrain the amount of hydrogen injected into the natural gas pressure reduction station ($PRS_{H_2,h,s}$, kmol per hour). It is a rearrangement of the equation used to calculate the concentration of hydrogen in the natural gas system, where the denominator ($PRS_{NG,h,s} + PRS_{H_2,h,s}$, kmol) is taken to the right hand side of the inequality. At a particular instant, the concentration of hydrogen within the natural gas system is constrained to a maximum of 5 vol.% **[40]**.

This limit is set by the notation θ in equation 7.10, that accounts for the molecular weight and density of hydrogen and natural gas to make sure the concentration limit in vol.% units is not exceeded:

$$PRS_{H_2,h,s} \leq \theta \times (PRS_{NG,h,s} + PRS_{H_2,h,s}) \tag{7.10}$$

Equation 7.11 is a simple energy balance equation that equates the energy content of the hydrogen and natural gas flow through the distribution pipeline to the hourly energy demand from the natural gas end user (ED_h, MMBtu per hour). The energy demand from the natural gas end user is not a stochastic random parameter and therefore does not have the subscript ‘s’ associated with it. The

terms HHV_{H_2} and HHV_{NG} are the high heating values of hydrogen and natural gas (in MMBtu per kmol):

$$\left(PRS_{H_2,h,s} \times HHV_{H_2}\right) + \left(PRS_{NG,h,s} \times HHV_{NG}\right) = ED_h \tag{7.11}$$

The power to gas energy hub sizes an on-site tank storage system used for the fuel cell vehicle refueling station. Equation 7.12 has been used to constrain the maximum hydrogen storage system capacity denoted by the variable St_{max} (kmol). Since the goal of the optimization is to minimize net cost (see equation 7.21), one can set a large enough arbitrary number as the upper bound for St_{max}:

$$St_{max} \leq 10000 \tag{7.12}$$

The optimization solver then decides the value that St_{max} should take such that it satisfies the inequality constraints shown in equation 7.13. Since the problem optimizes net cost, the value of St_{max} will most likely going to be a multiple of the maximum capacity of a single tank unit (C_{Max}). In this study, tanks with a maximum unit capacity of 45.4 kmol (or ~90 kg) at a maximum storage pressure of 172 bar have been used **[62]**:

$$N_{Tank} \times C_{Min} \leq St_{max} \leq N_{Tank} \times C_{Max} \tag{7.13}$$

A minimum inventory level inside each tank should be maintained so that the tank pressure does not fall below 70 bar. The lower inventory limit was calculated using the ideal gas equation with compressibility factor of hydrogen used to account for real gas behavior. The lower limit on the tank storage comes from the knowledge that hydrogen withdrawn from storage is sent to a booster compressor unit that can compress gas from 70 bar to 825 bar to complete a refueling cycle for a fuel cell vehicle that has maximum on-board tank storage pressure of 700 bar **[62,160]**.

The hydrogen inventory ($Inv_{H_2,h,s}$, kmol) in the tank storage system at the end of every hour for each scenario 's' cannot exceed St_{max}. This relation is portrayed by equation 7.14 below:

$$Inv_{H_2,h,s} \leq St_{max} \tag{7.14}$$

Equation 7.15 shows the tank storage system's inventory balance. The inventory is updated at the end of every hour based on the amount of hydrogen injected ($I_{H_2,h,s}$, kmol per hour) and/or withdrawn ($O_{H_2,h,s}$, kmol per hour) from storage:

$$Inv_{H_2,h,s} = Inv_{H_2,h-1,s} + I_{H_2,h,s} - O_{H_2,h,s} \quad (7.15)$$

The hydrogen goes through a compressor before being injected into the tank storage system. In this study a compressor module with a maximum flow handling capacity ($F_{Max,C}$) of 21 kmol per hour (or 42 kg per hour) has been used. The reciprocating compressor can take an inlet pressure of 42 psig and has an outlet pressure of 4500 psig. Therefore the optimization problem is constrained such that the product of number of compressors (N_C) and its unit flow capacity ($F_{Max,C}$, kmol per hour) is greater than or equal to the hydrogen flow directed to storage for injection ($I_{H_2,h,s}$, kmol per hour):

$$\varepsilon \times N_{C_1} \leq I_{H_2,h,s} \leq F_{Max,C} \times N_C \quad (7.16)$$

The hydrogen enriched natural gas used to satisfy end user energy demand offsets a certain fraction of the natural gas that would have been sent if no hydrogen is injected in to the distribution pipelines. Equation 7.17 calculates this offset ($NG_{Offset,h,s}$, kmol per hour) by subtracting the chosen values of natural gas flow through the distribution pipelines ($PRS_{NG,h,s}$, kmol per hour) by the optimization solver from the ratio of natural gas energy demand and high heating value of natural gas (HHV_{NG}, MMBtu per kmol):

$$NG_{Offset,h,s} = \frac{ED_h}{HHV_{NG}} - PRS_{NG,h,s} \quad (7.17)$$

There are two source points of emissions from the energy hub: (1) emissions associated with electricity bought for hydrogen production; and (2) emissions associated with hydrogen purchased from the market.

The emissions associated with the electricity bought is accounted for by multiplying the gas produced by the electrolyzers ($G_{H_2,h,s}$, kmol per hour) with the ratio of power grid emission factor in Ontario ($EF_{Grid,h}$, kg CO_2 per kWh) and electrolyzer efficiency (η_{El}, kmol per kWh).

The hydrogen purchased from the market is assumed to be produced from the steam methane reforming process. Therefore, the product of hydrogen purchased ($P_{H_2,h,s}$, kmol per hour) and the emission factor of the steam methane reforming process (EF_{SMR}, kg CO_2 per kmol H_2) **[111,161]** summed over all sets and hours gives in technicality, the CO_2 emissions purchased by the energy

hub. Equation 7.18 adds these two source points of CO_2 emission to give the total annual emission incurred (A_{CO_2}, kg of CO_2 emission incurred):

$$A_{CO_2} = \left[\frac{1}{p_s} \times \sum_s \sum_h G_{H_2,h,s} \times \frac{EF_{Grid,h}}{\eta_{El}}\right] + \left[\frac{1}{p_s} \times \sum_s \sum_h P_{H_2,h,s} \times EF_{SMR}\right] \quad (7.18)$$

In equation 7.18, the CO_2 emission offset associated with the use of hydrogen enriched natural gas (as described above) has been calculated by summing the product of natural gas usage offset at the end user ($NG_{Offset,h,s}$, kmol per hour) and the well-to-wheel emission factor of natural gas (EF_{NG}, kg CO_2 per kmol NG) **[111]**.

The second part of equation 7.18 calculates the emissions deferred by not using the steam methane reforming process to produce hydrogen. This is estimated by summing the product of total hydrogen flow coming from the electrolyzers ($G_{H_2,h,s}$, kmol per hour) and the emission factor of hydrogen produced by the steam methane reforming process (EF_{SMR}, kg CO_2 per kmol of H_2).

The CO_2 emissions offset from selling hydrogen enriched natural gas to the natural gas end user and deferring the use of the steam methane reforming process for producing hydrogen are summed to calculate the total CO_2 emission offsets possible on annual basis (S_{CO_2}, kg of CO_2 emissions offset):

$$S_{CO_2} = \left[\frac{1}{p_s} \times \sum_s \sum_h NG_{Offset,h,s} \times EF_{NG}\right] + \left[\frac{1}{p_s} \times \sum_s \sum_h G_{H_2,h,s} \times EF_{SMR}\right] \quad (7.19)$$

The difference between S_{CO_2} and A_{CO_2} give the net CO_2 emissions offset by the power to gas energy hub ($Net_{CO_2,Offset}$, kg of CO_2):

$$Net_{CO_2,Offset} = S_{CO_2} - A_{CO_2} \quad (7.19)$$

7.3.3.3 Objective function

The objective of the optimization study is to minimize the annual net cost ($Net\ Cost$, \$) of operating the energy hub, and is calculated from the difference between the annual cost (C, \$) and annual revenue (R, \$) (Equation 7.21):

$$Minimize: Net\ Cost = C - R \tag{7.21}$$

The different contributors to the annual cost variable 'C' have been shown in equation (7.22) below:

$$\begin{aligned} C = & \left[N_{Ele} \times \left(C_{Ele} + O\&M_{Ele} \right) \right] + \left[N_{Tank} \times C_{Tank} \right] + \left[N_C \times C_C \right] \\ & + \left[\frac{1}{p_s} \times \sum_s \sum_h \left(\left\{ E_{h,s} + \left(I_{H_2,h,s} \times ECF_C \right) \right\} \times \left\{ EP_{h,s} + TC \right\} \right) \right] \\ & + \left[C_{H_2O} \times WCR_{Ele} \times \frac{1}{p_s} \times \sum_s \sum_h G_{H_2,h,s} \right] \\ & + \left[TC_{NG} \times HHV_{H_2} \times \frac{1}{p_s} \times \sum_s \sum_h PRS_{H_2,h,s} \right] + \left[\frac{1}{p_s} \times \sum_s \sum_h X_{h,s} \right] \\ & + \left[MP_{H_2} \times \frac{1}{p_s} \times \sum_s \sum_h P_{H_2,h,s} \right] \end{aligned} \tag{7.22}$$

p_s denotes the probability associated with a scenario in the above equation.

Some of the new symbols in equation 7.22 that have not been described in earlier equations include:

- C_{Ele}: Annual amortized cost of a PEM electrolyzer unit **[44]**. This cost includes the cost of replacement of stacks which are assumed to have a stack life of 5 years. The replacement cost is taken to be equal to 15% of the capital cost **[162]**.
- $O\&M_{Ele}$: Annual operating and maintenance cost of an electrolyzer unit.
- C_{Tank}: Annual cost of a tank storage unit.
- C_C: Annual cost of a compressor unit.
- $EP_{h,s}$: Uncertain hourly electricity price realization in a particular hour and scenario 's' ($ per kWh).
- TC: Unit transmission cost of electricity ($ per kWh).
- C_{H_2O}: Unit cost of water ($ per liter).
- WCR_{Ele}: Water consumed per kmol of hydrogen produced (liter per kmol).
- ECF_C: Energy consumed per kmol of hydrogen compressed (kWh per kmol) **[91]**.
- TC_{NG}: Transmission cost per MMBtu of energy transmitted through natural gas pipelines. This includes the cost of running compressors along the natural gas pipeline **[139]**.

- MP_{H_2}: Unit market price of hydrogen ($ per kmol).

Note that all costs were updated to 2012 Canadian dollars and amortized for a project lifetime of 20 years and an interest rate of 8%.

The first three terms in equation 7.22 denote the cost of installing electrolyzer, tank and compressor units. The following terms in sequential order denote:

- The annual cost of buying and transmitting electricity to electrolyzers and compressors.
- Annual cost of buying water for H_2 production
- Annual cost of distributing H_2 through the natural gas distribution system.
- Annual clawback cost associated with participating and failing to provide demand response in the ancillary service market.
- Annual cost associated with the hydrogen purchased from a third party vendor.

Equation 7.23 shows the terms that are included the annual revenue:

$$\begin{aligned} R = & \left[SP_{H_2} \times \frac{1}{p_s} \times \sum_s \sum_h \left(O_{H_{2,h,s}} + B_{H_2,h,s} + P_{H_2,h,s} \right) \right] \\ & + \left[\frac{1}{p_s} \times \sum_s \sum_h HHV_{H_2} \times PRS_{H_2,h,s} \times MP_{NG,h} \right] \\ & + \left[Y_{DR} \times \frac{1}{p_s} \times \sum_s \sum_h \left(DR_{h,s} \times \alpha_h \right) \right] \\ & + \left[Net_{CO_2,Offset} \times MC_{CO_2} \right] \end{aligned} \tag{7.23}$$

The terms shown in equation 7.23 that have not been described earlier include:

- SP_{H_2}: The unit selling price of hydrogen when hydrogen is sold to the refueling station ($ per kmol) **[142]**.

- $MP_{NG,h}$: Market price of natural gas. In this case it is assumed to be the Henry Hub Spot Price ($ per MMBtu). Hydrogen injected into the distribution line is sold to the natural gas utility that distributes it to its end users on an energy basis at this price.
- MC_{CO_2}: Carbon tax credit earned per kg of CO_2 emissions offset ($ per kg CO_2) **[140]**.

In sequential order (as they appear), equation 7.23 includes:

- Annual revenue from selling hydrogen to fuel cell vehicles.
- Annual revenue from selling hydrogen to the natural gas utility on an energy value basis.
- Annual revenue from providing the demand response service.
- Annual revenue earned from offsetting CO_2 emissions at the end user and using a cleaner method in comparison to SMR for producing H_2.

Similar to what was mentioned in section 6.3.2.2, the hydrogen sold to the natural gas utility in this study is undervalued again. Therefore the optimization problem tries to minimize the price differential between its production price and selling price to the natural gas grid.

7.3.3.4 Design constraint – part 2

Equation 7.24 compares revenues earned from selling hydrogen to the natural gas utility at the Henry hub spot price with what can be earned if the gas is sold at the same value as SP_{H_2}, which is the selling price of hydrogen to fuel cell vehicles. This comparison yields the annual revenue loss (RL_{PRS,H_2}, \$):

$$RL_{PRS,H_2} = \left[SP_{H_2} \times \frac{1}{p_s} \times \sum_s \sum_h PRS_{NG,h,s}\right] - \left[HHV_{H_2} \times \frac{1}{p_s} \times \sum_s \sum_h (PRS_{NG,h,s} \times MP_{NG,h})\right] \quad (7.24)$$

Even though the cost of production based on electricity price is low in periods of low electricity price, the energy hub currently does not receive any additional incentive to account for the costs associated with its capital investment when it injects hydrogen into the natural gas system. Therefore there is a loss incurred in this pathway. In order to constrain this loss, equations 7.25–7.28 have been incorporated in to the optimization problem. Equation 7.25 is used to estimate the annual revenue earned from meeting fuel cell vehicle hydrogen demand (R_{FCV,H_2}). In this study, the selling price (SP_{H_2}) is set at \$16 per kmol. The National Hydrogen Association estimates market price of hydrogen as a transportation fuel between \$5–\$10 per kg (or \$10–\$20 per kmol) **[142]**:

$$R_{FCV,H_2} = \left[SP_{H_2} \times \frac{1}{p_s} \times \sum_s \sum_h (O_{H_2,h,s} + B_{H_{2,h,s}} + P_{H_2,h,s})\right] \quad (7.25)$$

The selling price of hydrogen set in this study can be marked up by \$4 per kmol. Equation 7.26 is used to estimate the additional revenue (Δ_{low}) that can be earned when the current selling price (SP_{H_2}) is increased by \$1 per kmol:

$$\Delta_{low} = \left[(SP_{H_2} + 1) \times \frac{1}{p_s} \times \sum_s \sum_h (O_{H_2,h,s} + B_{H_{2,h,s}} + P_{H_2,h,s})\right] - R_{FCV,H_2} \quad (7.26)$$

Similarly, equation 7.27 has been used to estimate the additional revenue that can be earned when (SP_{H_2}) is increased by \$4 per kmol:

$$\Delta_{up} = \left[(SP_{H_2} + 4) \times \frac{1}{p_s} \times \sum_{s} \sum_{h} (O_{H_2,h,s} + B_{H_{2,h,s}} + P_{H_2,h,s}) \right] - R_{FCV,H_2} \quad (7.27)$$

The variables Δ_{low} and Δ_{up} are then used to constrain the variable RL_{PRS,H_2} in equation 7.28. By adding equations 7.25-7.28 to the formulation, the solver ensures that there is injection of hydrogen in to the natural gas pressure reduction station's distribution pipelines.

$$\Delta_{low} \leq RL_{PRS,H_2} \leq \Delta_{up} \quad (7.28)$$

The power to gas energy hub acts as a supplier of hydrogen to a refueling station collocated with it. It is assumed that the power to gas energy hub is the sole provider of hydrogen to this refueling station, even if the energy hub has to purchase hydrogen to meet demand from the refueling station. Modeling of the components associated with dispenser, booster compressor system, and cascaded tank storage unit within the refueling station have been ignored to reduce the computational intensity required to solve the problem.

The goal of this study is to assess the benefit of accounting for the uncertainty associated in developing of power to gas systems supplying multiple services. The study does not focus on the different ways of addressing uncertainty and therefore does not include a robust optimization analysis.

7.3.4 Stochastic programming concepts: EVPI and VSS

The value of the solution obtained from a stochastic optimization problem can be determined with the help of two existing theories, namely: 1) the expected value of perfect information (EVPI); and 2) the value of stochastic solution (VSS) **[153]**.

The EVPI is a measure of the cost one is willing to pay in order to attain accurate information of the random parameters (or data sets/signals). This can also be interpreted as the cost one incurs for using 'prediction techniques' **[163]**. In order to estimate the EVPI, one needs to first define the terms RP solution and WSS. The solution from the two stage stochastic programming problem is called the recourse problem solution (RP solution). WSS is defined as the wait-and-see solution, and can be calculated by initially solving the optimization problem for each of the possible scenarios of the random parameters, one by one. In others, one needs to solve as many deterministic optimization problems as the number of scenarios for the random parameter one

considers in their work. Once the deterministic solutions are obtained, the mean of solutions to the objective function obtained from every deterministic optimization problem gives the WSS. The difference between the RP solution and WSS is called the EVPI (see equation 7.29):

$$\mathrm{EVPI} = \mathrm{RP} - \mathrm{WSS} \tag{7.29}$$

In order to estimate the VSS, one needs to first estimate the solution to the expected value (EV) problem. The solution to the optimization problem when it is solved by taking the expected value of the random parameter gives one the EV. The values of the first stage decision variables obtained for the expected value problem (EV) need to be then used and fixed in the two stage stochastic optimization problem. Upon fixing the first stage decision variables (based on the values obtained from the EV problem solution) and solving the RP, one can estimate the EEV (expected result of using the EV solution). The EEV helps in determining the solution to the second stage decision variables when the first stage decision variables have been fixed. Subsequently, the difference between EEV and the RP solution gives the VSS (see equation 7.30):

$$\mathrm{VSS} = \mathrm{EEV} - \mathrm{RP} \tag{7.30}$$

According to Birge and Louveaux **[153]**, the VSS helps in determining whether it is beneficial to set the first stage decision variables in the stochastic optimization problem (based on the solution obtained from the EV problem). In other words, if the difference between EEV and RP is negative, it is less beneficial to account for uncertainty in the parametric data sets/signals and the expected value solution is good enough.

7.4 Results

This section highlights the results of the stochastic optimization problem. The section presents analyses on the effects of the uncertain parameters on the first and second stage decision variables. The values of EVPI and VSS have also been estimated. The section ends with highlighting the importance of accounting uncertainty rather than taking a deterministic approach.

7.4.1 Effect of Uncertainty on second stage decision variables

Note that figure 7.5 is used to highlight how the energy hub operates in a particular hour for the five probabilistic scenarios. Each of the 5 scenarios have a realization associated with the

electricity price (denoted by the line), the amount refueled (kmol) and the number of refueling events. Since it is difficult to show the values of all the three uncertain parameters in the figure, the product of number of fuel cell vehicles (1766), and the 2 random parameters: amount refueled (kmol) and number of refueling events (%) has been represented as the hydrogen demand. In figure 7.5 the height of the bar graphs are representative of the hydrogen demand values.

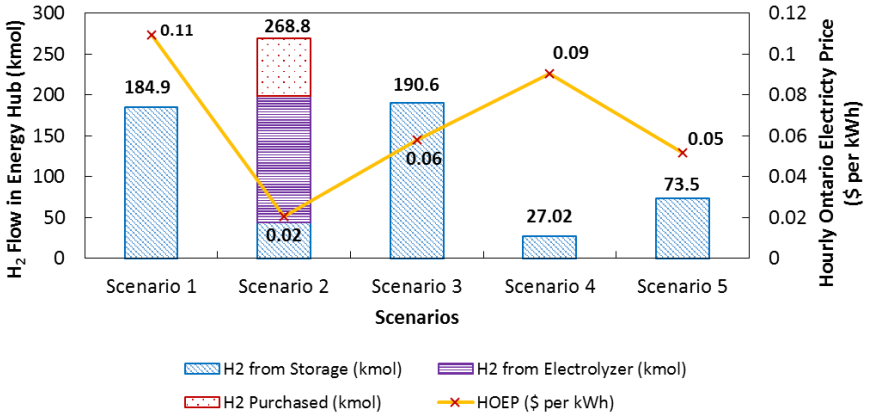

Figure 7.5: Variation in hydrogen stream flows used to meet hydrogen demand for 5 scenarios for a particular hour. Each scenario includes a realization of electricity price, amount refueled and number of refueling events. The line denotes the value of the electricity price realizations within the five probabilistic scenarios in a particular hour.

The hydrogen demand in a particular hour can be met by: (1) withdrawing from storage; (2) producing hydrogen from electrolyzer and directly sending it to a dispenser; and (3) purchasing hydrogen from the market. Figure 7.5 shows how the energy hub operates for a particular hour when the HOEP (Hourly Ontario Electricity Price), the amount refueled, and the number of refueling events are stochastic inputs to the optimization problem. In the above figure, it is observed that for scenarios 1, 3, 4 and 5, the HOEP is higher in comparison to scenario 2. Therefore, the hydrogen demand is met by withdrawing hydrogen from storage in scenarios 1, 3, 4 and 5. When the HOEP decreases for scenario 2, the share hydrogen coming directly from the electrolyzer is seen to increase. Despite the HOEP being the lowest in scenario 2, the high hydrogen demand value in scenario 2 leads the optimization problem to satisfy 25.9% of the demand by purchasing hydrogen from the market. The electrolyzers cover 57.8% of the total hydrogen demand in scenario 2. The remaining share (16.3%) of hydrogen demand in scenario 2 is satisfied by withdrawing hydrogen from on-site hydrogen storage tanks. Therefore, even if HOEP is low and the hydrogen demand is high for a particular scenario, the energy hub may have to purchase hydrogen from the market to satisfy demand.

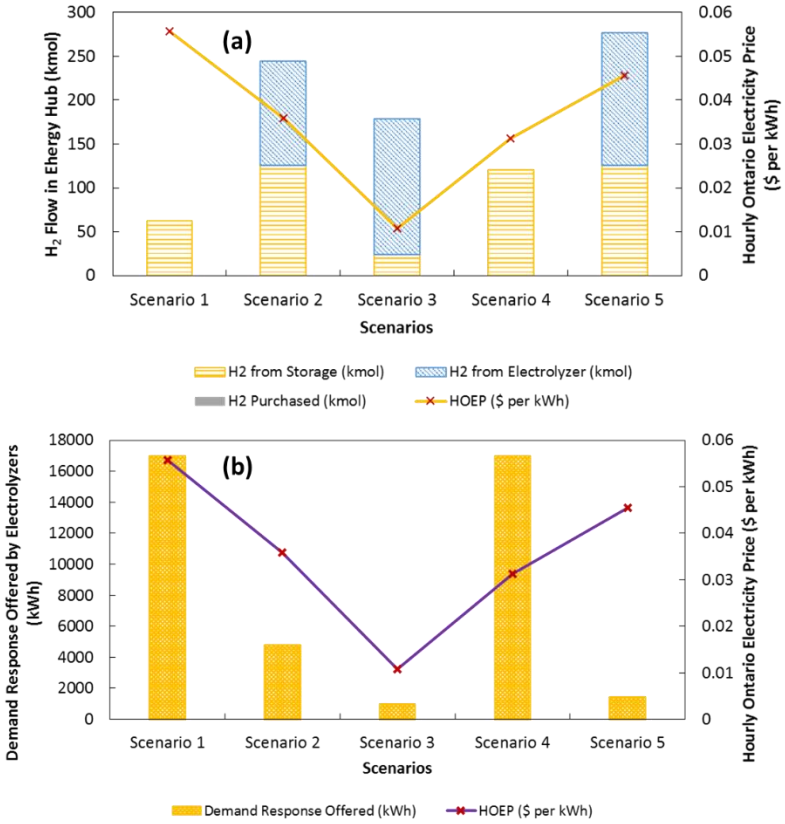

Figure 7.6: The bars in (a) show the different options utilized to meet the five probabilistic hydrogen demand scenario in an hour; (b) shows the change in demand response capacity offered for different realizations of electricity price and hydrogen demand in each of the 5 scenarios in an hour. (Note: hydrogen demand is only shown in (a)). (a, b) denote the value of the five probabilistic electricity price realizations in each scenario through the lines with markers.

Through figure 7.6, it is shown how the energy hub varies its operating regime to provide demand response while still meeting the stochastic hydrogen demand for a particular hour in the optimization time frame. The stochastic parameter HOEP is also plotted in figure 7.6 to show its influence in the energy hub operating regime. Figure 7.6(a) shows two similar trends to figure 7.5: (1) Hydrogen is withdrawn from storage to satisfy FCV demand in case of high HOEP; and (2) The share of hydrogen demand satisfied directly from electrolyzer increases when HOEP decreases.

At a particular hour, the maximum and minimum demand response capacity that can be offered by the electrolyzer system within the energy hub is 17,000 kWh and 1000 kWh. In figure 7.6(b), it is seen that the maximum demand response capacity is offered for scenarios 1, and 4. This trend can be easier to interpret when one looks at the high value of HOEP and low value of hydrogen flow

from storage (low hydrogen demand: implying low amount refueled and low number of refueling events) for scenario 1 in figure 7.6(a). Therefore when the two figures 7.6(a) and 7.6(b) are compared for scenario 1, it is seen that the electrolyzer is able to provide its full demand response capacity (Figure 7.6(b)) and satisfy the low hydrogen demand by only needing to withdraw hydrogen from on-site storage (Figure 7.6(a)).

Another interesting inference can be made when one looks at a scenario (3) where electricity price realization (HOEP) is low and hydrogen flow in the energy hub is high (implying that hydrogen demand is high or in other words the realizations for amount refueled, and number of refueling events are high, see scenario 3 in figure 7.6(a)). In this case the lower HOEP and higher hydrogen flow in comparison to scenario 1 (in figure 7.6(a)), leads the optimization problem to decide that running electrolyzers at a higher operating level and paying the clawback cost of not providing the entire demand response capacity (see figure 7.6(b)) is a more profitable decision. In other words, it can be concluded that the demand response offered by the electrolyzers is directly proportional to the value of HOEP realizations and inversely proportional to the realizations of (amount refueled and number of refueling events) hydrogen demand at any particular hour and scenario.

Implementing the power to gas energy hub concept within an energy economy transitioning towards increased share of renewable energy generation reduces the emissions associated with producing hydrogen. The net $CO_{2,e}$ emissions offsets achievable by the power to gas energy hub (see equations 7.17–7.20) accounts for : 1) the $CO_{2,e}$ emissions offset from utilizing the water electrolysis process to produce hydrogen in comparison to using the steam methane reforming technology; 2) The $CO_{2,e}$ emissions incurred while purchasing hydrogen from the market (based on the knowledge that the hydrogen bought is produced via the steam methane reforming process); and 3) The lifecycle $CO_{2,e}$ emissions (associated with using 100% natural gas) offset achieved by selling a cleaner blend of fuel to the natural gas end user (hydrogen-enriched natural gas). It is estimated that on an annual basis the energy hub can offset 9470.6 tonnes of $CO_{2,e}$ emissions.

7.4.2 EVPI and VSS Evaluation

From the solutions to the recourse problem (RP) and the EEV problem presented in table 7.2 below, the VSS is estimated to be 104,276.673 (VSS = EEV−RP). The positive VSS denotes that the accounting for uncertainty in the modeling of the energy hub is beneficial. The WSS for the

objective function (Net Cost) has been calculated to be −9241480.626. Based on this, the EVPI has been calculated to be 57,211.014 (EVPI = RP−WSS). The high value of EVPI shows that one must pay a high cost to obtain exact information on the values of the random parametric data sets/signals. Therefore adopting the usage of stochastic programming is beneficial and one can save 104,276.673 in cost. Based on this trend it is likely to see the saving increase for greater variances in the data set. However, the study does not go further in to validating this.

Table 7.2: Values of objective function and decision variables for the recourse problem (RP), expected value problem and EEV problem.

Results	Expected Value (EV) Solution	Recourse Problem (RP) Solution	Expected Value of Using EV Solution (EEV)
Objective Function: Net Cost ($ per year)	−8,959,896	−9,184,269	−9,079,992
Power to Gas System Capacity (MW_{el})	16	17	16
Compressed H_2 Storage Capacity (kg)	1958	1869	1958
H_2 Purchased (kg per year)	0	1814.142	3824.110
H_2 Produced (kg per year)	1,814,492	1,813,770	1,811,761

7.4.4 Comparison of H_2 and Gasoline Price

The levelized cost of producing hydrogen for the fuel cell vehicle fleet is estimated to be $3.145 per kg. Therefore, selling hydrogen to a fuel cell vehicle fleet at a premium price of $8 per kg **[39]** is a profitable energy recovery pathway for the power to gas energy hub. A kg of H_2 is equal to ~1 gallon gasoline equivalent. Therefore, the $8 per kg H_2 premium price and the $3.145 per kg production price if converted to gasoline equivalents, translate to a gasoline market price of $2.12 per liter and $0.83 per liter. The gasoline price in the region of Toronto was near $1 per liter of gasoline in 2016 **[164]**. The gasoline equivalent price of selling hydrogen ($2.12 per liter, above) is roughly twice at what gasoline is being sold in the present day. This price paid by the end user of hydrogen seems to be high and can be lowered further by either providing the refueling station/power to gas energy hub with tax rebates that allows them to maintain their profit and at the same time sell the hydrogen closer to their production price of $3.145 per kg or $0.83 per liter gasoline equivalent. Another option could be that the government provides price rebates to the end user for using a cleaner hydrogen fuel.

The cost associated with the purchase of the Toyota Mirai (a fuel cell vehicle) in the US market is $58,385 (CAD $ 78,105) **[160]**. Ontario, recently allocated incentives for the purchase of hydrogen powered fuel cell electric vehicles **[36]**. Early adopters of the fuel cell electric vehicle technology, will receive a maximum incentive of $14,000. Enabling both the development of refueling

infrastructure and incentivizing fuel cell electric vehicles will see a growth in the long awaited hydrogen economy.

7.4.5 Impact of Number of Scenarios on EVPI and VSS

This section highlights the impact of increasing the total number of scenarios on the expected value of perfect information (EVPI) and value of stochastic solution (VSS). The number of scenarios have been increased to 10 for every hour. Through unique combinations of the 5 realizations of each of the 3 uncertain parameters every hour, 5 new scenarios have been created.

The probability associated with all of the 10 scenarios are considered to be equal (0.1). The recourse problem has been solved again. The energy hub now requires 20 MW cap of electrolyzers, and 1997.2 kg of storage capacity. The recourse problem with 5 scenarios had a system configuration 17 MW electrolyzer capacity and 1869 kg of storage capacity. It is seen that the increasing the number of uncertain scenarios leads to the increase in the values of the first stage decision variables.

Table 7.3 compares the values of the objective function for 1) The recourse problem; 2) The expected value (EV) problem, and 3) The expected result of using the expected value solution (EEV).

Table 7.3:Comparison of objective function value for the 10 scenario RP problem with EV and EEV solutions

Results	Recourse Problem (RP) Solution	Expected Value (EV) Solution	Expected Value of Using EV Solution (EEV)
Objective Function: Net Cost ($ per year)	-9,150,804	-8,853,962.7	-9,063,791
Electrolyzer Capacity (MW)	20	16	16
Storage Capacity (kg H_2)	1997.2	1869	1869

The value of wait and see solution (WSS) has been estimated to -9,268,624. Using this the new EVPI (=RP – WSS) is calculated to be $117,820.45. The new VSS (=EEV-RP) is now estimated to be $87,012.08. The EVPI of the 10 scenario problem has increased by 105.9% in comparison to the 5 scenario problem (EVPI: $57,211). The VSS for the 10 scenario problem on the other hand is seen to decrease by 16% in comparison to the 5 scenario problem (VSS: $104,276). The increase in values of the first stage decision variables can be one of the reasons for the decrease in VSS. This result is indicative of stable solutions being achieved with increase in number of scenarios.

However due to the large number of time steps (8760 hours), the analysis is constrained to 5 and 10 scenarios. Future work would look at including a greater number of scenarios in the two-stage stochastic programming approach.

7.5 Conclusions

The study proposes the use of the two-stage stochastic programming approach to plan and operate a power to gas energy hub located in an urban area. The goal is to highlight the benefit of accounting for uncertainty in parameters that influence the operation of the power to gas energy hub. The energy hub system is modeled to be able to provide three services, namely: 1) meeting hydrogen demand from a fuel cell vehicle refueling station; 2) selling hydrogen to the natural gas end users as a mixed hydrogen enriched natural gas (HENG) fuel (not more the 5% hydrogen); and 3) provide hourly demand response service by participating in the demand response market (in this case as operated in Ontario by the IESO.

The hourly electricity price, amount refueled at the refueling station, and the number of refueling events have been taken as the random (uncertain) parameters. The two different stages of decisions taken by the stochastic optimization problem include: 1) First Stage: The size of the individual components of the power to gas energy hub (electrolyzer, tank, and compressor); and 2) Second Stage: Decisions taken to operate the components of the energy hub.

Due to the finer time index (hourly) adopted in the modeling study, the realizations of the uncertain parameters have been characterized into 2 categories high and low. The two stage stochastic programming problem is then formulated including the five most probable combinations of the 2 realization categories for each of the 3 uncertain parameters. In other words we have 5 scenarios with each scenario having 3 realization values, one for each of the 3 uncertain parameters. The refueling amount and the number of refueling amounts at a particular time point have been multiplied with an optimistic projection of fuel cell vehicle market penetration (1766 cars in GTA) to estimate the hydrogen demand.

The stochastic parameters are seen to affect the operation of the power to gas energy hub. Higher electricity price realizations for a particular scenario in an hour leads to the hydrogen storage being utilized to meet the hydrogen demand rather than direct from the electrolyzer. Consequently, when

the electricity price realization in a particular scenario in an hour is low, the share of hydrogen coming directly from the electrolyzer increases. So in a jurisdiction where electricity price is often low it is thus likely that the storage requirements would be lower, and the electrolyzer availability higher. When a scenario has a low realization of electricity price but high realization values of amount refueled and number of refueling events (in other words high hydrogen demand), the energy hub will need to purchase hydrogen from the market as shown in scenario 2 of figure 7.5.

The demand response service offered is also seen to be affected by the stochastic nature of electricity price and hydrogen demand. From the analysis presented in Section 3.0, it is observed that the demand response offered by the electrolyzers is directly proportional to the realization of electricity price and inversely proportional to the realization of amount refueled and number of refueling events for any particular scenario in an hour. The power to gas energy hub is also able to offset approximately 9470.6 tonnes of $CO_{2,e}$ emissions by forgoing the use of the steam methane reforming technology for producing hydrogen and using hydrogen enriched natural gas (HENG) that offsets lifecycle $CO_{2,e}$ emissions incurred in using 100% natural gas at the natural gas end user.

The benefit of accounting for uncertainty is highlighted through the two stochastic programming concepts called Value of Stochastic Solution (VSS) and Expected Value of Perfect Information (EVPI). A positive VSS shows that by accounting for uncertainty one can have an economic benefit of $104,276 over a deterministic solution. A positive EVPI of $57,211 highlights the cost one must pay to obtain exact information about the random parameters.

To highlight the change in values of EVPI and VSS, another study with 10 scenarios has been carried out. It has been observed that the component sizes of the power to gas energy hub change. The electrolyzer and storage tank capacity increase from 17 MW and 1869 kg of H_2 to 20 MW and 1997.2 kg of H_2, respectively. The EVPI and VSS values for the 10 scenario problem are $117,820.45 and $87,012.08, respectively. These values reflect a 105.9% increase in EVPI and 16% decrease in the VSS from the 5 scenario problem. The decrease in VSS for the 10 scenario problem is attributable to the first stage decision variables (electrolyzer and storage capacity) being of greater magnitude.

Due to a large number of time steps, increasing the number of scenarios for each time point increases the computational time significantly (5 scenario problem: ~2.5 hours, 10 scenario problem: ~4.6 hours). Therefore, this study constrains itself to assessing the sensitivity of VSS and EVPI for a 5 and 10 scenario stochastic programming problem. The change in VSS and EVPI as highlighted in the above paragraph shows that adding more scenarios will improve the reliability of the results. This would be an exercise for a future study.

Future work will focus on looking at different ways for accounting for uncertainty, like adding risk to the stochastic optimization study and also assessing further how the incentive program can be developed for the hydrogen economy by taking the example of the existing electric vehicle incentive program in Ontario.

Chapter 8: Contributions, Conclusions and Recommendations

This thesis explores the case for curbing surplus baseload electricity exports from Ontario and repurposing the available excess within the province's natural gas and transportation sectors. The concept of a power to gas energy hub and its ability to interlink different energy sectors while using hydrogen as an energy vector has been explored.

8.1 Global Trends and Challenges for Energy Storage in Ontario

Through the analysis presented in this thesis some of the potential barriers for the implementation of such technologies has been highlighted in this section chapter 8. Some of the primary challenges that have acted as a barrier for proliferation of energy storage within the province stem from the limited or unsteady policies that exist within the province.

A clear challenge for such technologies currently includes them being subject to market uplift charges such as global adjustment, transmission connection charges (these can be high depending on their location), administration fees which significantly increases their cost to be competitive. Another issue lies in how the Ontario electricity market price is set. The Independent Electricity System Operator in Ontario does not account for energy storage technologies acting as potential dispatchable loads during hours of predicted surplus baseload generation. The electricity system operator's dispatch scheduling optimization engine needs to be modified to account for dispatchable loads. This would reduce some of the uplift charges especially the global adjustment) as a result of electricity market clearing price increasing and reaching values close to what contracted generation facilities need to be paid.

Energy storage technologies have not been included in the provinces industrial conservation initiatives. Locating energy storage technologies on-site at an industrial location will help conservation efforts. Currently, there are no clear rules, regulations (including safety standards) defined by the Ontario Energy Board or in other legislations within the province. Having a clear role definition of such technologies will help clear ambiguities.

The additional services (e.g., emission reduction, surplus baseload generation management, enabling higher penetration of renewables) provided by them have also not been studied well enough by regulators within the province.

Finally in order to drive investment in energy storage projects, the regulators of the electricity sector need to provide better access to reliable, and current data. This will help investors to understand the regions where there are potential opportunities for such projects within the province.

Regions such as California, countries in Europe especially Germany, the United Kingdom **[165]** realize the potential for hydrogen production technologies to help maintain grid reliability in electricity systems transitioning towards intermittent generation. They also realize how the hydrogen produced can be utilized in other energy sectors to offset $CO_{2,e}$ emissions **[166,167]**. Germany has been a proponent for developing power to gas co-located in regions with intermittent wind and solar farms. Injecting hydrogen and renewable/synthetic natural gas in to their natural gas grids has been a prime focus **[71]**.

The proliferation of hydrogen as an energy vector within Europe primarily lies in the fact that the European Union has a better structured approach to address the transition to the intermittent renewables, and they have invested in developing clear guidelines (including safety and market regulations) through insights from demonstration projects (e.g. The Store&GO initiative that has looked at developing hydrogen injection guidelines in natural gas systems **[168]**).

Despite Canada having world renowned companies developing hydrogen technologies (e.g., Ballard, Hydrogenics, NextHydrogen etc.), these companies have found most of their business market in Europe. This is primarily because of development of more stable policies that complement clean generation and energy storage within Europe.

Canadian provinces transitioning towards cleaner generation sources would require to develop policies that complement both energy storage and clean energy generation. The most important hurdle lies in developing policies that are stable irrespective of changing political parties.

8.2 Contribution: Techno-economic and life cycle emissions analyses

Through techno-economic optimization models presented in chapters 4, 6 and 7 the study has assessed how the components of the power to gas energy hubs can be sized and operated while minimizing cost subject to technology specific constraints. Chapter 4 in particular also includes a life-cycle emissions estimation and environmental benefit of using hydrogen and renewable natural as cleaner alternative fuels within the natural gas sector.

8.3 Contribution: Market Mechanism Analyses

Chapter 4 compares the cost effectiveness of existing battery electric vehicles and power to gas energy hubs to reduce emissions via utilizing surplus electricity from Ontario's power grid. Through this the existing rebate structure outlined in Ontario's electric and hydrogen vehicle incentive program is compared to potential costs that could be incurred by the province for promoting the use of blend of hydrogen enriched natural gas or renewable and conventional natural gas.

Chapter 6 on the other had develops an incentive mechanism to value the services offered by a 2 MW power to gas energy hub subject to meeting set payback periods. These services include: 1) Providing hydrogen as a fuel for a potential refueling station; 2) Providing ancillary services to the power grid, and 3) Offsetting $CO_{2,e}$ emissions at natural gas end users.

8.4 Contribution: Market opportunities for power to gas in different electricity power zones within Ontario

Chapter 5 highlights the potential scale of power to gas system size required to absorb all of Ontario's surplus electricity. This chapter also shows that cost of hydrogen production can be significantly low when economies of scale is achieved by large scale power to gas systems.

Based on the contribution of baseload generation and the load, and demographic characteristics of the ten different power zones in Ontario, a brief discussion on the market opportunities for power to gas energy hubs have been suggested as well.

8.5: Contribution: Stochastic analyses of power to gas systems

Chapter 7 assesses the impact of accounting for uncertainty in parametric data inputs associated to power to gas energy hubs. The parameters of interest are the hourly electricity price, the amount of hydrogen refueled and the number of fuel cell vehicles serviced. Accounting for uncertainty associated with hydrogen refueling characteristics is a contribution of this work.

8.6: Conclusions and Recommendations

The analyses presented in chapter 4, 5, 6 and 7 show that hydrogen can be a viable energy vector and is well suited for playing a role in managing Ontario's surplus baseload electricity exports. There is a potential for large scale power to gas energy hubs to increase the renewable content of natural gas via hydrogen enriched or renewable natural gas. It is seen that larger power to gas energy hubs between 20-30 MW (see chapter 4) are only able to reach the 5 vol.% of hydrogen content in a segment of Enbridge's distribution pipelines within the greater Toronto area only ~51% of the hours throughout a year. This implies that there is a potential for even larger power to gas systems to be installed along transmission pipelines going through power zones prone to surplus electricity generation. This will help in effective management of surplus electricity.

Although it is environmentally beneficial to increase the renewable content of natural gas, the price of carbon needs to be greater than at least $87.8 per tonne of $CO_{2,e}$ for hydrogen enriched natural gas to be economically feasible. A low price on carbon implies that power to gas energy hubs will have to be catered to primarily provide hydrogen as an alternative fuel source to the transportation sector. Secondary and tertiary revenue streams for power to gas energy hubs will be the ancillary service and cap and trade market.

From a technical perspective, accounting for uncertainty in services offered by power to gas energy hubs (e.g.: hydrogen at a refueling station) is valuable as metrics such as value of stochastic solution and expected value of perfect information have been estimated to be high (see chapter 7).

Some of the recommendations for future work in this area would be developing further complex stochastic models such as Markowitz approach that also account for variance in uncertain parametric data. This thesis has primarily focused on sizing of power to gas energy hubs at one location within Ontario. Therefore, future work could include an Ontario wide model that analyses the potential for such energy hubs to offer a variety of services in the different electricity power zones.

References

[1] Stokes, L. C. (2013). The politics of renewable energy policies: The case of feed-in tariffs in Ontario, Canada. Doi: https://doi.org/10.1016/j.enpol.2013.01.009

[2] Transmission Connected Generation: Supply Overview, Independent Electricity System Operator. (2018). Retrieved from http://www.ieso.ca/en/power-data/supply-overview/transmission-connected-generation (Accessed on 10/04/2018)

[3] Ontario's energy capacity: Independent Electricity System Operator. (2018). Retrieved from http://www.ieso.ca/learn/ontario-supply-mix/ontario-energy-capacity (Accessed on 10/04/2018)

[4] A Progress Report on Contracted Electricity Supply: Fourth quarter 2017. (2017). Ontario: Independent Electricity System Operator.

[5] Historical Demand: Demand Overview, Independent Electricity System Operator. (2018). Retrieved from http://www.ieso.ca/power-data/demand-overview/historical-demand (Accessed on 12/05/2018)

[6] 18-month outlook: An Assessment of the Reliability and Operability of the Ontario Electricity System, October 2017 to March 2019. (2017). Ontario: Independent Electricity System Operator.

[7] FIT/micro FIT Price Schedule. (2016). Ontario: Independent Electricity System Operator.

[8] Large Renewable Procurement: Energy Procurement Programs and Contracts. (2018). Retrieved from http://www.ieso.ca/sector-participants/energy-procurement-programs-and-contracts/large-renewable-procurement (Accessed on 12/05/2018)

[9] Featured Reports, Independent Electricity System Operator, Surplus Baseload Generation Report. (2018). Retrieved from http://www.ieso.ca/power-data/data-directory (Accessed on 13/04/2018)

[10] Wind and the Electrical Grid - Mitigating the Rise in Electricity Rates and Greenhouse Gas Emissions. (2012), Ontario Society of Professional Engineers.

[11] Defining Ontario's Typical Electricity Customer. (2016). (No. EB-2016-0153). Ontario: Ontario Energy Board.

[12] Understanding the global adjustment - Ontario power authority. Retrieved from http://www.powerauthority.on.ca/about-us/electricity-pricing-ontario/understanding-electricity-system-costs/understanding-global-adjustment (Accessed on 14/04/2018)

[13] 2015 Annual Report. (2015). (No. ISSN 1911-7078).Office of Auditor General of Ontario.

[14] Surplus Baseload Electricity Generation in Ontario: Environmental Commissioner of Ontario. (2017). Retrieved from https://eco.on.ca/blog/surplus-baseload-electricity-generation-in-ontario/ (Accessed on 13/04/2018)

[15] RFP for Energy Storage Services Backgrounder. (2014). Ontario: Independent Electricity System Operator.

[16] Energy Storage Procurement - Phase II Backgrounder. (2015). Ontario: Independent Electricity System Operator.

[17] Ontario's five year climate change action plan: 2016-2020. (2016). Ontario: Minister of Environment and Climate Change.

[18] Ontario's Electric Vehicle Incentive Program: Ministry of Transportation, Ontario. (2017). Retrieved from http://www.mto.gov.on.ca/english/vehicles/electric/electric-vehicle-incentive-program.shtml

[19] Stevens, M. (2017). Electric Vehicle Sales in Canada: 2016 Final Update. Retrieved from https://www.fleetcarma.com/ev-sales-canada-2016-final/ (Accessed on 24/10/2017)

[20] S. Walker, U. Mukherjee, M. Fowler and A. Elkamel, "Benchmarking and Selection of Power-to-Gas Utilizing Electrolytic Hydrogen as an Energy Storage Alternative," International Journal of Hydrogen Energy, 2015.
[21] Mazloomi, K., & Gomes, C. (2012). Hydrogen as an energy carrier: Prospects and challenges. Renewable and Sustainable Energy Reviews, 16(5), 3024-3033.
[22] Peng, D. (2013). Enabling utility-scale electrical energy storage through underground hydrogen-natural gas co-storage. (Master of Applied Science in Chemical Engineering, University of Waterloo).
[23] Braun, H. (2008). The Phoenix Project: Shifting to a Solar Hydrogen economy by 2020. Chemical Industry & Chemical Engineering Quarterly, 14(2), 107-118.
[24**]** Liu, H., Almansoori, A., Fowler, M., & Elkamel, A. (2012). Analysis of Ontario's hydrogen economy demands from hydrogen fuel cell vehicles. International Journal of Hydrogen Energy, 37(11), 8905-8916.
[25] Jørgensen, C., & Ropenus, S. (2008). Production price of hydrogen from grid connected electrolysis in a power market with high wind penetration. International Journal of Hydrogen Energy, 33(20), 5335-5344.
[26] Sustainable Development Business Case Report: Renewable Fuel - Hydrogen. (2006). (No. BC_RFH_V7.12.1_EG_061123). Canada: Sustainable Development Technology Canada.
[27] Bartels, J. R., Pate, M. B., & Olson, N. K. (2010). An economic survey of hydrogen production from conventional and alternative energy sources. International Journal of Hydrogen Energy, 35(16), 8371-8384.
[28] Laperche-Riteau, Y. (2018). (2018). Country update: Initiatives on hydrogen and fuel cells (Canada). Paper presented at the European hydrogen energy conference in Malaga, Spain.
[29] Petrunic, J. (2015). Automotive and Transportation Innovation across Canada & Regional Transportation Needs and Capacities as Targeted Research, Development & Demonstration (RD&D) projects. (). Ottawa, Canada: Canadian Urban Transit Research & Innovation Consortium.
[30] Mccarthy, S. (2018). Toronto's hydrogen village. Retrieved from https://www.theglobeandmail.com/news/national/torontos-hydrogen-village/article1077291/ (Accessed on 21/04/2018)
[31] Barker, E. H. (2017). International Partnership for Hydrogen and Fuel Cells in the Economy, Country Update: Canada. Retrieved from https://www.iphe.net/canada (Accessed on 21/04/2018)
[32] Pan-Canadian Framework on Clean Growth and Climate Change: Canada's plan to address climate change and grow the economy. (2016). (No. En4-294/2016E-PDF).Federal Government of Canada.
[33] Low carbon Smart Mobility Innovation Initiative: Creating knowledge-based jobs in B.C. for a cleaner future. (2018). British Columbia, Canada: Canadian Urban Transit Research and Innovation Consortium.
[34] Clean Electric Vehicle Incentive Program: British Columbia, Canada. (2018). Retrieved from cevforbc™ Vehicle Incentive Program.
[35] Cap and Trade: Program overview (Ministry of Environment and Climate Change). (2017). Retrieved from https://www.ontario.ca/page/cap-and-trade-program-overview (Accessed on 01/09/2018)

[36] Electric and Hydrogen Vehicle Incentive Program: Ontario Ministry of Transportation. (2018). Retrieved from http://www.mto.gov.on.ca/english/vehicles/electric/electric-vehicle-incentive-program.shtml (Accessed on 09/05/2018)
[37] Ontario investing up to $100M in renewable natural gas: Ministry of the Environment and Climate Change. (2016). Retrieved from https://news.ontario.ca/ene/en/2016/05/ontario-investing-up-to-100m-in-renewable-natural-gas.html (Accessed on 13/05/2018)
[38] Aubry, A. (2016). Canada's Natural Gas Utilities Propose Target for Renewable Natural Gas Content: Canadian Gas Association. Retrieved from http://www.cga.ca/news_item/canadas-natural-gas-utilities-propose-target-for-renewable-natural-gas-content/(Accessed on 13/05/2018)
[39] Van der Zwaan, B. C. C., Schoots, K., Rivera-Tinoco, R., & Verbong, G. P. J. (2011). The cost of pipelining climate change mitigation: An overview of the economics of CH4, CO2 and H2 transportation. Applied Energy, 88(11), 3821-3831.
[40] Melaina, M., Antonia, O., & Penev, M. (2013). Blending hydrogen into natural gas pipeline networks: A review of key issues. (No. NREL/TP-5600-51995).NREL.
[41] Ulleberg, Ø. (2003). Modeling of Advanced Alkaline Electrolyzers: A System Simulation Approach. International Journal of Hydrogen Energy, 28(1), 21-33.
[42] Electrolysis - Hydrogenics. (2013). Retrieved from http://www.hydrogenics.com/technology-resources/hydrogen-technology/electrolysis (Accessed on 19/12/2014)
[43] Carmo, M., Fritz, D. L., Mergel, J., & Stolten, D. (2013). A comprehensive review on PEM water electrolysis. International Journal of Hydrogen Energy, 38(12), 4901-4934.
[44] Harvey, R. (2014). Electrolyzer Specifications: Personal Communication. Hydrogenics.
[45] Schiebahn, S., Grube, T., Robinius, M., Tietze, V., Kumar, B., & Stolten, D. (2015). Power to gas: Technological overview, systems analysis and economic assessment for a case study in Germany doi:https://doi.org/10.1016/j.ijhydene.2015.01.123
[46] Awasthi, A., Scott, K., & Basu, S. (2011). Dynamic Modeling and Simulation of a Proton Exchange Membrane Electrolyzer for Hydrogen Production. International Journal of Hydrogen Energy, 36(22), 14779-14786.
[47] Natural gas consumption in Ontario, Canadian Association of Petroleum Producers. (2013). Retrieved from: http://www.capp.ca/canadaindustry/industryacrosscanada/Pages/Ontario.aspx (Accessed on 18/11/2018)
[48] Making choices: Reviewing Ontario's Long-Term Energy Plan. (2013). Toronto, Ontario: Ministry of Energy.
[49] Natural Gas Regulation in Ontario: A Renewed Policy Framework, Report on the Ontario Energy Board, Natural Gas forum. (2005), Ontario Energy Board.
[50] TransCanada Pipeline. (2012). Retrieved from: http://en.wikipedia.org/wiki/transcanada_pipeline (Accessed on 18/11/2013)
[51] Energy facts & statistics, Center for Energy. (2010). Retrieved from: http://www.centreforenergy.com/factsstats/mapscanada/ON-energymap.asp (Accessed on 18/11/2013)
[**52**] Fielden, S. (2013). Return to sender natural gas exports - the battle for a new dawn. Retrieved from: https://rbnenergy.com/return-to-sender-the-battle-for-a-new-dawn(Accessed on 30/07/2014)
[53] Underground Storage-Reservoirs, Ministry of Natural Resources, Ontario. (2012). Retrieved from: http://www.mnr.gov.on.ca/en/Business/OGSR/2columnsubpage/STEL02_167108.html (Accessed on 21/11/2013)
[54] Teichroeb, D. (2013). Large, long-duration energy storage, Mindfirst Storage Seminar.

[55] Tabkhi, F., Azzaro-Pantel, C., Pibouleau, L., & Domenech, S. (2008). A mathematical framework for modelling and evaluating natural gas pipeline networks under hydrogen injection. International Journal of Hydrogen Energy,33(21), 6222-6231.
[56] Hydrogen delivery technical team roadmap. (2017). (United States Driving Research and Innovation for Vehicle efficiency and Energy Sustainability.
[57] Parker, N. (2004). Using natural gas transmission pipeline costs to estimate hydrogen pipeline costs.
[**58]** Öney, F., Veziroglu, T. N., & Dülger, Z. (1994). Evaluation of pipeline transportation of hydrogen and natural gas mixtures. International Journal of Hydrogen Energy, 19(10), 813-822.
[59] Altfeld, K. & Pinchbeck, D Admissible Hydrogen Concentrations in Natural Gas Systems
[60] Haeseldonckx, D., & d'haeseleer, W. (2007). The use of the natural-gas pipeline infrastructure for hydrogen transport in a changing market structure. International Journal of Hydrogen Energy, 32(10–11), 1381-1386.
[61] Von der Grün, G. T. M., Hotopp, S, & Müller-Kirchenbauer, J. (2013). Transport and usage of hydrogen via natural gas pipeline systems. Clean Energy Systems in the Subsurface: Production, Storage and Conversion Springer Series in Geomechanics and Geoengineering, 421-436.
[62] Parks, G., Boyd, R., Cornish, J., Remick, R. (2014). Hydrogen station compression, storage, and dispensing technical status and costs. (No. NREL/BK-6A10-58564).National Renewable Energy Laboratory.
[63] Taylor, J. B., Alderson, J. E. A., Kalyanam, K. M., Lyle, A. B., & Phillips, L. A. (1986). Technical and economic assessment of methods for the storage of large quantities of hydrogen. International Journal of Hydrogen Energy, 11(1), 5-22.
[64] Gahleitner, G. (2013). Hydrogen from renewable electricity: An international review of power-to-gas pilot plants for stationary applications.International Journal of Hydrogen Energy, 38(5), 2039-2061.
[65] Hydrogenics - Falkenhagen Power-to-Gas Plant, Germany. (2013). Retrieved from http://www.hydrogenics.com/about-the-company/news-updates/2013/06/14/largest-power-to-gas-facility-in-the-world-now-operational-with-hydrogenics-technology(Accessed on 29/07/2014)
[66] Audi e-gas project. (2013). Retrieved from http://www.powertogas.info/power to gas/pilotprojekte-im-ueberblick/audi-e-gas-projekt/ (Accessed on 18/01/2017)
[67] de Boer, H. S., Grond, L., Moll, H., & Benders, R. (2014). The application of power-to-gas, pumped hydro storage and compressed air energy storage in an electricity system at different wind power penetration levels. Energy, 72, 360-370. Doi:http://dx.doi.org/10.1016/j.energy.2014.05.047
[68] Nastasi, B., & Lo Basso, G. (2016). Hydrogen to link heat and electricity in the transition towards future smart energy systems. Energy, 110, 5-22. Doi:http://dx.doi.org/10.1016/j.energy.2016.03.097
[69] Collet, P., Flottes, E., Favre, A., Raynal, L., Pierre, H., Capela, S., & Peregrina, C.Techno-economic and life cycle assessment of methane production via biogas upgrading and power to gas technology. Applied Energy,doi:http://dx.doi.org.proxy.lib.uwaterloo.ca/10.1016/j.apenergy.2016.08.181
[70] Maroufmashat, A., Fowler, M., Sattari Khavas, S., Elkamel, A., Roshandel, R., & Hajimiragha, A. (2016). Mixed integer linear programing based approach for optimal planning and operation of a smart urban energy network to support the hydrogen economy. International Journal of Hydrogen Energy, 41(19), 7700-7716. Doi:http://dx.doi.org/10.1016/j.ijhydene.2015.08.038

[71] Götz, M.; Lefebvre, J.; Mörs, F.; mcdaniel Koch, A.; Graf, F.; Bajohr, S.; Reimert, R.; Kolb, T. Renewable power-to-gas: A technological and economic review. Renew. Energy **2016**, 85, 1371–1390. Doi:http://dx.doi.org/10.1016/j.renene.2015.07.066.
[72] Rönsch, S.; Schneider, J.; Matthischke, S.; Schlüter, M.; Götz, M.; Lefebvre, J.; Prabhakaran, P.; Bajohr, S. Review on methanation—From fundamentals to current projects. Fuel **2016**, 166, 276–296. Doi:http://dx.doi.org/10.1016/j.fuel.2015.10.111.
[73] Otto, A.; Robinius, M.; Grube, T.; Schiebahn, S.; Praktiknjo, A.; Stolten, D. Power-to-steel: Reducing CO2 through the integration of renewable energy and hydrogen into the German steel industry. Energies **2017**, 10, 451. Doi:10.3390/en10040451.
[74] Astiaso Garcia, D.; Barbanera, F.; Cumo, F.; Di Matteo, U.; Nastasi, B. Expert opinion analysis on renewable hydrogen storage systems potential in Europe. Energies **2016**, 9, 963. Doi:10.3390/en9110963.
[75] Jempa, C., van Leeuwen C., & Hulshof, D. (2017). Innovative large-scale energy storage technologies and power-to-gas concepts after optimisation: Exploring the future of green gases. (No. D8.1). University of Groningen: European Union.
[76] J. Eichman, K. Harrison and M. Peters, "Novel Electrolyzer Applications: Providing More Than Just Hydrogen. (No. NREL/TP-5400-61758)," NREL, Golden, 2014.
[77] M. Albadi and E. El-Saadany, "A summary of demand response in electricity markets," Electric Power Systems Research, vol. 78, no. 11, pp. 1989-1996, 2008.
[78] Independent Electricity Systems Operator, "Demand Response Pilot: IESO," 2015. Retrieved from: http://www.ieso.ca/Pages/participate/Demand-Response-Pilot/default.aspx. (Accessed 8 September 2015).
[79] B. Kirby, "Demand response for power system reliability: FAQ (No. ORNL/TM-2006/565)," Oak Ridge National Laboratory, Oak Ridge,, 2006.
[80] IESO, "Proposed market rule changes - Ancillary Service Contract Terms No. IESO TP 257-3b," IESO Technical Panel, Toronto, 2012.
[81] IESO, "Operating Reserve Markets," 2015. Retrieved from: http://www.ieso.ca/Pages/Participate/Markets-and-Programs/Operating-Reserve-Markets.aspx. (Accessed 04/03/2015).
[82] Independent Electricity Systems Operator, "Demand Response: A New Form of Regulation Service (IESO)," 2015. Retrieved from: http://www.ieso.ca/Pages/Ontario's-Power-System/Reliability-Through-Markets/DR%20%26%20Regulation%20Service.aspx. (Accessed 10/09/2015).
[83] IESO, "Demand Response in Ontario," 2015. Retrieved from: http://www.ieso.ca/Pages/Ontario's-Power-System/Reliability-Through-Markets/Demand-Response.aspx. (Accessed 04/03/2015).
[84] Charles River Associates, "Primer on Demand Side Management with an Emphasis on Price Responsive Programs," The World Bank, Washington DC, 2005.
[85] Center for Energy, Economic, and Environmental Policy, "Assessment of Customer Response to Real Time Pricing," State University of New Jersey, Rutgers, 2005.
[86] IESO, "Demand response auction," 2015. Retrieved from: http://www.ieso.ca/Pages/Participate/Demand-Response-Auction/default.aspx. (Accessed 10/01/2015).
[87] IESO, "Demand Response-Pre Auction Report," 2015. Retrieved from: http://reports.ieso.ca/public/DR-preauction/PUB_DR-preauction.xml. (Accessed 11/11/2015).

[88] D. Kirschen, " Demand-Side View of Electricity Markets," IEEE Transactions on Power Systems, vol. 18, no. 2, pp. 520-527, 2003.
[89] P. Jazayeri, A. Schellenberg, W. Rosehart, J. Doudna, S. Widergren, D. Lawrence and S. Jones, "A survey of load control programs for price and system stability," IEEE Transactions on Power Systems, vol. 20, no. 3, pp. 1504-1509, 2005.
[90] S. Chan, K. Tsui, H. Wu, H. Yunhe, W. Yik-Chung and F. Wu, "Load/Price forecasting and managing demand response for smart grids: Methodologies and challenges," IEEE Signal Processing Magazine, vol. 29, no. 5, pp. 68-85, 2012.
[91] National Renewable Energy Laboratory, "H2A hydrogen delivery infrastructure analysis models and conventional pathway options analysis results. Interim Report No. DE-FG36-05GO15032," Office of Energy Efficiency & Renewable Energy, Washington D.C., 2008.
[92] Aicher, T., Gonzalez, M. I., & Götz, M. (2014). Work package 5: Considerations of the overall system in terms of dynamics and process integration for methanation reactors (energy and water practice). Germany.
[93] Components of natural gas: Enbridge. (2018). Retrieved from https://www.enbridgegas.com/gas-safety/about-natural-gas/components-natural-gas.aspx (Accessed on 11/01/2018)
[94] J. Lefebvre, Interviewee, Methanation Reactor Ramping Characteristics: Personal Communication with Deutscher Verein des Gas- und Wasserfaches (German Association for Gas and Water).
[95] Global, E. V. (2016). Outlook 2016: Beyond One Million Electric Cars. International Energy Agency: Paris, France.
[96] Requia, W. J., Adams, M. D., Arain, A., Koutrakis, P., & Ferguson, M. (2017). Carbon dioxide emissions of plug-in hybrid electric vehicles: A life-cycle analysis in eight canadian cities doi:https://doi.org/10.1016/j.rser.2017.05.105
[97] Ellingsen, L. A. W., Singh, B., & Strømman, A. H. (2016). The size and range effect: Lifecycle greenhouse gas emissions of electric vehicles. Environmental Research Letters, 11(5).
[98] Vehicle size classes: US department of energy. (2017). Retrieved from https://www.fueleconomy.gov/feg/info.shtml#sizeclasses (Accessed on 18/01/2017)
[99] Find and compare cars (Database: US Department of Energy). (2017). Retrieved from http://www.fueleconomy.gov/feg/findacar.shtml (Accessed on 18/01/2017)
[100] Axsen, J., S. Goldberg, J. Bailey, G. Kamiya, B. Langman, J. Cairns, M. Wolinetz, and A. Miele (2015). Electrifying Vehicles: Insights from the Canadian Plug-in Electric Vehicle Study. Simon Fraser University, Vancouver, Canada.
[101] Hawkins, T. R., Singh, B., Majeau-Bettez, G., & Strømman, A. H. (2013). Comparative environmental life cycle assessment of conventional and electric vehicles. Journal of Industrial Ecology, 17(1), 53-64. Doi:10.1111/j.1530-9290.2012.00532.x
[102] Data directory, independent electricity system operator, generator output and capability report. (2018). Retrieved from http://www.ieso.ca/power-data/data-directory (Accessed on 18/04/2018)
[103] Greenhouse gas emissions associated with various methods of power generation in Ontario. (2016). (Technical No. 20-22285). Ontario: Intrinsik Corp.
[104] Emission factors for greenhouse gas inventories. (2014). United States Environmental Protection Agency. Retrieved from https://www.epa.gov/sites/production/files/2015-07/documents/emission-factors_2014.pdf (Accessed on 20/04/2018)

[105] Time-of-use price periods for electricity users: Ontario energy board. (2017). Retrieved from https://www.oeb.ca/newsroom/2017/time-use-price-periods-electricity-users-changing-november-1 (Accessed on 25/04/2018)
[106] Al-sharrah, G. K., Hankinson, G., & Elkamel, A. (2006). Decision-making for petrochemical planning using multiobjective and strategic tools. Chemical Engineering Research and Design, 84(11), 1019-1030. Http://dx.doi.org.proxy.lib.uwaterloo.ca/10.1205/cherd.05198
[107] Featured Reports, Independent Electricity System Operator, Surplus Baseload Generation Report. (2018). Retrieved from http://www.ieso.ca/power-data/data-directory (Accessed on 18/04/2018)
[108] CCI bioenergy: Toronto projects. (2012). Retrieved from https://www.ccibioenergy.com/projects-toronto-ontario/ (Accessed on 06/08/2017)
[109] Toronto zoo anaerobic digester: Project description report. (2013). Toronto: Riepma Consultants Inc.
[110] Successful startup of the disco road organics processing facility (DROPF) Toronto, Canada. (2014). Retrieved from http://www.btai.de/en/aktuelles/newsletter/newsletter-2014-02/startup-toronto-disco-road.html (Accessed on 06/08/2017)
[111] Life cycle greenhouse gas emissions of natural gas: A literature review of key studies comparing emissions from natural gas and coal. (2012). ICF Consulting Canada.
[112] Guide: Greenhouse gas emissions reporting. (2016). Retrieved from https://www.ontario.ca/page/guide-greenhouse-gas-emissions-reporting (Accessed on 06/09/2017)
[113] CHERUBINI, F., PETERS, G. P., BERNTSEN, T., STRØMMAN, A. H., & HERTWICH, E. (2011). CO2 emissions from biomass combustion for bioenergy: Atmospheric decay and contribution to global warming. GCB Bioenergy, 3(5), 413-426. Doi:10.1111/j.1757-1707.2011.01102.x
[114] Nguyen, T. T., & Wilson, B. G. (2010). Fuel consumption estimation for kerbside municipal solid waste (MSW) collection activities. Waste Management and Research, 28(4), 289-297. Doi:10.1177/0734242X09337656.
[115] DISCO Road Biogas Utilization Project: Emission summary and dispersion modelling report. (2015). (No. 13-1155-0028-DOC9). Ontario: Golder Associates.
[116] McKenna, R. C., Bchini, Q., Weinand, J. M., Michaelis, J., König, S., Köppel, W., & Fichtner, W. (2018). The future role of power-to-gas in the energy transition: Regional and local techno-economic analyses in baden-württembergHttps://doi.org/10.1016/j.apenergy.2017.12.017
[117] Ausfelder, F., & Bazzanella, A. (2008). Verwertung und speicherung von CO2 (recycling and storage of CO2): Discussion paper. Dechema. Retrieved from https://dechema.de/dechema_media/diskussionco2-view_image-1-called_by-dechema-original_site-dechema_ev-original_page-124930.pdf (Accessed on 06/11/2017)
[118] Spath, P., & Mann, M. (2004). Life cycle assessment of renewable hydrogen production via Wind/Electrolysis: Milestone completion report. (No. NREL/MP-560-35404). Colorado, USA: National Renewable Energy Laboratory.
[119] Melaina, M., & Penev, M. (2013). Hydrogen station cost estimates: Comparing hydrogen station cost calculator results with other recent estimates. (No. NREL/TP-5400-56412). Golden, Colorado: National Renewable Energy Laboratory.
[120] J. Ruf, Interviewee, Methane Upgrading Equipment: Personal Communication with Deutscher Verein des Gas- und Wasserfaches (German Association for Gas and Water).

[121] Budzianowski, W. M., & Budzianowska, D. A. (2015). Economic analysis of biomethane and bioelectricity generation from biogas using different support schemes and plant configurationshttp://dx.doi.org/10.1016/j.energy.2015.05.104
[122] Riva, C., Schievano, A., D'Imporzano, G., & Adani, F. (2014). Production costs and operative margins in electric energy generation from biogas. Full-scale case studies in italyhttp://dx.doi.org/10.1016/j.wasman.2014.04.018
[123] Hourly Ontario electricity price, independent electricity system operator. (2018). Retrieved from http://www.ieso.ca/Pages/Power-Data/Data-Directory.aspx#
[124] Rate order - 2015 uniform electricity transmission rates. (2015). (No. EB-2014-0357).Hydro-One. Retrieved from https://www.hydroone.com/abouthydroone/regulatoryinformation/rateschedules/Documents/Transmission%20Rates/Rate%20Order_%202015%20UTR_20150108.pdf
[125] Water Rate: City of Markham, Ontario. (2015).
[126] Snyder, J. (2017). Proposal to build major transmission line between Canada and US receives critical regulatory approval. Retrieved from http://business.financialpost.com/commodities/energy/proposal-to-build-major-transmission-line-between-canada-and-u-s-receives-critical-regulatory-approval (Accessed on 09/12/2017)
[127] Population by year, by province and territory: Statistics Canada. (2017). Retrieved from http://www.statcan.gc.ca/tables-tableaux/sum-som/l01/cst01/demo02a-eng.htm (Accessed on 08/09/2017)
[128] Motor vehicle registrations, by province and territory: Statistics Canada. (2016). Retrieved from http://www.statcan.gc.ca/tables-tableaux/sum-som/l01/cst01/trade14a-eng.htm (Accessed on 08/09/2017)
[129] Alsubaie, A. (2017). Implementation of power-to-gas to reduce carbon intensity and increase renewable content in liquid petroleum fuels Retrieved from http://hdl.handle.net/10012/12242
[130] De Sisternes, F. J., Jenkins, J. D., & Botterud, A. (2016). The value of energy storage in decarbonizing the electricity sector. Applied Energy, 175, 368-379.
[131] IESO report: Energy storage. (2016). Ontario: Independent Electricity System Operator.
[132] Biogas projects in Ontario: Canadian biogas association. (2018). Retrieved from https://biogasassociation.ca/about_biogas/projects_ontario (Accessed on 06/05/2018)
[133] P. Hill and M. Penev, "Hydrogen Fueling Station in Honolulu, Hawaii Feasibility Analysis," Office of Energy Efficiency & Renewable Energy (No. INL/EXT-14-31624), Honolulu, 2014.
[134] J. Pratt, D. Terlip, C. Ainscough, J. Kurtz and A. Elgowainy, "H2FIRST Reference Station Design Task (Technical No. NREL/TP-5400-64107)," National Renewable Energy Laboratory, Washington, D.C., 2015.
[135] netinform, "Hydrogen filling stations worldwide," 2016. [Online]. Available: http://www.netinform.net/h2/H2Stations/Default.aspx. [Accessed 3 March 2016].
[136] U. Mukherjee, S. Walker, A. Maroufmashat, M. Fowler, & A. Elkamel. (2016). Power-to-gas to meet transportation demand while providing ancillary services to the electrical grid. 2016 IEEE Smart Energy Grid Engineering (SEGE), 221-225. Doi:10.1109/SEGE.2016.7589529
[137] IESO, "Load Following: Impact of New Supply," 2007. Retrieved from: http://www.ieso.ca/Documents/consult/se38/se38-20070403-Load-Following.pdf. (Accessed on 03/02/2016).
[138] B. Kirby and E. Hirst, " Customer-Specific Metrics for the Regulation and Load-Following Ancillary Services. (No. ORNL/CON-474)," Oak Ridge National Laboratory, Oak Ridge, 2000.

[139] Union Gas, "M -12 schedule C fuel rates," 2014.
[140] Huffington Post, "Alberta extends climate change rules, including $15 tonne carbon levy," 19 December 2014. Retrieved from: http://www.huffingtonpost.ca/2014/12/19/alberta-climate-change_n_6357480.html. (Accessed on 02/03/2016).
[141] IESO, "Demand-response pilot program: program details," 2015. Retrieved from: http://www.ieso.ca/Documents/procurement/DR-Pilot-RFP/IESO-Demand_Response_Pilot_Program-Program_Details.pdf. (Accessed 12/10/2015).
[142] Hydrogen and Fuel Cells: The U.S. market report. (2010). National Hydrogen Association, and Technology Transition Corporation.
[143] Province of Alberta, "Carbon Levy and Rebates: Putting a Price on Carbon is the Most Cost-Effective Way to Reduce Greenhouse Gas Emissions that cause Climate Change," Retrieved from: http://www.alberta.ca/climate-carbon-pricing.cfm. (Accessed on 04/07/2016).
[144] Carbon Pricing: Insight Briefing, Analyzing the issues that matter to the clean revolution. (2013).The Climate Group.
[145] Juan, A.A.; Mendez, C.A.; Faulin, J.; de Armas, J.; Grasman, S.E. Electric Vehicles in Logistics and Transportation: A Survey on Emerging Environmental, Strategic, and Operational Challenges. Energies 2016, 9, 86.
[146] Franzitta, V.; Curto, D.; Rao, D.; Viola, A. Hydrogen Production from Sea Wave for Alternative Energy Vehicles for Public Transport in Trapani (Italy). Energies **2016**, 9, 850.
[147] Blanco-Fernández, P.; Pérez-Arribas, F. Offshore Facilities to Produce Hydrogen. Energies 2017, 10, 783.
[148] Kim, J.; Lee, Y.; Moon, I. Optimization of a hydrogen supply chain under demand uncertainty. Int. J. Hydrog. Energy 2008, 33, 4715–4729. Doi:http://dx.doi.org.proxy.lib.uwaterloo.ca/10.1016/j.ijhydene.2008.06.007.
[149] Almansoori, A.; Shah, N. Design and operation of a stochastic hydrogen supply chain network under demand uncertainty. Int. J. Hydrog. Energy 2012, 37, 3965–3977. Doi:http://dx.doi.org/10.1016/j.ijhydene.2011.11.091.
[150] Dayhim, M.; Jafari, M.A.; Mazurek, M. Planning sustainable hydrogen supply chain infrastructure with uncertain demand. Int. J. Hydrog. Energy 2014, 39, 6789–6801. Doi:http://dx.doi.org/10.1016/j.ijhydene.2014.02.132.
[151] Nunes, P.; Oliveira, F.; Hamacher, S.; Almansoori, A. Design of a hydrogen supply chain with uncertainty. Int. J. Hydrog. Energy 2015, 40, 16408–16418. Doi:http://dx.doi.org/10.1016/j.ijhydene.2015.10.015.
[152] Taljan, G; Fowler, M.; Cañizares, C.; Verbič, G. Hydrogen storage for mixed wind–nuclear power plants in the context of a hydrogen economy. Int. J. Hydrog. Energy 2008, 33, 4463–4475. Doi:http://dx.doi.org.proxy.lib.uwaterloo.ca/10.1016/j.ijhydene.2008.06.040.
[153] Birge, J.R.; François, L. Introduction to Stochastic Programming, 2nd ed.; Mikosch, T.V., Resnick, S.I., Robinson, S.M., Eds.; Springer: New York, NY, USA, 2011.
[154] Independent Electricity System Operator (IESO). Historical Hourly Ontario Electricity Price; IESO: Toronto, ON, USA, 2017. Available online: http://www.ieso.ca/Pages/Power-Data/Data-Directory.aspx# (Accessed on 15/01/2017).
[155] Greene, D.L.; Leiby, P.N.; James, B.; Perez, J.; Melendez, M.; Milbrandt, A.; Unnasch, S.; Rutherford, D.; Hooks, M. Analysis of the Transition to Hydrogen Fuel Cell. Vehicles & the Potential Hydrogen Energy Infrastructure Requirements; No. ORNL/TM-2008/30; Oak Ridge National Laboratory: Oak Ridge, TN, USA, 2008.

[156] US and World Population: United States Census Bureau. 2017. Available online: http://www.census.gov/popclock/ (Accessed on 10/01/2017).
[157] Population of Census Metropolitan Areas: Statistics Canada. 2016. Available online: http://www.statcan.gc.ca/tables-tableaux/sum-som/l01/cst01/demo05a-eng.htm (Accessed on 10/01/2017).
[158] Sprik, S.; Kurtz, J.; Ainscough, C.; Peters, M.; Jeffers, M.; Saur, G. Performance Status of Hydrogen Stations and Fuel Cell Vehicles: 2015 Fuel Cell Seminar and Energy Exposition; California State University, Los Angeles: Los Angeles, CA, USA, 2015.
[159] Histogram of Fueling Amounts Vehicle and Infrastructure: National Renewable Energy Laboratory. 2011. Retrieved from: http://www.nrel.gov/hydrogen/docs/cdp/cdp_39.jpg (accessed on 05/06/2016).
[160] Toyota. 2016 Mirai Product Information. Retrieved from: http://toyotanews.pressroom.toyota.com/releases/2016+toyota+mirai+fuel+cell+product.htm (Accessed on 10/12/2016).
[161] Olateju, B.; Monds, J.; Kumar, A. Large scale hydrogen production from wind energy for the upgrading of bitumen from oil sands. Appl. Energy 2014, 118, 48–56. Doi:http://dx.doi.org/10.1016/j.apenergy.2013.12.013.
[162] Shaner, M.R.; Atwater, H.A.; Lewis, N.S.; mcfarland, E.W. A Comparative Techno-economic Analysis of Renewable Hydrogen Production Using Solar Energy. R. Soc. Chem. 2016, 9, 2354–2371. Doi:10.1039/C5EE02573G.
[163] Narayan, A.; Ponnambalam, K. Risk-Averse Stochastic Programming Approach for Microgrid Planning Under Uncertainty. Renew. Energy **2017**, 101, 399–408. Doi:http://dx.doi.org/10.1016/j.renene.2016.08.064.
[164] Gasoline and fuel oil, average retail prices by urban center (monthly) (Toronto)—Statistics Canada. 2017. Available online: http://www.statcan.gc.ca/tables-tableaux/sum-som/l01/cst01/econ152h-eng.htm (Accessed on 18/01/2017).
[165] Corfield, G. (2018). UK.gov: Here's £8.8m to plough into hydrogen-powered car tech. Retrieved from https://www.theregister.co.uk/2018/03/27/ukgov_8m_hydrogen_car_project/ (Accessed on 9/08/2018).
[166] Hydrogen Mobility Europe. (2018). Retrieved from https://h2me.eu/about/hydrogen-refuelling-infrastructure/ (Accessed on 9/08/2018).
[167] English, C. (2018). Alstom confirms plans to bring hydrogen trains to the UK. Retrieved from https://www.alstom.com/press-releases-news/2018/5/alstom-confirms-plans-to-bring-hydrogen-trains-to-the-uk (Accessed on 9/08/2018).
[168] Store&Go: Power-to-Gas Regulations. (2018). Retrieved from https://www.storeandgo.info/ (Accessed on 9/08/2018).

Appendix A: List of Parameters and Variables

Appendix A.4.1: List of Symbols for Electric Vehicle Lifecycle Analysis

Symbols	Description
$Emissions_{Production\ Phase}$ (Tonnes, $CO_{2,e}$)	Production phase emissions from all 9056 electric vehicles.
W (Tonnes)	Weight of electric vehicle model
N	Number of electric vehicles of a particular make.
$EMF_{EV,Production}$ (Tonnes of $CO_{2,e}$ per tonne of car)	Emission factor for the production of an electric vehicle model's size category.
$Emissions_{End\ of\ Life\ Treatment\ Phase}$ (Tonnes, $CO_{2,e}$)	End of life treatment phase emissions from all 9056 electric vehicles.
$EMF_{EV,EOL}$	End of life treatment emission factor for an electric vehicle model's size category.
E_{1,BEV_k} (kWh per day)	Total daily energy consumed by all battery electric vehicles of model '*k*' in scenario 1.
$E_{1,PHEV_n}$ (kWh per day)	Total daily electrical energy consumed by all plug-in hybrid electric vehicles of model '*n*' in scenario 1.
$E_{2,V}$ (kWh per day)	Daily electricity consumed by all electric vehicles under model '*V*' in scenario 2.
D_{Daily} (km)	Ontario average daily trip distance of 61 km.
$D_{PHEV,n}$ (km)	Electric range of PHEV model '*n*'.
$\eta_{BEV_k,El}$ (kWh per km)	The electric range efficiency for battery electric vehicle model '*k*'.
$\eta_{PHEV_n,Gas}$ (liters of gasoline per km)	Gasoline drive cycle efficiency of the PHEV model '*n*'.
$G_{1,PHEV_n}$ (liters of gasoline)	Total daily gasoline consumed by all plug-in hybrid electric vehicles of model '*n*' in scenario 1.
$E_{Home,i}$ (kWh)	Total energy consumed every hour at home by all the PHEVs and BEVs in scenario '*i*'.
$E_{Public+Work,i}$ (kWh)	Total energy consumed every hour at public and work charging stations by all the PHEVs and BEVs in scenario '*i*'.
$E_{BEV,i}$ (kWh per day)	Total daily electrical energy consumed by all BEVs in scenario '*i*'.
$E_{PHEV,i}$ (kWh per day)	Total daily electrical energy consumed by all PHEVs in scenario '*i*'.
t_{Home} (hours per day)	Time spent charging vehicle at home per day.
$t_{Public+Work}$ (hours per day)	Time spent charging vehicle at public and work charging stations per day.

$\emptyset_{Home}$ (%)	Share of total daily energy consumed by all 9056 EVs at home.
$\emptyset_{Public+Work}$ (%)	Share of total daily energy consumed by all 9056 EVs at public and work place charging stations.

Appendix A.4.2: List of Indices for Electric Vehicle Lifecycle Analysis

Indices	Description
V	Electric vehicle model index 'V' = 1,..,26.
s	Size category of electric vehicle
BEV_k	Battery electric vehicle model 'k' = 1,..,9.
$PHEV_n$	Plug-in hybrid electric vehicle model 'n'= 1,..,17.
1	Denotes scenario 1 where utility factor of all PHEVs among 9056 EVs is 51.5%.
2	Denotes scenario 2 where utility factor of all PHEVs among 9056 EVs is 100%.
i	Denote 2 scenarios and can have values of 1 (51.5% Utility factor case for PHEVs), and 2 (100% Utility factor case for PHEVs),

Appendix A.4.3: List of Variables for Power to Gas Energy Hub Models in Chapter 4

Variables	Description
$Emissions\ Offset_{Case\ 1,Max}$ (Tonnes of $CO_{2,e}$ per year)	Maximum annual emission offset at the natural gas end user via a blend of conventional and renewable natural gas.
$Emissions\ Offset_{Case\ 2,Max}$ (Tonnes of $CO_{2,e}$ per year)	Maximum annual emission offset at the natural gas end user via a blend of conventional natural gas and hydrogen.
$Emissions\ Offset_{Case\ 1}$(Tonnes of $CO_{2,e}$ per year)	Annual emissions offset in ε-constraint problem in case 1: RNG/NG.
$Emissions\ Offset_{Case\ 2}$(Tonnes of $CO_{2,e}$ per year)	Annual emissions offset in ε-constraint problem in case 2: HENG.
$Emissions_{NG}$ (Tonnes of $CO_{2,e}$ per year)	Annual emissions incurred when only conventional natural gas is used to meet the demand of natural gas
$Emissions_{RNG,NG}$ (Tonnes of $CO_{2,e}$ per year)	Annual lifecycle emissions incurred by natural gas end users when a blend of conventional and renewable natural gas is delivered to them.
E_h (kWh)	Hourly energy consumption of electrolyzer.

$CO_{2,h}$ (m^3 per hour)	Hourly biogenic CO_2 drawn from biogas plants.
RNG_h (m^3 per hour)	Hourly renewable natural gas produced at the methanation reactor and sent to end user.
NG_h (m^3 per hour)	Hourly conventional natural gas sent to end user.
$H_{2,h}$ (m^3 per hour)	Hourly hydrogen production at the electrolyzer.
$Total\ Cost_{Case\ 1}$ ($)	Total lifetime cost including capital and operating cost of energy hub in case 1: RNG/NG.
$CAPEX_{Case\ 1}$($)	Lifetime capital cost of energy hub components in case 1: RNG/NG.
$OPEX_{Annual,Case\ 1}$($)	Annual operating cost of the energy hub in case 1: RNG/NG.
$CAPE2$($)	Lifetime capital cost of energy hub components in case 2: HENG.
$OPEX_{Annual,Case\ 2}$($)	Annual operating cost of the energy hub in case 2: HENG.
RNG_{Max} (m^3 per hour)	Maximum methanation reactor capacity chosen by optimization problem.
α_i	Binary variable
$N_{Electrolyzer}$	Number of electrolyzers chosen.
$Emissions_{HENG}$	Annual emissions associated with HENG in case 2.

Appendix: A.4.4: List of Parameters and Indices for Power to Gas Energy Hub Models in Chapter 4

Parameter	Description	Value
EMF_{NG} (kg $CO_{2,e}$ per m^3 of NG)	Lifecycle emission factor of conventional natural gas	2.41
HHV_{NG} (MMBtu per m^3)	Higher heating value of natural gas.	0.036
D_h (MMBtu per hour)	Hourly energy demand at natural gas pressure reduction station.	Hourly data for a year.
δ	Coefficient to convert kg to tonnes.	0.001
h	Hourly index	1, …., 8784
i	Index used to denote electrolyzer system size.	1, 2,…,30
EMF_{WtP} (kg $CO_{2,e}$ per m^3 of NG)	Well to pump emission factor or the emissions incurred during	0.54

	pre-production, processing, and transmission of natural gas	
$EMF_{CO_2,Combustion}$ (kg $CO_{2,e}$ per m^3 of NG)	Emissions incurred when a cubic meter of natural gas is combusted at the end user	1.863
$EMF_{CH_4,Combustion}$ (kg CH_4 per m^3 of NG)	kg of CH_4 emissions occurring when a cubic meter of natural gas is combusted at either a residential, commercial, or manufacturing industry.	0.000037
EMF_{N_2O} (kg N_2O per m^3 of NG)	kg of N_2O emissions occurring when a cubic meter of natural gas is combusted at either a residential, commercial, or manufacturing industry.	0.000035
GWP_{CH_4}	Global warming potential of CH_4 for a 100 year time horizon or residence time within the atmosphere.	25
GWP_{N_2O}	Global warming potential of N_2O for a 100 year time horizon or residence time within the atmosphere.	298
$EMF_{Combustion,RNG}$ (kg $CO_{2,e}$ per m^3 of RNG)	Post-combustion emission factor of renewable natural gas	0.011355
$EMF_{Nuclear}$ (kg of $CO_{2,e}$ per kWh)	Emission factor of nuclear power plants.	0.017
$EMF_{Biogenic\ CO_2}$	Tonnes of $CO_{2,e}$ per m^3 of biogenic carbon dioxide produced	0.000225637
$EMF_{Electrolyzer}$(Tonne of $CO_{2,e}$ per m^3 of H_2 produced)	Production and End of Life Treatment Emission Factor for Electrolyzer	0.000003866
$EMF_{Reactor}$, (Tonne of $CO_{2,e}$ per m^3 of RNG produced)	Production and End of Life Treatment Emission Factor for Methanation Reactor	0.0000153
$Emissions_{Facility\ Operation}$ (Tonnes of $CO_{2,e}$ per year)	Emissions associated with natural gas consumption at biogas facilities (CCI Dufferin andCCI Disco)	481.4
$Emissions_{Waste\ Collection}$ (Tonnes of $CO_{2,e}$ per year)	Emissions associated with organic waste collection	928
$CO_{2,Total}$ (m^3 per year)	Aggregate annual biogenic-CO_2 coming from CCI Dufferin, CCI Disco, and Zooshare.	6,246,451

TVM	The time value of money is estimated based on an interest rate of 8% and a project lifetime of 20 years.	9.818
β	Replacement cost + capital cost factor of electrolyzers	1.35
$C_{Electrolyzer,i}$(\$)	Total capital cost of electrolyzer system for size index 'i'	Set of Values
γ (\$ per m^3 of reactor capacity)	Slope of methanation reactor capital cost trend line.	1714.8
k (\$)	Intercept of methanation reactor capital cost trend line.	2,000,000
$C_{Upgrading}$(\$ per m3 of methanation reactor capacity)	Total capital cost of a methane upgrading unit.	1172.3
C_o(\$ per kW)	The base cost of a 1 MW (or 1000 kW) unit.	1324.3
C^*(\$ per kW)	Updated unit cost of a scaled up electrolyzer system size.	Depends on system size
$CO_{2,avialable,h}$(m^3 per hour)	Hourly flow of CO_2 available from 3 biogas plants.	1300.26
$\dot{V}_o$(m^3 per hour)	The base hydrogen production capacity of the 1 MW (or 1000 kW) unit (m^3 per hour).	222
$\dot{V}$(m^3 per hour)	Production capacity of a scaled up electrolyzer system size.	Depends on system size
μ	Scaling factor used for electrolyzer capital cost.	0.707
C_{CO_2}(\$ per m^3)	Cost of biogenic CO_2	0.172
$HOEP_h$(\$ per kWh)	Hourly Ontario Electricity Price	Hourly time series data for 2016.
TC(\$ per kWh)	Transmission charge of electricity price.	0.008804
WCR(liter per m^3)	Water consumption rate of electrolyzer of 1000 kW unit.	0.4
C_{H_2O}(\$ per liter)	Unit cost of water	0.00314
$OPEX_{Annual,Upgrading}$(\$ per m^3)	Annual operating cost of upgrading unit of methane.	146.5
$SBG_{Toronto\ Zone,h}$(kWh)	Available hourly surplus baseload electricity in the Toronto power zone.	Hourly time series data of surplus electricity in 2016.
$\emptyset$	Parameter used in ε-constraint methodology.	0.1, 0.2,…,0.9,1

Appendix A.6.1: List of Parameters for Chapter 6

Parameter	Description	Value
$C_{Booster\ Compressor}$ ($)	Annual investment on total capital cost of booster compressor	37367.92334
$C_{Compressor,Pre-Storage}$ ($)	Annual investment on total capital cost of compressor pre-storage	25441.99036
$C_{Electricity}$ ($ per kWh)	Hourly Ontario energy price	Time series data of electricity price for a year (2012-2013).
$C_{Electrolyzer}$ ($)	Annual investment on total capital cost of electrolyzer	Confidential
CR_{Water} ($l\ of\ Water\ per\ kmol\ of\ H_2\ produced$)	Water consumption rate of electrolyzer	Confidential
$C_{Tank\ Storage}$ ($)	Annual investment on total capital cost of tank storage	30421.51423
$D_{H_2}(kmol)$	Hourly hydrogen demand at a fuel cell vehicle refueling station	Time series data of hydrogen demand over the course of a year.
$D_{NG}(MMBtu)$	Hourly natural gas energy demand at a natural gas pressure reduction station.	Time series data of varying natural gas energy demand for a year (2012-2013).
$ECF_{Compressor,Pre-Storage}$ ($kWh\ per\ kmol\ H_2$)	Energy consumed by compressor per kmol of H_2 compressed	2.5042
$EF_{Electrolyzer}$	kmol of H_2 produced per kWh energy consumed by electrolyzer	Confidential
E_{max} (kWh)	Maximum energy rating of electrolyzer	2000
$F_{Max,Booster\ compressor}$ ($kmol$)	Maximum inflow to the compressor	43.5
$F_{Max,Compressor,Pre-Storage}$ ($kmol$)	Maximum inflow to the compressor	21
I_{Max} ($kmol$)	Upper limit on hydrogen inventory inside tank	45.39133304

I_{Min} $(kmol)$	Lower limit on hydrogen inventory inside tank	8.516043857
$N_{Booster\ Compressor}$	Number of booster compressors	1
$N_{Compressor,Pre-Storage}$	Number of compressors Pre-storage	1
N_{Tank}	Number of tanks used for storing hydrogen	1
P_{out} (bar)	Output pressure of booster compressor, based on refueling station requirements	350
$P_{tank,min}$ (bar)	Minimum pressure level to be maintained in tank	30
R_{CO_2} $(\$\ per\ kg\ of\ CO_2)$	Emission credits for reducing a kilogram of CO_2 emissions	0.015
$R_{Load\ Reduction}$ $(\$\ per\ kWh)$	Monetary incentive provided per kWh of demand response offered	0.0215
$R_{NG}(\$\ per\ MMBtu)$	Hourly Henry hub natural gas spot price.	Time series data of natural gas price for a year (2012-2013).
R_{comp} $(kJ\ per\ K-mol)$	Universal gas constant used for booster compressor	8.314
UC_{Water} $(\$\ per\ liter\ of\ Water)$	Unit cost of water	0.00314
n'	Set project lifetime (years)	8, 9 and 10
η	Booster compressor efficiency	0.65
CCA (kWh)	Contracted curtailment amount	2000
DR	Binary parameter denoting hours in which demand response needs to be provided.	0 or 1
EMF_{H_2} $(kg\ of\ CO_2\ per\ kmol\ of\ H_2)$	Emission factor of hydrogen produced via electrolysis.	Time series data that varies with emission factor of the electricity produced by power grid.
$EMF_{NG,production}$ $(kg\ CO_{2,e}\ per\ kmol\ of\ NG\ produced)$	Emissions incurred in producing a kmol of natural gas	12.074
EMF_{NG} $(kg\ of\ CO_{2,e}\ per\ kmol\ of\ NG)$	CO_2 equivalent emissions released per kmol of natural gas combusted	42.129
H	Total number of hours in a year	8760

HHV_{H_2} $(MMBtu\ per\ kmol)$)	High heating value of hydrogen	0.27176
HHV_{NG} $(MMBtu\ per\ kmol)$	High heating value of natural gas	0.8053
$O\&M_{Electrolyzer}$ ($)	Annual operating and maintenance cost of electrolyzer	Confidential
R $(m^3\ bar\ per\ K-mol)$	Universal gas constant	8.314 x 10^{-5}
$T\ (K)$	Temperature inside tank	294.15
TC $(\$\ per\ kWh)$	Fee charged for transmission of electricty	0.008652778
$V\ (m^3)$	Maximum volume capacity of tank	7.0523
i (%)	Discount rate	8%
k	Heat capacity ratio of hydrogen	1.4091
n	Project lifetime in years	20
γ $(\$\ per\ MMBtu)$	Rate charged by gas utility to supply fuel for operating pipeline compressors	0.054839982
δ (%)	The amount of natural gas fuel supplied to gas utility to run their pipeline compressors, on top of the gas being transported. Denoted as a ratio of fuel to gas being transported through pipelines.	0.00844
θ	Molar hydrogen injectability limit in natural gas (NG) grid	0.052632
τ($)	Total investment needed for installing the energy hub	5915379.754

Appendix A.6.2: List of Variables for Chapter 6

Variable	Description
ASP_{H_2} $(\$\ per\ kmol)$	Adjusted selling price of H_2 to fuel cell vehicles
$C_{Capital,Annual}$($)	Annual cash outflow for capital cost of energy hub components
C_{H_2} ($)	Annual cost of producing hydrogen
C_{DR} $(\$\ per\ h)$	Amount of monetary clawback if the contracted curtailment amount (CCA) is not offered as demand response
$E_{Booster\ compressor}$ (kWh)	Hourly energy consumption of booster compressor

$EO_{NG}\ (kg)$	Emission offset from combustion of hydrogen enriched natural gas compare to combustion of pure natural gas
$F_{H_2,In,Tank}\ (kmol\ per\ h)$	Hydrogen injected in the tank
$F_{H_2,Pipe,h}\ (kmol\ per\ h)$	Amount of hydrogen injected in to the pipeline every hour
$F_{H_2}\ (kmol\ per\ h)$	Amount of H_2 produced every hour
$F_{H_2,Out,Tank}\ (kmol\ per\ h)$	Hydrogen withdrawn from the tank
$F_{NG,Pipe,h}\ (kmol\ per\ h)$	Amount of natural gas flowing through the pipeline every hour
$I_{H_2}\ (kmol)$	Amount of hydrogen in tank at a given time point
$UPC_{H_2}\ (\$\ per\ kmol)$	Unit production cost of H_2
$P_{tank}\ (bar)$	Pressure inside the hydrogen storage tank
$R_{H_2,FCV}\ (\$)$	Annual revenue from selling hydrogen to FCVs
$T_{H_2,FCV}$	Total hydrogen sold to FCVs throughout the year
$T_{H_2}\ (kmol)$	Total annual hydrogen production
$W_{Booster\ compressor,theoretical}\ (kJ\ per\ kmol)$	Theoretical work required to operate the booster compressor
$\bar{z}$	Compressibility factor of hydrogen going in to booster compressor as function of Pressure and Temperature (which is assumed to be constant).
CF	Annual cash flow of the energy hub
$E\ (kWh)$	Hourly energy consumption level of electrolyzer
$Ereduce\ (kWh)$	Hourly reduction in energy consumption of electrolyzer
L	Annual revenue lost in selling hydrogen at natural gas spot price ($)
$LR\ (kWh)$	Hourly load reduction (demand response) offered by electrolyzer
NPV	Net present value
$NR\ (\$)$	Net annual revenue
$O\ (kmol\ per\ h)$	Amount of natural gas replaced by hydrogen
UF	Unavailability factor, fraction of CCA not offered
z	Compressibility factor of hydrogen as a function of temperature and pressure inside tank
α	Binary variable to decide if a scheduled demand response signal is satisfied by the electrolyzers or not.
$\beta\ (\$)$	New net annual revenue

Appendix A.7.1: List of Variables for Chapter 7

Variables	Description
G_{H_2}	Hydrogen gas produced (kmol)
B_{H_2}	Hydrogen flow bypassing storage (kmol)
E	Energy consumed (kWh)
O_{H_2}	Hydrogen output from tank storage (kmol)
P_{H_2}	Hydrogen purchased from market (kmol)
SF_{H_2}	Short fall in meeting hydrogen demand (kmol)
I_{H_2}	Hydrogen inflow to the tank (kmol)
$PRS_{H_2,h,s}$	Hydrogen injected into pressure reduction station (kmol)
$PRS_{NG,h,s}$	Natural gas flowing through pressure reduction station (kmol)
N_{Ele}	Number of electrolyzers on-site
N_{C_1}	Number of pre-storage compressor modules on-site
N_{Tank}	Number of tanks on-site
ER	Amount of energy consumption reduced (kWh)
DR	Energy consumption reduced to provide demand response (kWh)
St_{max}	Maximum amount of hydrogen stored on-site (kmol)
Inv_{H_2}	Stored hydrogen inventory on-site (kmol)
NG_{Offset}	Amount of natural gas offset at the pressure reduction station (kmol)
A_{CO_2}	Total $CO_{2,e}$ emissions associated with production and purchase of hydrogen (kg)
S_{CO_2}	Total $CO_{2,e}$ emissions curbed while substituting natural gas with hydrogen and from not using steam methane reforming to produce on-site hydrogen. (kg)
$Net_{CO_2,Offset}$	Net $CO_{2,e}$ emissions offset (kg)
X	Clawback cost for not offering scheduled demand response ($ per kWh)
$O\&M_{C_2}$	Operating and maintenance cost of booster compressor modules that includes electricity consumption and transmission charges ($)
RL_{PRS,H_2}	Annual revenue loss in selling hydrogen at natural gas spot price ($)
R_{FCV,H_2}	Annual revenue earned from meeting hydrogen demand ($)
Δ_{low}	The additional annual revenue that can be earned when hydrogen as a transportation fuel is sold at $17 per kmol
Δ_{up}	The additional annual revenue that can be earned when hydrogen as a transportation fuel is sold at $20 per kmol
CF_{Ele}	Annual average capacity factor of electrolyzers
$\beta_0, \dots, \beta_3, \dots, \beta_5$	Binary variables
$\gamma_0, \dots, \gamma_3, \dots, \gamma_5$	Not Sure how to define it: Product of geometric series of constant ratio 2 and capacity factor variable

Appendix A.7.2: List of Indices for Chapter 7

Indices	Description
h	Represents hour of the year
s	Represents a particular scenario for electricity price as well as hydrogen demand
n	Number of terms in the geometric series

Appendix A.7.3: List of Parameters for Chapter 7

Parameter	Description	Value
p_s	Probability of occurrence of a scenario	0.2
a	First term of the geometric series	1
r	Recurrence ration of the geometric series	2
RE_{H_2}	Time Variant Stochastic Parameter	Percentage of total number of refueling events (%)
RA_{H_2}	Time Variant Stochastic Parameter	Refueling Amount of hydrogen (kmol)
η_{El}	Confidential	Electrolyzer efficiency factor (kmol per kWh)
E_{Min}	0	Minimum operating level of an electrolyzer module (kWh)
E_{Max}	1000	Maximum operating level of an electrolyzer module (kWh)
α	$\begin{cases} 0, when\ no\ demand\ response\ is\ required \\ 1, when\ demand\ response\ is\ required \end{cases}$	Binary parameter depicting hours in which demand response should be provided.
DR_{min}	1000	Minimum demand response to be provided in an hour (kWh)
Y_{DR}	0.0215	Incentive received for providing demand response ($ per kWh)
ED	Time series data for the period of November 2012–October 2013	Natural gas energy demand (kmol)
θ	0.05	Upper limit on acceptable fraction of hydrogen injection to natural gas pipeline
C_{Min}	19.5	Minimum storage capacity of tank module (kmol)
C_{Max}	45.4	Maximum storage capacity of tank module (kmol)
HHV_{H_2}	0.272	Higher heating value of hydrogen (MMBtu per kmol)
HHV_{NG}	0.805	Higher heating value of natural gas (MMBtu per kmol)

$F_{Max,C}$	21	Maximum flow handling capacity of pre-compressor storage (kmol)
ε	0.00001	Very small number
EF_{Grid}	Time series value of Emission factor of power grid between November 2012–October 2013	Emission factor of power grid in Ontario (kg CO_2 per kWh)
EF_{NG}	54.203	Well-to-Wheel emission factor of natural gas (kg $CO_{2,e}$ per kmol of NG)
EF_{SMR}	18	Emission factor of steam methane reforming process for hydrogen production (kg $CO_{2,e}$ per kmol H_2)
C_{Ele}	Confidential	Amortized electrolyzer capital cost ($)
$O\&M_{Ele}$	Confidential	Annual operating and maintenance cost of electrolyzer cost ($)
C_{Tank}	$30,421.5	Amortized capital cost of tank ($)
C_{C_1}	$25,442	Amortized capital cost of pre-storage compressor ($)
EP	Time Variant Stochastic Parameter	Hourly Ontario electricity price ($ per kWh)
TC	$0.008 per kWh	Transmission service charge ($ per kWh)
C_{H_2O}	0.00314	Unit cost of Water ($ per liter)
WCR_{Ele}	Confidential	Water consumption rate of electrolyzer (liter per kmol)
ECF_C	2.5042	Energy consumption factor of pre-storage compressor (kWh per kmol H_2)
TC_{NG}	0.055	Natural gas pipeline system service charge ($ per MMBtu)
MP_{H_2}	13.88	Market price of hydrogen ($ per kmol) purchased
SP_{H_2}	8	Selling price of H_2 ($ per kmol)
MP_{NG}	Time series data for the period of November 2012–October 2013	Henry Hub Natural gas spot price ($ per MMBtu)
MC_{CO_2}	0.015	Carbon credit ($ per kg $CO_{2,e}$)
$SP_{H_2,min}$	17	Lower limit on selling price of H_2 ($ per kmol)
$SP_{H_2,max}$	20	Upper limit on selling price of H_2 ($ per kmol)

$CF_{Ele,min}$	0.65	Lower limit on annual average capacity factor of electrolyzer
μ	43800	Product of number of hours in a year (8760) and total number of scenarios (5) considered in the stochastic study)